

**METALLURGICAL STUDIES OF LOCALLY PRODUCED  
AND IMPORTED LOW CARBON STEEL RODS ON THE  
GHANAIAN MARKET**

**by**

**Cephas Thywill Komla Dzogbewu, BSc. Physics (Hons.)**

**A Thesis submitted to the department of Physics,  
Kwame Nkrumah University of Science and Technology  
in partial fulfilment of the requirements for the degree of**

**MASTER OF SCIENCE**

**Faculty of Physical Sciences, College of Science**

**February 2010**

**DECLARATION**

I hereby declare that this thesis is my original work towards the Master of Science and has not been presented for a degree in any other University, except where due acknowledgment has been made in the text.

Cephas Thywill Komla Dzogbewu

.....

Student

Signature

Date

This thesis has been certified by:

1) Dr. A.B.C. Dadson

.....

Supervisor

.....

Signature

.....

Date

2) Prof. S.K. Danuor

.....

Head of Department

.....

Signature

.....

Date

## ABSTRACT

The objective of the research was to undertake a comparative metallurgical study of locally produced and imported iron rods on the Ghanaian market. The iron rods were cut, 40 cm for tensile test, 2.5 cm for microstructural studies and 2.5 cm for elemental analysis. The rod samples of length 40 cm and diameter 19 mm were machined at the mid portions to diameters of 14 mm. The samples were then subjected to tensile loading in an Avery Hydraulic Tensile testing machine. The loads were read from a dial on the machine and the extensions with a set of pre-gauged callipers. The average ultimate tensile strength of the local rods was  $535 \pm 14$  MPa and  $455 \pm 23$  MPa for the imported rods. These values compared well with the standard values of 400 MPa to 1860 MPa for low carbon steels. The toughness test was carried out in two ways: by finding the percentage elongation and the area under the stress-strain curve. The imported rods had an average value of  $30.0 \pm 0.2$  % elongation and  $23.9 \pm 1.1$  % elongation for the local rods. These values fall within the range of the standard values of 4 % to 40 %. From the area under the curve, the imported and locally rods had values of  $101.1 \pm 2.67$  MJ/m<sup>3</sup> and  $87.7 \pm 4.2$  MJ/m<sup>3</sup> respectively, making the imported rods tougher than the local rods. The Young's modulus for the local rods and imported rods were  $16.3 \pm 0.4$  GPa and  $10.9 \pm 0.5$  GPa respectively. The hardness value for the local rods was  $239 \pm 9$  BHN and  $176 \pm 2$  BHN for the imported rods. The local rods were stronger and harder than the imported rods. However the imported rods were more ductile and tougher than the local rods. The difference in the mechanical properties and behaviour were attributed to the difference in the microstructure as a result of the processing methods used, manganese and phosphorus content.

## TABLE OF CONTENTS

TITLE PAGE	i
CERTIFICATION PAGE	ii
ABSTRACT	iii
TABLE OF CONTENTS	iv-vii
LIST OF TABLES	vii
LIST OF FIGURES	viii-x
ACKNOWLEDGEMENT	xi
CHAPTER ONE                      INTRODUCTION	1-11
1.1 General Introduction	1-2
1.2.1 History and production of Steel	2-3
1.2.2 Blast furnace	3-6
1.2.3 Steel furnaces	6
1.2.4 Finishing processes	7
1.3.1 Observation of iron rod production at Tema Steel Works	7-8
1.3 .2 Iron Rods	9-10
1.3.3 Reinforcement of concrete with steel bars (iron rods)	10-11
1.4 Objective of the project	11
1.5 Justification of the project	11

CHAPTER TWO	LITERATURE REVIEW	12-45
2.1	Definition and history	12-14
2.2	Iron	14-15
2.3	Carbon	15-16
2.4	Role of Inclusions and alloying elements in steel	17-18
2.5.1	Iron – carbon phase diagram	18-27
2.5.1	Phases	18-20
<b>2.5.2</b>	<b>Ferrite</b> – solid solution of carbon in $\alpha$ -iron	20-21
<b>2.5.3</b>	<b>Austenite</b> – interstitial solid solution of carbon in $\gamma$ -iron	21
2.5.4	Cementite	22
2.5.5	Pearlite	22-23
2.6	Critical temperatures on the iron – carbon phase diagram	23-24
2.7	Hypoeutectoid and Hypereutectoid steels	24-27
2.8	Transformation on high cooling rates	27-29
2.8.1	Bainite	30-31
2.8.2	Martensite	31-32
2.9.1	Mechanical properties of steel	33
2.9.2	Tensile test	33-34
2.3.3	Type of tensile strength	34-37
2.10.1	Hardness test	38
2.10.2	Hardness measurement methods	38-40

2.11.1 Microstructural studies	40
2.11.2 Cutting and Mounting Metallic Samples	40-41
2.11.3 Grinding	41
2.11.4 Polishing	41
2.11.5 Etching	42
2.12 Determination of elemental composition of the iron rods	43-45
CHAPTER THREE            EXPERIMENTAL DETAILS	46-55
3.1 Introduction	46-47
3.2.1 Preparation of the specimens for tensile test	48-49
3.2.2 Tensile test	50
3.3.1 Preparation of samples for microstructural studies	51-52
3.4 Etching of samples	52-53
3.5 Observing the microstructure under the microscope	53-54
3.6 Hardness test	54-55
CHAPTER FOUR            RESULTS AND DISCUSSIONS	56-78
4.1 Locally produced iron rods	56-63
4.2 Imported iron rods	63-66
4.3 Comparison between locally produced iron rods and imported rods	67-74
4.3.2 Elemental composition	74-76
4.4 Grains size Calculation	77-78

CHAPTER SIX	CONCLUSIONS AND RECOMMENDATIONS	79-81
6.1	Conclusions	79 -81
6.2	Recommendations	81
REFERENCES		82 -86
APPENDICES		87-125
Appendix A–	Calculations	87-91
Appendix B -	Stress Strain curves for imported and locally produced iron rods	92-95
Appendix C- Load - extension tables and calculated values for imported and locally produced iron rods		96-109
Appendix D- The convention chart for hardness test		110-112
Appendix E – Microstructure of the imported and local samples		113-124

#### LIST OF TABLES

Table 1.1	Dimensions of iron rods on the Ghanaian market and their uses	9-10
Table 3.1	Sample codes and their descriptions	47
Table 4.1	Elemental composition of iron rods	61
Table.4.3	The results of hardness test using Brinell hardness testing method	62-63
Table 4.2	Approved elemental composition of mild steel from Ghana standard board...	76

## LIST OF FIGURES

Fig.1.1 Schematic diagram of a blast furnace	4
Fig.1.2 A Schematic diagram of iron rod production	8
Fig. 2.1 Effect of carbon in solid solution on the yield strength of iron	16
Fig. 2.4 A micrograph of ferrite – cementite	21
Fig. 2.5 Different stages of formation of pearlite	23
Fig. 2.6 Iron–Carbon phase diagram	25
Fig.2.7 Microstructure of hypoeutectoid steel	26
Fig.2.8 Microstructure of hypereutectoid steel	27
Fig. 2.9 Time, Temperature, Transformation phase diagram of eutectoid steel	28
Fig.2.10 (a) TTT Diagram and microstructures obtained by different types of cooling rates, (b) Austenite , (c) Pearlite , (d) Martensite, (e) bainite	29
Fig.2.11 Microstructure of upper bainite	30
Fig .2.12Microstructure of lower bainite	31
Fig.2.13 Electron microstructure of martensites: (a) Martensite, (b) Tempered Martensite, (c) Heavily Tempered Martensie	32
Fig.2.14 Stress-strain curve	35
Fig.2.15 Stress vs. Strain curve of typical of structural steel (showing 1:Ultimate strength, 2:Yield strength , 3:Rapture , 4:Strain hardening region , 5:Necking region , A:Apparent stress and B:Actual stress)	36
Fig. 2.16 A schematic diagram of internal structure of a mass spectrometer	45

Fig. 3.1 A Picture of the sample in the jaw of the Center Lathe machine	48
Fig. 3.2 A Picture of the machined samples	48
Fig. 3.3 Schematic diagram of a prepared tensile test sample	49
Fig. 3.4 A Picture of the sample in the jaw of the Avery tensile testing machine	50
Fig.3.5 A Picture of dividers used at incremental interval of 0.00127 m	50
Fig. 3.6 A picture showing the grinding table	51
Fig. 3.7 A Picture showing a sample being polished on a rotating wheel	52
Fig. 3.8 A fume chamber for etchant preparation	53
Fig. 3.9 Picture showing a sample mounted on a computerized microscope and its microstructure displace on the screen	54
Fig. 3.10 A schematic diagram of a 10 mm steel ball indenter on a test specimen	55
Fig. 4.3 Stress-Strain curve of locally produced iron rods (Tema Steel Works [T] and Ferro Fabrik [F] )	56
Fig.4.2 Transverse section of Tema steel sample 1	.58
Fig.4.3 Longitudinal section of Tema steel sample 1	58
Fig.4.4 Transverse section of Ferro Fabric sample 1	59
Fig.4.5 Longitudinal section Ferro Fabric sample 1	59
Fig. 4.6 Stress-Strain curve for imported iron rods (Ukraine [U] and Spain [S])	64
Fig.4.7 Transverse section of Ukraine sample 1	65
Fig.4.8 Longitudinal section of Ukraine sample 1	65
Fig.4.9 Transverse section of Spain sample 1	66
Fig.4.10 Longitudinal section of Spain sample 1	66

Fig. 4.11 Average Stress-Strain curve for imported and locally produced iron rods (Ukraine [U], Spain [S], Tema Steel Works [T], Ferro Fabrik [F])	67
Fig.4.12 Average Stress-Strain curves for the imported (I) and locally produced (L) iron rods	68
Fig. 4.13 Comparing the Ultimate tensile strength and Toughness of locally produced and imported iron rods	71
Fig. 4.14 Comparing the Ultimate tensile strength and Percentage elongation of locally produced and imported iron rods	72
Fig. 4.15 Comparing the Young's modulus and Percentage elongation of locally produced and imported iron	73

## **ACKNOWLEDGEMENT**

I thank the almighty God for making this project a success. For His profound love and guidance are insatiable. Thank you Lord, indeed you have been my sharpard on KNUST campus.

I would like to give special thanks to my research supervisor, Dr. A.B.C. Dadson, who offered tireless guidance and contribution throughout this work. The successful completion of this work depended significantly on his suggestions and creative ideas. His fatherly advice and support to me have undoubtedly made this work a reality.

My heartfelt acknowledgement is made to Tema steel company for permitting me to use their equipment for my chemical analysis and hardness test of my samples. I sincerely acknowledge the constant selfless help of Mr. Emmanuel Amoah a technician in the Department of Physics and Mr. Joseph Amuzu, Mr. Amoaku both technicians at Civil Engineering Department for their dedicated support during the tensile test and polishing of the samples for microstructural studies.

I am indebted to those who have given their invaluable assistance and suggestions in the writing of this thesis.

Lastly, I would like to thank my parents for their financial support and encouragement through out my study on KNUST campus.

# CHAPTER ONE

## INTRODUCTION

### 1.1 General Introduction

Steel is the common name for a large family of iron alloys which are easily malleable after the molten stage. Steel is most common alloy of iron. Alloy steels contain varying amounts of carbon as well as other metals, such as chromium, vanadium, molybdenum, nickel, tungsten etc. Steels are commonly made from iron, coal and limestone. When these raw materials are put in to the blast furnace, the result is a pig iron [1].

Steel has been part of some of the greatest achievements in the history of man's discovery. It was the 'iron horse ' and steel rails that helped carve a nation out of the frontier. Steel is the backbone of bridges, the skeleton of skyscrapers, and the framework for automobiles.

Steel continue to revolutionize the way we live even in the twenty first century, it is the high-strength lighter-than plastic frames for eyeglasses. It is the stronger and the more durable frame in the construction buildings; it is the high technological alloy used in the Space Shuttle's solid fuel rocket motor cases; and it is the precise surgical instruments used in hospital operating rooms around the world [2].

The differences between the various types of iron and steel are sometimes confusing because of the nomenclature used. Steel is generally an alloy of iron and carbon, with other alloying elements. Steels of various types contain from 0.04 percent to 2.25 percent

by weight of carbon while Cast iron and pig iron contain about 2 to 4 percent. A special form of malleable iron, containing virtually no carbon, is known as white-heart malleable iron. A special group of iron alloys, known as ferroalloys, is used in the manufacture of iron and steel alloys; they contain from 20 to 80 percent of an alloying element, such as manganese, silicon, and chromium [3].

### **1.2.1 History and production of Steel**

The exact date at which people discovered the technique of smelting iron ore to produce usable metal is not known. The earliest iron implements discovered by archaeologists in Egypt dates from about 3000 BC and iron ornaments were used even earlier; the comparatively advanced technique of hardening iron weapons by heat treatment was known to the Greeks about 1000 BC.

The alloys produced by early iron workers and all the iron alloys made until about the 14th century would be classified today as wrought iron. They were made by heating a mass of iron ore and charcoal in a forge or furnace having a forced draft. Under this treatment the ore was reduced to the sponge of metallic iron filled with a slag composed of metallic impurities and charcoal ash. This sponge of iron was removed from the furnace while still incandescent and beaten with heavy sledges to drive out the slag and to weld and consolidate the iron. The iron produced under these conditions usually contained about 3 percent of slag particles and 0.1 percent of other impurities. Occasionally, this technique of iron making was produced by accident, a true steel rather than wrought iron. Iron workers learned to make steel by heating wrought iron and

charcoal in clay boxes for a period of several days. By this process the iron absorbed enough carbon to become true steel [4, 48].

After the 14th century the furnaces used in smelting were increased in size, and increased draft was used to force the combustion gases through the “charge,” the mixture of raw materials. In these larger furnaces, the iron ore in the upper part of the furnace was first reduced to metallic iron and then took on more carbon as a result of the gases forced through it by the blast. The product of these furnaces was pig iron, an alloy that melts at a lower temperature than steel or wrought iron. Pig iron (so called because it was usually cast in stubby, round ingots known as pigs) was then further refined to make steel.

Over the years various countries have excelled in making steel. During the eighteenth century a relatively small amount of steel was made, but Sweden was the main producer. In the nineteenth century, Great Britain became dominant. In the twentieth century the United States was the largest steel producer in the world until about 1970, when it was surpassed by the Soviet Union. At the start of the twenty-first century, China led the world in steel production [5].

### **1.2.2 Blast furnace.**

There are three main installations in an integrated steel plant; they are the blast furnace, the steel furnaces, and the rolling mills. The blast furnace converts iron ore to pig iron and the steel furnaces convert the pig iron to steel. Rolling mills were used to shape the steel into sheets, slabs, or bars.

A blast furnace is a chimney-like structure in which iron ores (mainly FeO, Fe<sub>2</sub>O<sub>3</sub>, and Fe<sub>3</sub>O<sub>4</sub>) are converted into iron metal. Iron ore, coke, and limestone are loaded into the top of the furnace, while hot air is blown in from below. The coke is converted to carbon monoxide (CO), which then acts as the reducing agent and reduce the iron ore to molten iron:



[2]

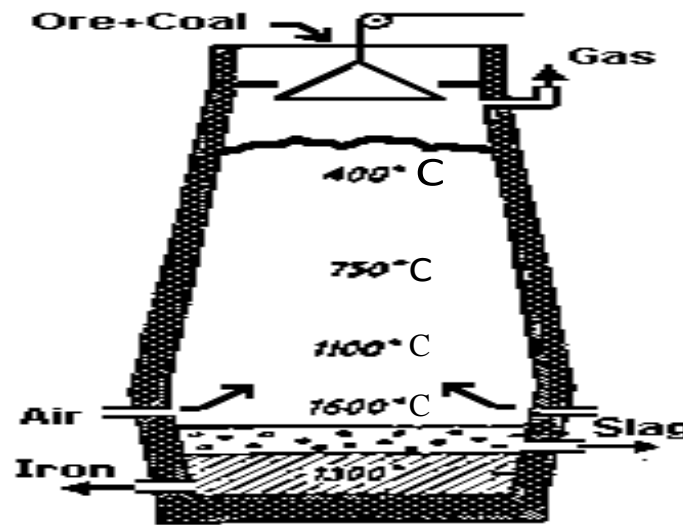


Fig.1.1 Schematic diagram of a blast furnace [6,49]

The limestone in the furnace charge is used as an additional source of carbon monoxide and as a “flux” to combine with the infusible silica present in the ore to form fusible calcium silicate. Without the limestone, iron silicate would be formed, with a resulting loss of metallic iron. Calcium silicate plus other impurities form a slag that floats on top of the molten metal at the bottom of the furnace. Ordinary pig iron as produced by blast

furnaces contains about 92 percent iron , 3 or 4 percent carbon, 0.5 to 3 percent silicon, 0.25 to 2.5 percent manganese , phosphorus and trace of sulphur.

A typical blast furnace consists of a cylindrical steel shell lined with a refractory, which is any nonmetallic substance such as firebrick. The shell is tapered at the top and at the bottom and is widest at a point about one-quarter of the distance from the bottom. The lower portion of the furnace, called the bosh, is equipped with several tubular openings or tuyeres through which the air blast is forced. Near the bottom of the bosh is a hole through which the molten pig iron flows when the furnace is tapped, and above this hole, but below the tuyeres, is another hole for draining the slag. The top of the furnace contains vents for the escaping gases, and a pair of round hoppers closed with bell-shaped valves through which the charge is introduced into the furnace. [6]

Blast furnaces operate continuously. The raw material to be fed into the furnace is divided into a number of small charges that are introduced into the furnace at 10- to 15- minutes intervals. Slag is drawn off from the top of the melt about once every 2 hr, and the iron itself is drawn off or tapped about five times a day.

The air used in the blast furnace is preheated to temperatures between 540° and 870° C. The heating is performed in stoves, cylinders containing networks of firebrick. An important development in blast furnace technology, the pressurizing of furnaces, was introduced after World War II. The pressure within the furnace may be built up to 1.7 atm or more. The pressurizing technique makes possible better combustion of the coke and higher output of pig iron. The output of many blast furnaces can be increased 25

percent by pressurizing. Experimental installations have also shown that the output of blast furnaces can be increased by enriching the air blast with oxygen.

The process of tapping consists of knocking out a clay plug from the iron hole near the bottom of the bosh and allowing the molten metal to flow into a clay-lined runner and then into a large, brick-lined metal container, which may be either a ladle or a rail car capable of holding as much as 100 tons of metal. Any slag that may flow from the furnace with the metal is skimmed off before it reaches the container. The container of molten pig iron is then transported to the steel furnace [5, 6]

### **1.2.3 Steel furnaces.**

In the steel furnace, sulfur and phosphorus impurities and excess carbon are burned out, and manganese and other alloying ingredients are added. During the nineteenth century most steel was made by the Bessemer process, using big pear-shaped converters. During the first half of the twentieth century, the open hearth furnace became the main type of steel furnace. This gave way mid-century to the basic oxygen process, which used pure oxygen instead of air, cutting the process time from all day to just a few hours. In the twenty-first century, most new steel plants use electric furnaces, the most popular being the electric-arc furnace. It is cheaper to build and more efficient to operate than the basic oxygen furnace. In the electric-arc furnace a powerful electric current jumps (or arcs) between the electrodes, generating intense heat, which melts the iron scrap that is typically fed into it. The most modern process for making steel is the continuous process, which bypasses the energy requirements of the blast furnace. Instead of using coke, the iron ore is reduced by hydrogen and CO derived from natural gas. This direct reduction

method is especially being used in developing countries where there are not any large steel plants already in operation [2].

#### **1.2.4 Finishing processes.**

A final step in processing steel is shaping. Liquid steel can be cast into ingots or various other forms. They can then be sent to rolling mills. There are hot rolling mills and cold rolling mills. Various kinds of steel slabs are rolled into sheets, strips, bars, or other kinds of products. Sometimes the steel is forged into shape with hammers or presses, or the hot steel is extruded through dies to give it some desired shape. For example, steel wire is made by drawing hot steel rods through smaller and smaller dies. Some steel is finished by grinding or polishing, and some is coated with zinc or electroplated with tin [5].

#### **1.3 Observation of iron rod production at Tema Steel Works**

The first stage of the production is the segregation of the scrap. The selection of the scrap basically depends on the type of steel which would be produced. For a high carbon steel scraps from engine part are selected while for a low carbon steel scrap from automobile body parts are mainly selected. The scraps are sent to the balling press for compacting so that the bucket can contain a larger volume. After the segregation the bucket is charge and the overhead crane would convey the segregated scrap to the Electric Arc Furnace. The roof of the furnace is removed and the bottom of the basket is open and the scrap fell into the furnace. During the charging of the furnace lime is introduce to prevent early slaging, including oxygen for the oxidation process. The scrap is melted and at a temperature of 1500 °C the first slag (the scavenger slag) is removed to take away

phosphorus, sulfur and other impurities. As the oxidation process continues more of the impurities are moved to the surface of the slag. The furnace is tilted at an angle of 15° and another slag is removed. At a temperature of about 1560 °C the molten metal should be cleared of slag three times. When the molten metal composition is tested and it agrees with the kind of steel desired to be produced the temperature is raised to the tapping temperature of 1640 °C and the molten metal is then tap into a ladle.

Some slag is left at the top of the molten metal in the ladle to minimized temperature loss and the overhead crane is used to transport the ladle to the Ladle Refinery furnace, where the molten metal chemistry is fine tune by adding of manganese and sea shell. Nitrogen is then introduced into the molten metal to bring out any non-metallic inclusion to the surface of the molten metal. The molten metal is conveyed to the continuous casting machined before the casting the metal under goes thermo metallurgical treatment (TMT). Thermo metallurgical treatment is the quenching of molten metal as it passes through the casting machined to make it solidified. The molten metal is cast into billet. The billet is preheated and passed through a series of rollers depending on the dimension and surface texture desired.

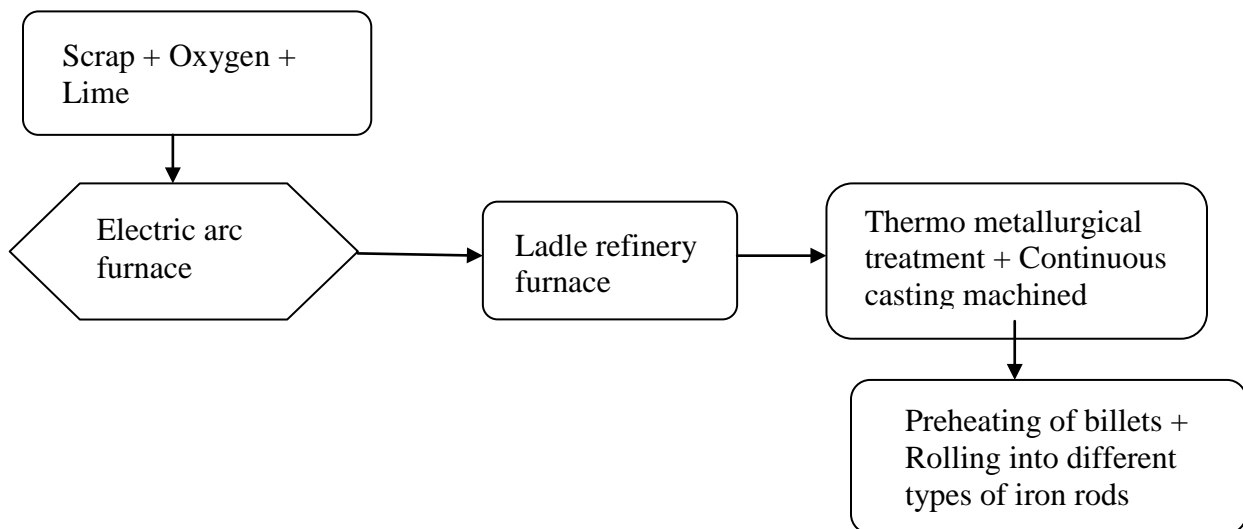


Fig.1.2 Flow chart diagram of iron rod production at Tema Steel Company [5]

### 1.4.1 Iron Rods

Iron rods belong to a large family of iron alloys called steel. Which are easily malleable after the molten stage. Iron rods are obtained after the ingot is rolled into rods of different diameter at the rolling mills. They are used in buildings and heavy constructional works [7].

Table 1.1 Dimensions of iron rods on the Ghanaian market and their uses (Information provided by Kwasi Opong Co. Ltd Kumasi-Fumesua)

TYPE OF IRON RODS ON THE GHANAIAN MARKET AND USES		
Item	Surface texture	Uses
10 mm	Rough	Window design (Burglar proofing) ,flow, mat
10.5 mm	Rough	Window design(Burglar proofing ), flow, mat
11.5 mm	Rough	Window design(Burglar proofing), flow, mat
12 mm	Rough	Reinforced concrete columns and beams
14 mm	Rough	Window design( Burglar proofing), Reinforced concrete columns and beams
15 mm	Rough	Pillar, Window
19 mm	Rough	Beam, Column of story building
24 mm	Rough	Story building (heavy duty)
32 mm	Rough	Story building (heavy duty)
8 mm	Rough	Ring
5.5 mm	Rough	Gate design

12 mm	Smooth	Gate design
15 mm	Smooth	Window design(Burglar proofing), Gate design, Welding
19 mm	Smooth	Window design, Gate design, Welding
24 mm	Smooth	Window design(Burglar proofing), Gate design, welding

#### **1.4.2 Reinforcement of concrete with steel bars (iron rods)**

The introduction of steel concrete also known as ferroconcrete, or reinforced concrete is generally attributed to Joseph Monier, a French gardener, who about the year 1868 was anxious to build some concrete water basins. Concrete has considerable compressive or crushing strength, but is somewhat deficient in shearing strength, and distinctly weak in tensile or pulling strength. Steel, on the other hand, have a good tensile strength and is easily procurable in simple forms such as long bars. If a concrete slab be "reinforced" with a network of small steel rods on it's under surface where the tensile stresses occurs, its strength will be enormously increased.

Any steel bar should be capable of being bent cold to the shape of the letter U without breaking. The structures in which steel concrete is used normally are: walls, columns, piles, beams, slabs and arches. The effect of reinforcing walls with steel is that they can be made much thinner. The steel reinforcement is generally applied in the form of vertical rods built in the wall at intervals, with lighter horizontal rods which cross the vertical ones, and thus form a network of steel which is buried in the concrete. These rods assist in taking the weight, and the whole network binds the concrete together and

prevents it from cracking under a heavy load. To meet tensile stresses the steel is nearly always inserted in the form of bars running along the beam [8, 12].

### **1.5 Objective of the project**

The objective of this project is to study the metallurgical differences between locally produced and imported iron rods on the Ghanaian market. Usually routine tests like tensile test, hardness test, microstructural studies are carried out to established whether or not a product of a metal meets the required specification. Efforts have been made to established the relationship between the mechanical properties of the rods and their microstructures. Since there are all kinds of iron rods in the country, there is a need for a study to characterize the properties of the iron rods used.

### **1.6 Justification of the project**

There is high demand for iron rods in the country which the two functioning local industries (Tema Steel Company and Ferro Fabrik Company) can not supply. This has created the need for the importation of iron rods into the country.

Some of the countries that provide either billets or iron rods for Ghanaian market are; Ukraine, Turkey, Spain, Brazil and Ivory Coast.

This project seeks to study the metallurgy of the locally produced iron rods and some of the imported iron rods.

## **CHAPTER TWO**

### **LITERATURE REVIEW**

#### **2.1 Definition and history**

Metallurgy is a domain of materials science that studies the physical and chemical behavior of metallic elements, their intermetallic compounds, and their mixtures, which are called alloys. It is the technology of extracting metals from their ores, or purifying metals and casting useful items from them. It involves knowledge and study of metals and their phases and properties at bulk and atomic levels. Metallurgy is commonly used in the craft of metalworking [9].

No substance has been as important as metal in the story of man's control of his environment. Advances in agriculture, warfare, transport, even cookery are impossible without metals. So is the entire Industrial Revolution, from steam to electricity.

Nature entices man into the adventure of metallurgy by an initial gift of gold, the most attractive and precious of metals in every society, is also the easiest for primitive man to acquire.

Metallurgy is one of the oldest applied sciences. Its history can be traced back to 6000 BC. Currently there are 86 known metals. Before the 19th century only 24 of these metals had been discovered. There were seven metals known as the Metals of Antiquity upon which civilization was based. These metals and the year of discovery are as follow: Gold (6000BC), Copper (4200BC), Silver (4000BC), Lead (3500BC), Tin (1750BC), Iron smelted (1500BC) and Mercury (750BC).

These metals were known to the Mesopotamians, Egyptians, Greeks and the Romans. Five of these metals can be found in their native states, e.g., gold, silver, copper, iron (from meteors) and mercury. However, the occurrence of these metals was not in abundant and the first two metals to be used widely were gold and copper [10].

The origin of metallurgy in Africa is disputed by archaeologists. The first evidence of metallurgical work in Africa dates back as far as the second millennium BC. The vast scale of the continent, accessibility, political and cultural barriers have caused difficulties in finding a good database of evidence to help diagnose when and where origins lie. The metallurgical work in Africa was based around the agricultural revolution, driven by the use of iron tools. Tools for cultivation and farming made production far more efficient and possible on much larger scales. Fishing hooks, arrow heads and spears aided hunting and iron weapons also influenced warfare [42].

However, the Africans were the first to create a sophisticated pre-heated furnace than any developed in Europe until the mid-19th century. It has also been discovered that near Lake Victoria were 13 Iron Age furnaces that proved a technologically superior culture developed in Africa more than 1, 500 years ago. The temperature achieved in the blast furnace of the African steel-smelting machine was higher than any achieved in European machine until the industrial revolution [43].

The most ancient mines in the world were found in the southern part of Africa. One of several discoveries was reported early in 1970, which was of an ancient mine in an

iron-ore mountain in Swaziland, in southeast Africa. Stone as mining tools were found, and samples of charcoal remaining from old fires were also detected. Sacrifices were also made to the gods of various metals [43].

## **2.2 Iron**

Iron is a chemical element. It is a strong, hard, heavy gray metal. Among all the metals, iron is second only to aluminum in natural abundance, making up 4.7 percent of the earth's crust, and occurring mainly in its various oxides, it is also found in meteorites. Iron is also found combined in many mineral compounds in the earth's crust. Iron rusts easily. It can be magnetized and is strongly attracted to magnets. It is used to make many things such as gates and railings. Iron is also used to make steel, an even harder and tougher metal compound. Steel is formed by treating molten iron with intense heat and mixing it (alloying) with carbon. Steel is used to make machines, cars, tools, knives, and many other things. The main product made from iron is steel, the least expensive and most widely used of all metals [11].

Typical iron-containing minerals include  $\text{Fe}_2\text{O}_3$ —the form of iron oxide found as the mineral hematite, and  $\text{FeS}_2$ —pyrite (fool's gold).

Pure iron is quite different from chromium or copper. When heated to the correct temperature, it has the ability to transform from one cubic arrangement to another, a phenomenon called a polymorphic transition. The temperature transformation stages of pure iron are as follows: It is body-centered cubic at room temperature. Once the metal is heated to 910 °C, it fully transforms to the face-centered cubic form. It stays FCC until it

reaches 1390 °C. At that temperature, it transforms back to the body-centered cubic form. Heating pure iron above 1390 °C to its melting temperature of 1532 °C has no effect on the BCC form. Another temperature worth mentioning is the Curie point, or magnetic change point. At 768 °C and above, iron is nonmagnetic. This Curie point is not a structural change point [7,13].

### **2.3 Carbon**

Carbon is the most common alloying element in steel. It is inexpensive and has a strong influence on hardness and strength. It is the basic and essential alloying element in all plain-carbon, low-alloy steels. When carbon in small quantities is added to iron, 'Steel' is obtained. Since the influence of carbon on mechanical properties of iron is much larger than other alloying elements because the atomic diameter of carbon is less than the interstices between iron atoms and the carbon goes into solid solution of iron. As carbon dissolves in the interstices, it distorts the original crystal lattice of iron. This mechanical distortion of crystal lattice interferes with the external applied strain to the crystal lattice, by mechanically blocking the dislocation of the crystal lattices. In other words, they provide mechanical strength. Obviously adding more and more carbon to iron (up to solubility of iron) results in more and more distortion of the crystal lattices and hence provides increased mechanical strength. However, solubility of more carbon influences negatively with another important property of iron called the 'ductility' (ability of iron to undergo large plastic deformation). Increase in carbon content is not the only way, and certainly not the desirable way to get increased strength of steels. More amount of carbon causes problems during the welding process [14].

The influence of carbon on the strength of iron can be seen in Figure 2.1. Carbon can increase yield strength of pure iron (0% C) to a strength of about 28–190MPa with only 0.005% C [15]

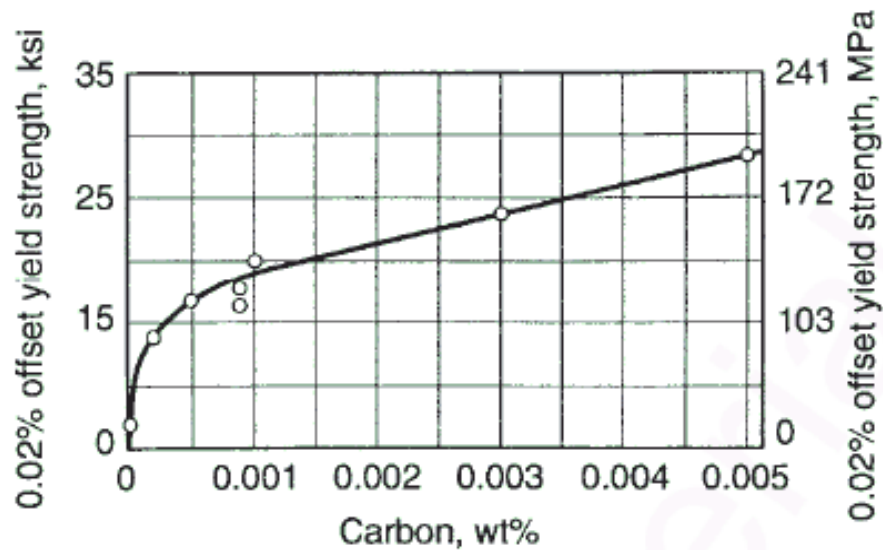


Fig. 2.1 Effect of carbon in solid solution on the yield strength of iron [15].

Any excess carbon, above 0.005% C, will form an iron carbide compound called cementite ( $\text{Fe}_3\text{C}$ ).

Thus, carbon in the form of cementite has a further influence on the strength of steels. These properties are for carbon steels in the air-cooled condition. In a 0.8% C content, a further increase in strength can be achieved if faster cooling rates are used to produce a finer pearlite interlamellar spacing. In a fully pearlitic, the yield strength can increase to 860MPa and tensile strength to 1070MPa [15].

## **2.4 Role of Inclusions and alloying elements in steel**

In the concept of hardenability, the alloying elements have a profound effect on depth of hardness. The elements actually act as a hardening agent, preventing dislocations in the iron atom crystal lattice from sliding past one another. Varying the amount of alloying elements and form of their presence in the steel (solute elements, precipitated phase) controls qualities such as the hardness, ductility, and tensile strength of the resulting steel [15].

Steel contains impurities such as phosphorous and sulfur and they eventually form phosphides and sulfides which are harmful to the toughness of the steel.

Hence, it is desirable to keep these elements less than 0.05%. Phosphorous could be easily removed compared to sulfur. If manganese (Mn) is added to steel, it forms a less harmful manganese sulfide (MnS) rather than the harmful iron sulphide. Sometimes calcium, cerium, and other rare earth elements are added to the refined molten steel.

They combine with sulfur to form less harmful elements. Steel treated this way has good toughness and such steels are used in special applications where toughness is the criteria. The addition of manganese also increases the undercooling before the start of the formation of ferrite and pearlite. This gives fine-grained ferrite and more evenly divided pearlite. Since the atomic diameter of manganese is larger than the atomic diameter of iron, manganese exists as 'substitutional solid solution' in ferrite crystals, by displacing the smaller iron atoms. This improves the strength of ferrite because of the distortion of crystal lattice due to the presence of manganese which blocks the movement of dislocation in the crystal lattices. However, manganese content cannot be increased

unduly, as it might become harmful. Increased manganese content increases the formation of martensite, and hence, hardness and raises its ductile -to -brittle transition temperature (temperature at which steel which is normally ductile becomes brittle). Because of these reasons, manganese is restricted to 1.5% by weight [5]

In recent years, micro alloyed steels or high strength low alloy (HSLA) steels have been developed. They are basically carbon manganese steels in which small amounts of Aluminum, Vanadium or other elements are used to help control the grain size.

These steels are controlled rolled and/or controlled cooled to obtain fine grain size. They exhibit a best combination of strength and toughness and also are generally weldable without precautions such as preheating or post heating. Sometimes 0.5% molybdenum is added to refine the lamellar spacing in pearlite, and to make the pearlite evenly distributed. The micro alloyed steels are more expensive than ordinary structural steels, however, their strength and performance outweigh the extra cost. Weldability of steel is closely related to the amount of carbon in steel. Weldability is also affected by the presence of other elements [16].

## **2.5 Iron – carbon phase diagram**

### **2.5.1 Phases**

A "Phase" is a form of material having characteristic structure and properties. It is a form of the material which has identifiable composition, structure and boundaries separating it from other phases in the material volume. The iron-carbon equilibrium phase diagram is a plot of transformation of iron with respect to carbon content and temperature. Fig.2.2

below shows the iron-carbon system of alloys containing up to 6.67% of carbon, which discloses the phase's compositions and their transformations occurring with the alloys during their cooling or heating. Carbon content 6.67% corresponds to the fixed composition of the iron carbide  $\text{Fe}_3\text{C}$ . A study of the microstructure of all steels usually starts with the metastable iron-carbon (Fe-C) binary phase diagram .

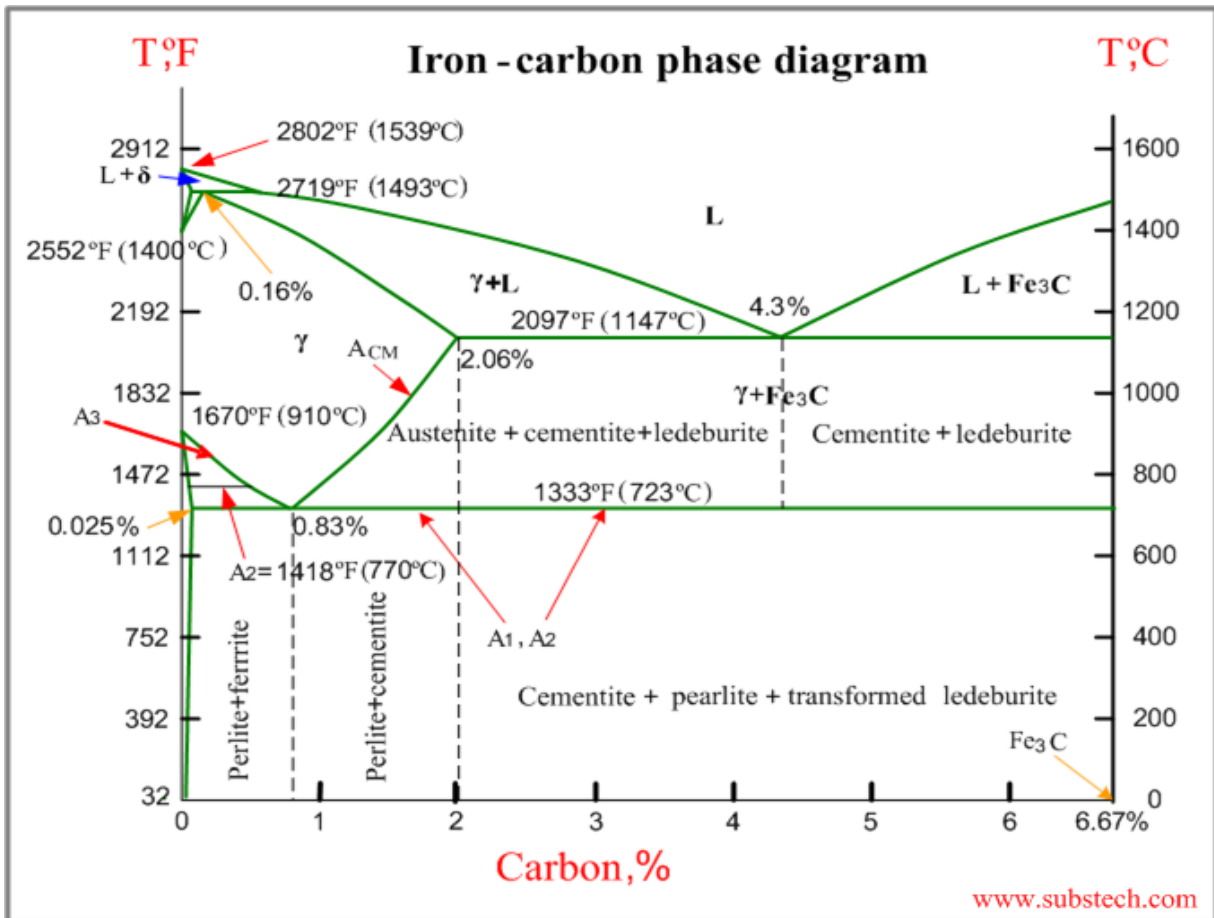


Fig. 2.2 Iron carbon phase diagram [18,].

The following phases are involved in the transformation, occurring with the iron-carbon phase diagram in Figure 2.2:

- **L** - Liquid solution of carbon in iron;
- **$\delta$ -ferrite** – Solid solution of carbon in iron.

Maximum concentration of carbon in  $\delta$ -ferrite is 0.09% at 1493°C – temperature of the peritectic transformation. The crystal structure of  $\delta$ -ferrite is BCC (cubic body centered).

This has no real practical significance in engineering.

### 2.5.2 Ferrite – solid solution of carbon in iron.

Ferrite: Virtually pure iron with body centered cubic crystal structure (bcc) with low solubility of carbon – up to 0.025% at 723°C). It is stable at all temperatures. The carbon solubility in ferrite depends upon the temperature [17].

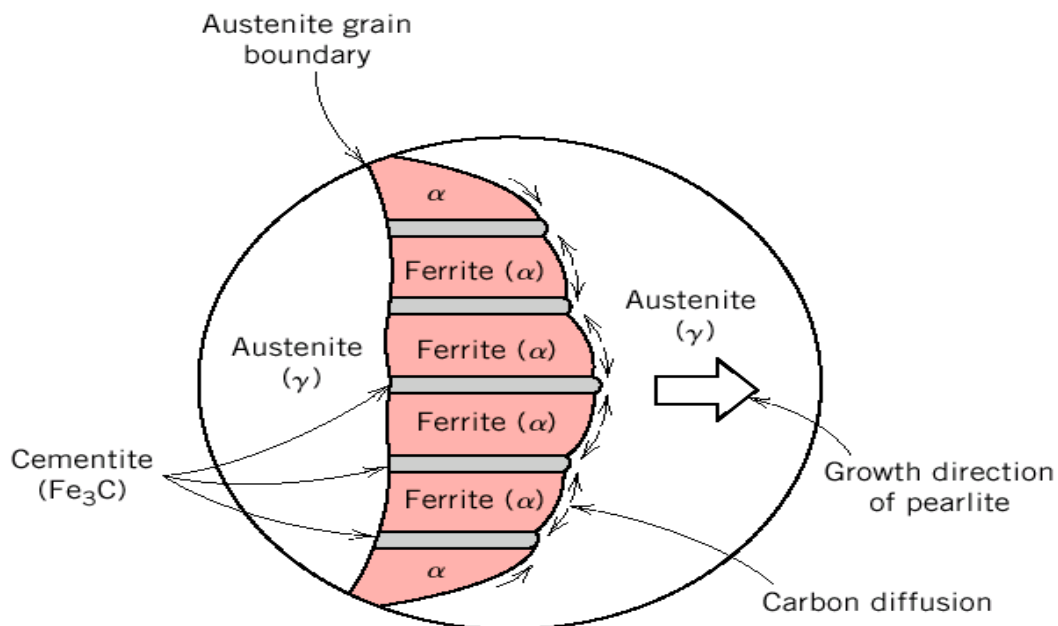


Fig. 2.3 A schematic diagram of formation of ferrite-cementite alternation layer [44]

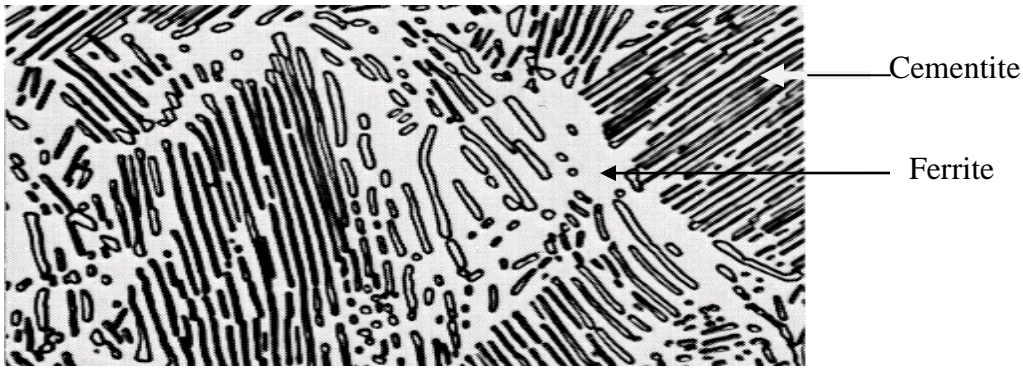


Fig. 2.4 A micrograph of ferrite (white region) and cementite (dark region) [44]

### 2.5.3 Austenite – interstitial solid solution of carbon in iron.

Austenite has FCC (cubic face centered) crystal structure, permitting high solubility of carbon – up to 2.06% at 1147 °C.

Austenite does not exist below 733°C and maximum carbon concentration at this temperature is 0.83%. The maximum solubility of carbon in the form of  $\text{Fe}_3\text{C}$  in iron is 6.67%. Addition of carbon to iron beyond this percentage would result in formation of free carbon or graphite in iron. At 6.67% of carbon, iron transforms completely into cementite or  $\text{Fe}_3\text{C}$  (Iron Carbide). Generally carbon content in structural steels is in the range of 0.12-0.25%. Up to 2% carbon, we get a structure of ferrite + pearlite or pearlite + cementite depending upon whether carbon content is less than 0.8% or beyond 0.8%. Beyond 2% carbon in iron, brittle cast iron is formed [18, 50].

#### **2.5.4 Cementite**

Unlike ferrite and austenite, cementite is a very hard intermetallic compound consisting of 6.7% carbon and the remainder iron, its chemical symbol is  $\text{Fe}_3\text{C}$ . Cementite is very hard, but when mixed with soft ferrite layers as shown in Fig.2.3 its average hardness is reduced considerably. Slow cooling gives coarse perlite; soft easy to machine but poor toughness. Faster cooling gives very fine layers of ferrite and cementite; harder and tougher.

#### **2.5.5 Pearlite**

A mixture of alternate strips of ferrite and cementite in a single grain. The distance between the plates and their thickness is dependant on the cooling rate of the material; fast cooling creates thin plates that are close together and slow cooling creates a much coarser structure possessing less toughness. The name for this structure is derived from its mother of pearl appearance under a microscope. A fully pearlitic structure occurs at 0.8% Carbon. Further increases in carbon will create cementite at the grain boundaries, which will start to weaken the steel. It is stable at all temperatures below  $723^\circ\text{C}$ .

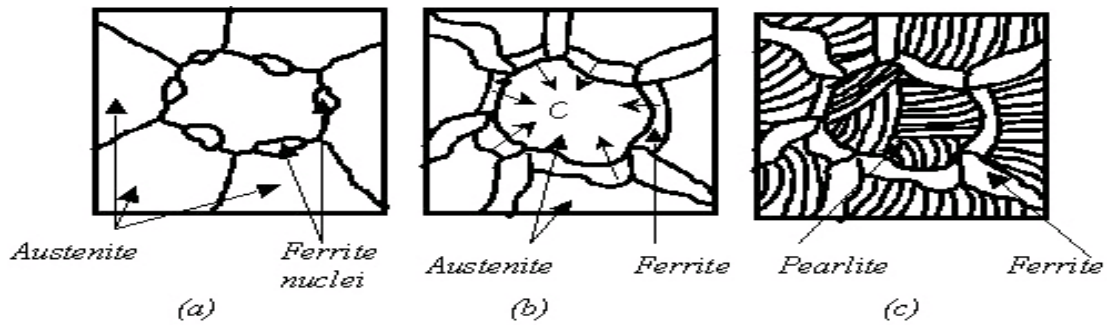


Fig.2.5. Different stages of formation of pearlite

The latter decomposes by eutectic mechanism to a fine mixture of austenite and cementite, called ledeburite [18].

## 2.6 Critical temperatures on the iron – carbon phase diagram

- **Upper critical temperature (point) A3 (Hypoeutectoid Steel)** as in Fig. 2.2 is the temperature, below which ferrite starts to form as a result of ejection from austenite in the hypoeutectoid alloys.
- **Upper critical temperature (point) ACT (Hypereutectoid Steel)** as in Fig. 2.2 is the temperature, below which cementite starts to form as a result of ejection from austenite in the hypereutectoid alloys.
- **Lower critical temperature (point) A1** as in Fig. 2.2 is the temperature of the austenite-to-pearlite eutectoid transformation. Below this temperature austenite does not exist.
- **Magnetic transformation temperature A2** as in Fig. 2.2 is the temperature below which  $\alpha$ -ferrite is ferromagnetic.[17]

## **2.7 Hypoeutectoid and Hypereutectoid steels**

The part of the iron-carbon phase diagram portion that is of interest to structural engineers is shown in Fig.2.6. The phase diagram is divided into two parts called “hypoeutectoid steels” (steels with carbon content to the left of eutectoid point [0.8% carbon] and “hypereutectoid steels” which have carbon content to the right of the eutectoid point. It is seen from the fig.2.6 that iron containing very low percentage of carbon (0.002%) called very low carbon steels will have 100% ferrite microstructure (grains or crystals of ferrite with irregular boundaries) .

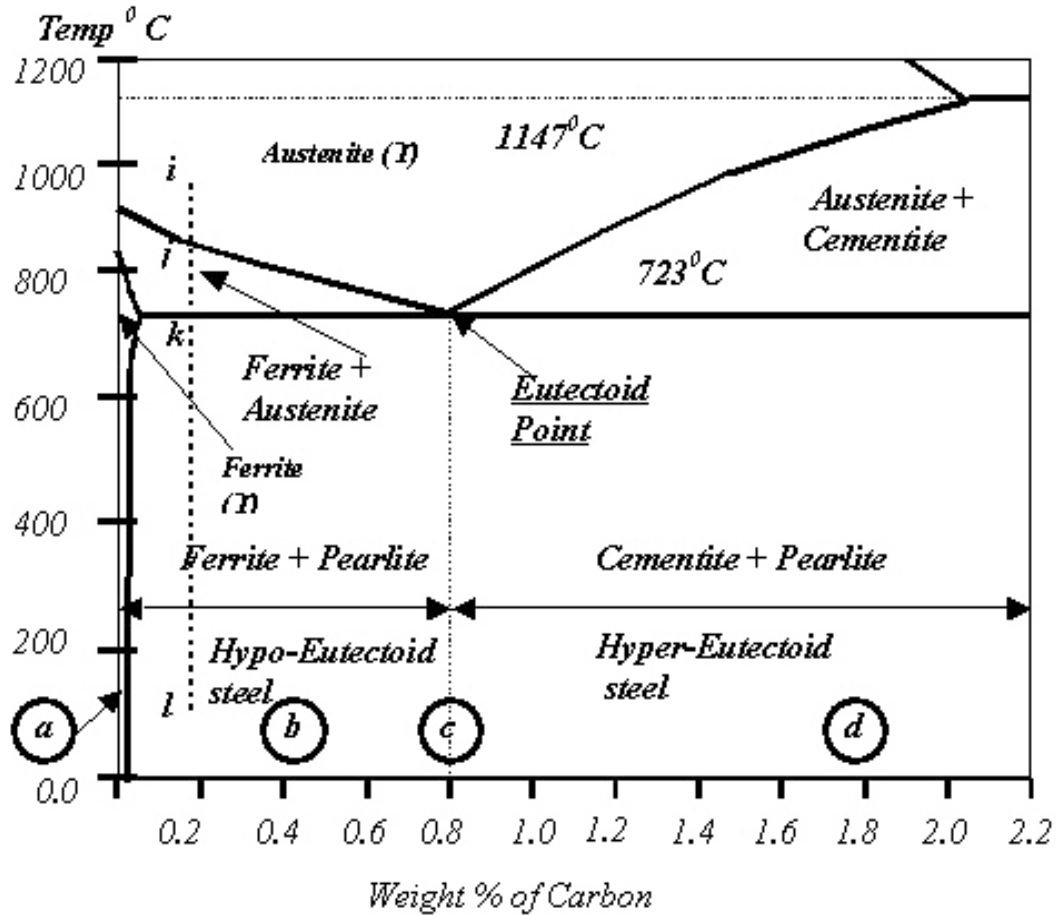


Fig. 2.6 Iron–Carbon phase diagram [17].

Ferrite is soft and ductile with very low mechanical strength. This microstructure at ambient temperature has a mixture of what is known as ‘pearlite and ferrite’ as can be seen in Fig. 2.6. Hence, we see that ordinary structural steels have a pearlite + ferrite microstructure. However, it is important to note that steel of 0.20% carbon ends up in pearlite + ferrite microstructure, only when it is cooled very slowly from higher temperature during manufacturing. When the rate of cooling is faster, the normal pearlite+ ferrite microstructure may not form, instead some other microstructure called bainite or martensite may result. At about 900°C, steel has austenite microstructure. This is shown as point ‘i’ in Fig. 2.6. When steel is slowly cooled, the transformation would

start on reaching the point 'j'. At this point, the alloy enters a two-phase field of ferrite and austenite. On reaching the point, ferrite starts nucleating around the grain boundaries of austenite as shown in Fig. 2.5(a). By slowly cooling to point 'k', the ferrite grains grow in size and diffusion of carbon takes place from ferrite regions into the austenite regions as shown in Fig. 2.5(b), since ferrite cannot retain carbon above 0.002% at room temperature. At this point it is seen that a network of ferrite crystals surrounds each austenite grain. On slow cooling to point 'l' the remaining austenite gets transformed into 'pearlite' as shown in Fig 2.5(c). Pearlite is a lamellar mixture of ferrite and cementite.

The higher the carbon content, the higher would be the pearlite content and hence higher mechanical strength. Conversely, when the pearlite content increases, the ferrite content decreases and hence the ductility is reduced [18, 19].

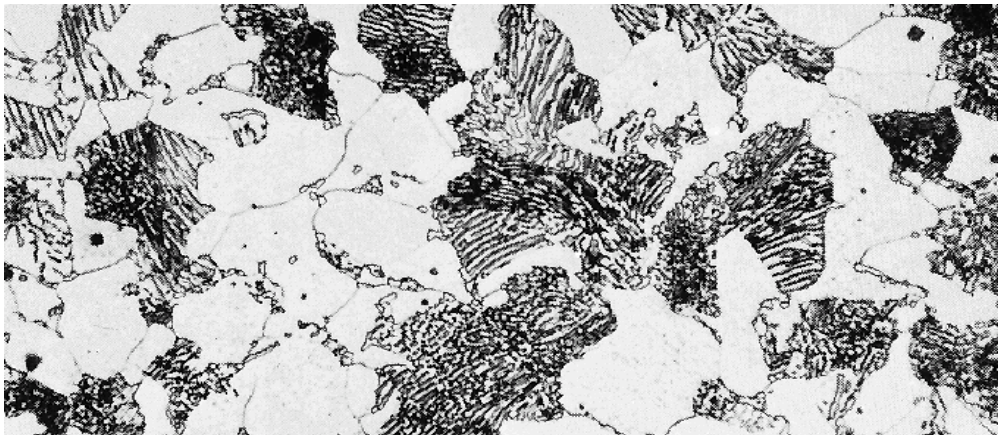


Fig.2.7 Microstructure of hypoeutectoid steel [44]



Fig.2.8 Microstructure of hypereutectoid steel [44]

### **2.8 Transformation on high cooling rates**

Fast cooling rate of steel from austenite region to room temperature produces different microstructures, which imparts different mechanical properties. The TTT (Time, Temperature, Transformation) curve for a eutectoid steel test piece which has been rapidly cooled in a bath at a set temperature, held for a time and then water quenched produces a different phase diagram as shown below in fig.2.9.

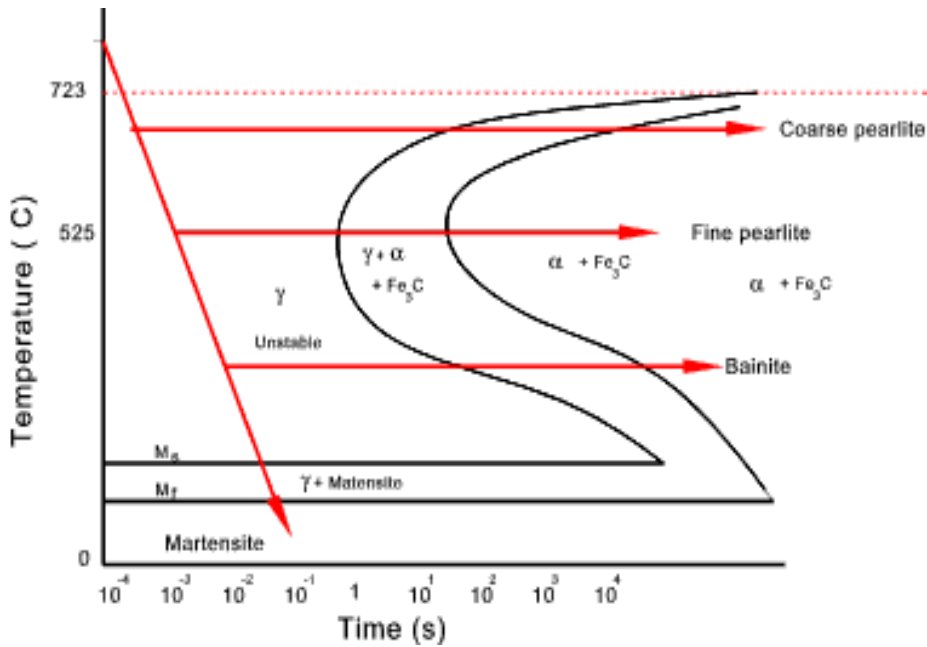


Fig. 2.9 Time, Temperature, Transformation phase diagram of eutectoid steel [18]

It can be seen that if the transformation is allowed to take place at regular cooling rate and at a higher temperature then, coarse pearlite is formed but if allow to cooled to a lower temperature in a bath a finer pearlitic structure results. If the test piece is rapidly cooled to a temperature below a value  $M_s$  (which varies with the carbon content) then a new metastable phase called martensite is produced; this is a supersaturated solid solution of carbon in ferrite. If the test piece is cooled rapidly to a temperature between 220°C and 525°C a phase structure between pearlite and martensite is formed, called Bainite [18].

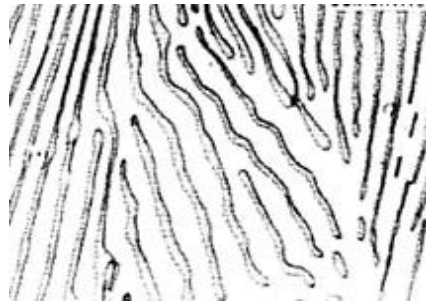
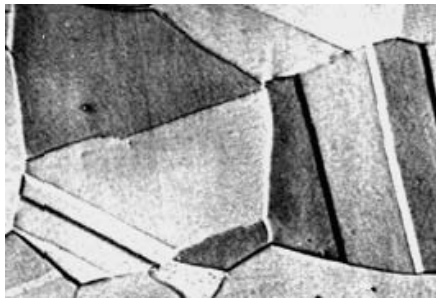
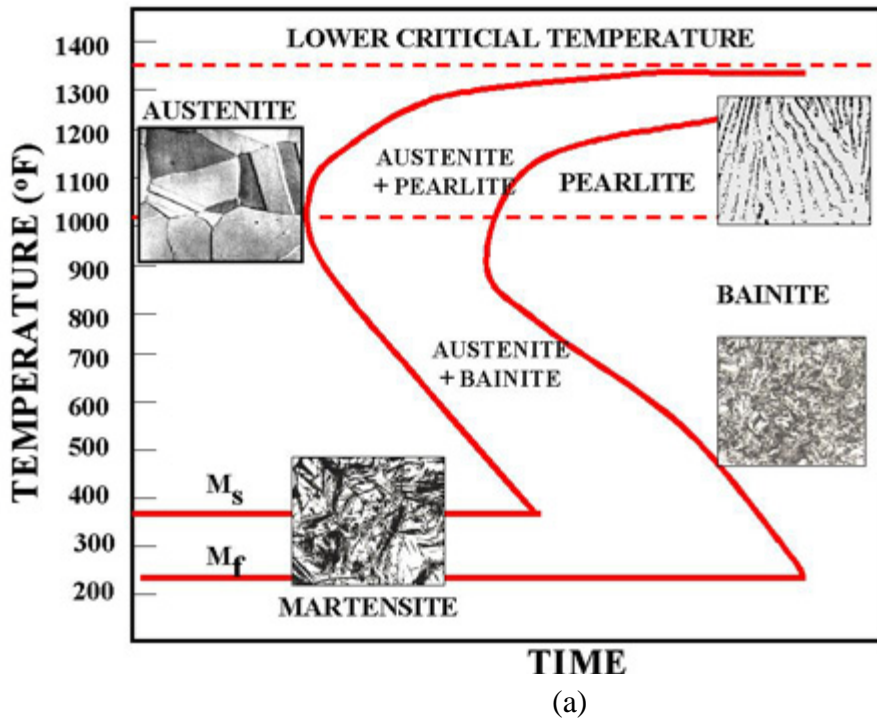


Fig.2.10 (a) TTT Diagram and microstructures obtained by different types of cooling rates, (b) Austenite , (c) Pearlite , (d) Martensite, (e) bainite

### 2.8.1 Bainite

It is a constituent which forms from austenite in a temperature range below  $530^{\circ}\text{C}$  and above  $M_s$  temperature. It forms together with pearlite in steel which are cooled somewhat too fast to form a complete pearlite structure. It is like pearlite a mixture of ferrite and iron carbide but in a different form. The bainite structure varies from a featherlike pattern of lens shaped particles depending on the temperature range of formation. (Featherlike constituent in upper temperature range and lens-like in the lower temperature range). Bainite is harder, stronger than ferrite-pearlite structures at lower temperatures.

There are two kinds of bainite ; upper bainite and lower bainite. Upper bainite is formed between a temperature range of  $300\text{-}540^{\circ}\text{C}$ , which consists of needles of ferrite separated by long cementite particles. Lower bainite is also formed between temperatures range of  $200\text{-}300^{\circ}\text{C}$ , which consists of thin plates of ferrite containing very fine rods or blades of cementite.

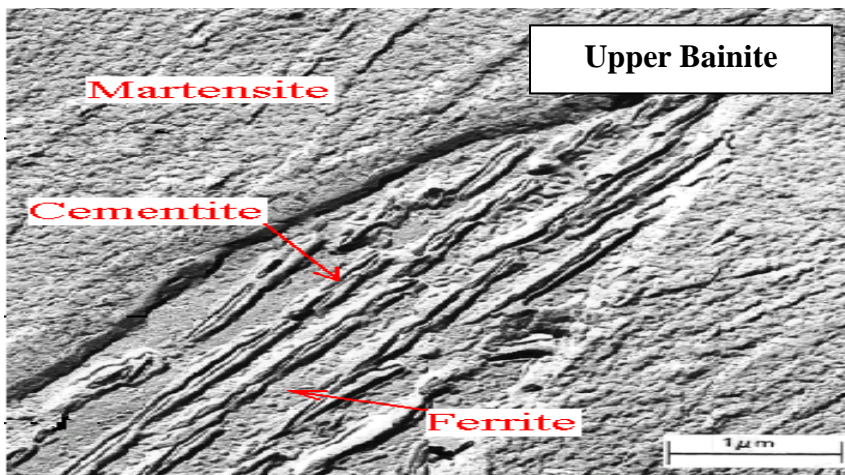


Fig.2.11 Microstructure of upper bainite [44]

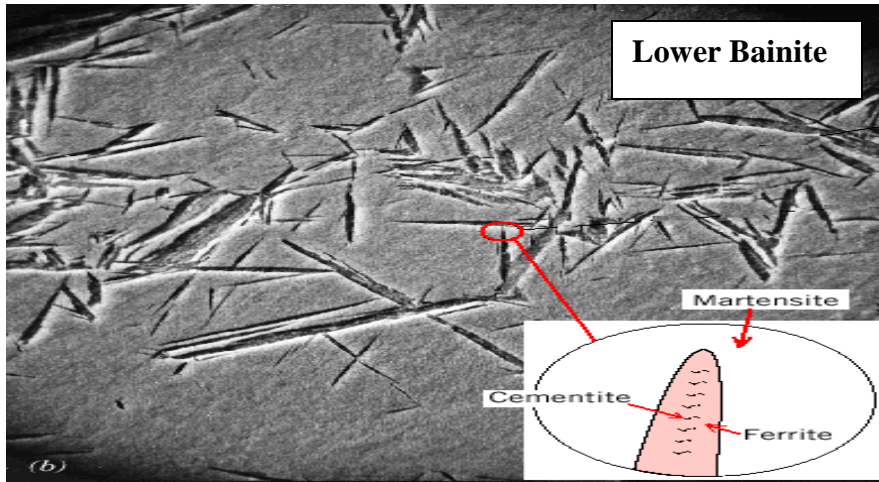


Fig.2.12 Microstructure of lower bainite [44]

### 2.8.2 Martensite

It is named after the German metallurgist Adolf Martens (1850–1914).

The martensite is formed by rapid cooling (quenching) of austenite which traps carbon atoms that do not have time to diffuse out of the crystal structure. This martensitic reaction begins during cooling when the austenite reaches the martensite start temperature ( $M_s$ ) and the parent austenite becomes mechanically unstable. At a constant temperature below  $M_s$ , a fraction of the parent austenite transforms rapidly, and then no further transformation will occur. When the temperature is decreased, more of the austenite transforms to martensite. Finally, when the martensite finish temperature ( $M_f$ ) is reached, the transformation is complete as shown in Fig.2.9 and Fig.2.10.

One of the differences between austenite and martensite is that, martensite has a body centered tetragonal crystal structure, whereas austenite has a face centred cubic (FCC)

structure. The transition between these two structures requires very little thermal activation energy which results in the subtle but rapid rearrangement of atomic positions. Martensite is not shown in the equilibrium phase diagram of the iron-carbon system because it is a metastable phase.

Martensite is so brittle that it needs to be modified for practical applications. This is done by heating it to 250-650 °C for some time known as tempering which produces tempered martensite, an extremely fine-grained and well dispersed cementite grains in a ferrite matrix. Since quenching can be difficult to control, many steels are quenched to produce an overabundance of martensite, and then tempered to gradually reduce its concentration until the right structure for the intended application is achieved. Too much martensite leaves steel brittle, too little leaves it soft. It is the hardest structure formed from austenite. [19, 53].

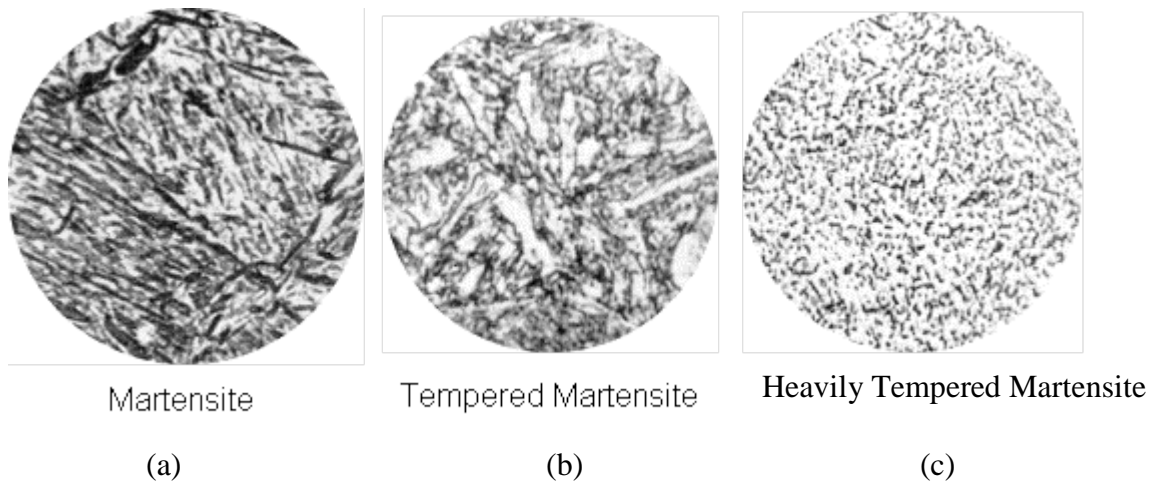


Fig.2.13 Electron microstructure of martensites: (a) Martensite, (b) Tempered Martensite, (c) Heavily Tempered Martensite [45]

### **2.9.1 Mechanical properties of steel**

It is the mechanical properties of a material that reveal its elastic and inelastic behavior when a force is applied thereby indicating its suitability for mechanical applications, e.g. modulus of elasticity, tensile strength, percentage elongation, hardness and fatigue limit. The mechanical properties of steels are almost always requirements of the specification used to purchase the product. For flat rolled products the properties usually specified are tensile strength, yield stress (or proof stress), elongation and Brinell or Rockwell hardness. These properties give a guarantee that the material in question has been correctly produced, and are also used by engineers to calculate the working loads or pressures that the product can safely carry in service. [21]

### **2.9.2 Tensile test**

Tensile properties indicate how the material will react to forces being applied in tension. It measures the force required to pull something such as rope, wire, or a structural beam to the point where it breaks. It is measured in units of force per unit area. In the SI system, the units are Newton per square meter or Pascal. Specially, the tensile strength of a material is the maximum amount of tensile stress that it can be subjected to before failure. The definition of failure can vary according to material type and design methodology. This is an important concept in engineering, especially in the fields of material science, material engineering and structural engineering.

A tensile test is a fundamental mechanical test where a carefully prepared specimen is loaded in a very controlled manner while measuring the applied load and the elongation of the specimen over some distance. Tensile tests are used to determine the tensile

strength, toughness, and modulus of elasticity, elastic limit, elongation, yield point and other tensile properties.

Tensile strength is an intensive property and, consequently, does not depend on the size of the test specimen. However, it is dependent on the preparation of the specimen and the temperature of the test environment and material [21, 22,].

### **2.9.3 Types of mechanical strength**

There are three typical definitions of tensile strength:

- (i) Yield strength : The stress at which a material strain changes from elastic deformation to plastic deformation, causing it to deform permanently.
- (ii) Ultimate strength: The maximum stress a material can withstand when subjected to tension, compression or shearing. It is the maximum stress on the stress-strain curve.
- (iii) Breaking strength: The stress coordinates on the stress-strain curve at the point of rupture.

The various definitions of tensile strength are shown in the following stress-strain graph Fig.2.14. [23].

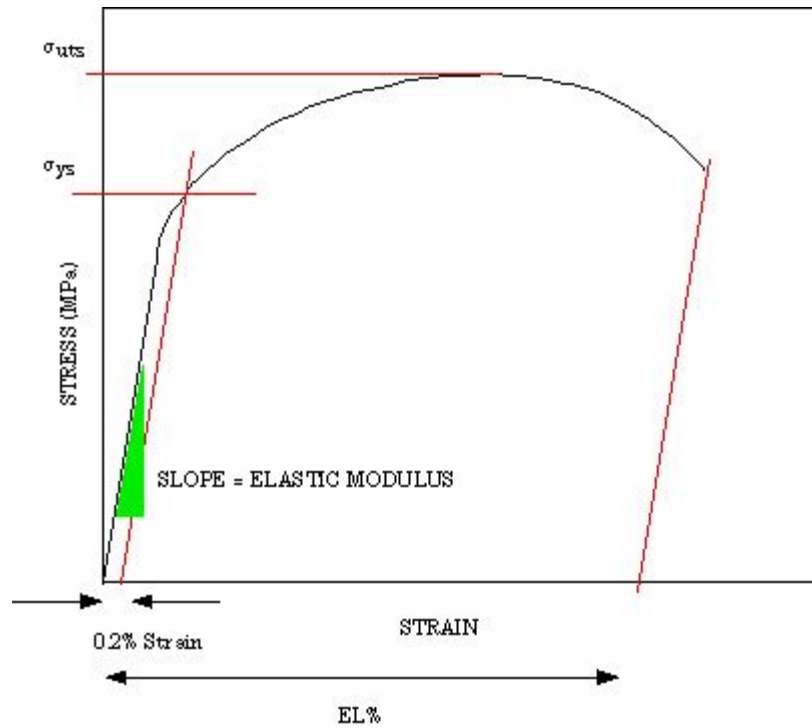


Fig.2.14 Stress-strain curve [24]

Metals including steel have a linear stress-strain relationship up to the yield point, as shown in the Fig.2.14. Up to the yield point the material obeys Hook's law that is the strain in a material under tension is proportional to the applied stress within the elastic limit. In some steels the stress falls after the yield point. This is due to the interaction of carbon atoms and dislocations in the stressed steel. Cold worked and alloy steels do not show this effect. For most metals yield point is not sharply defined. Below the yield strength all deformation is recoverable, and the material will return to its initial shape when the load is removed. This recoverable deformation is known as elastic deformation. For stresses above the yield point the deformation is not recoverable, and the material will not return to its initial shape. This unrecoverable deformation is known as plastic

deformation. For many applications plastic deformation is unacceptable, and the yield strength is used as the design limitation.

After the yield point, steel and many other ductile metals will undergo a period of strain hardening, in which the stress increases again with increasing strain up to the ultimate strength. [24, 25]

After a metal has been loaded to its yield strength it begins to "neck" as the cross-sectional area of the specimen decreases due to plastic flow. When necking becomes substantial, it may cause a reversal of the engineering stress-strain curve, where decreasing stress correlates to increasing strain because of geometric effects. This is because the engineering stress and engineering strain are calculated assuming the original cross-sectional area before necking. If the graph is plotted in terms of true stress and true strain the curve will always slope upwards and never reverse, as true stress is corrected for the decrease in cross-sectional area. Curve B is the true stress – strain curve while curve A is the engineering stress-strain curve as shown in Fig.2.15 below

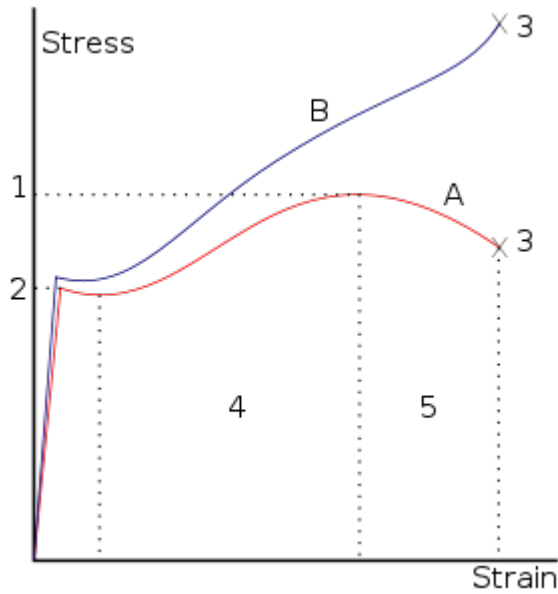


Fig.2.15 Stress vs. Strain curve of typical of structural steel (showing 1:Ultimate strength, 2:Yield strength , 3:Rapture , 4:Strain hardening region , 5:Necking region , A:Apparent stress and B:Actual stress) [23, 26].

Necking is not observed for materials loaded in compression. The peak stress on the engineering stress-strain curve is known as the ultimate strength. After a period of necking, the material will rupture and the stored elastic energy is released as noise and heat. The stress on the material at the time of rupture is known as the breaking strength.

Some metals do not have a well defined yield point. The yield strength is typically defined by the "0.2% offset strain". The yield strength at 0.2% offset is determined by finding the intersection of the stress-strain curve with a line parallel to the initial slope of the curve which intercepts the abscissa at a strain of 0.002 [24,25]

### **2.10.1 Hardness test**

It is defined as resistance of metal to plastic deformation, usually by indentation. However, the term may also refer to stiffness or temper, scratching, abrasion, cutting, resistance to local penetration, machining and yielding. It is the property of a metal, which gives it the ability to resist being permanently deformed (bent, broken, or have its shape changed), when a load is applied. The greater the hardness of the metal, the greater resistance it has to deformation.

The multiplicity of definitions, and corresponding multiplicity of hardness measuring instruments, together with the lack of a fundamental definition, indicates that hardness may not be a fundamental property of a material, but rather a composite of: yield strength, work hardening, true tensile strength, modulus of elasticity, and others [28].

### **2.10.2 Hardness measurement methods**

The three most popular hardness methods are: Brinell hardness test, Rockwell hardness test and Vickers hardness test. The way the three of these hardness tests measure a metal's hardness is to determine the metal's resistance to the penetration of a non-deformable ball or cone. The tests determine either the width or depth of indentation the indenter will make on or into metal, under a given load, within a specific period of time. The Rockwell hardness test is the most used and versatile of the hardness tests. Compared to the other hardness test methods, the Brinell ball makes the deepest and widest indentation, so the test averages the hardness over a wider amount of material, which will more accurately account for multiple grain structures and any irregularities in

the uniformity of the material. This method is the best for achieving the bulk or macro-hardness of a material, particularly those materials with heterogeneous structures. For a extremely hard metals a Brinell tester will substitute a tungsten carbide ball for the steel ball. The hardness number is not really a true property of the material; it is an empirical value that should be seen in conjunction with the experimental methods and the hardness scale used. When doing the hardness tests the distance between indentations must be more than 2.5 indentation diameters apart to avoid interaction between the work-hardened regions. The other hardness testing methods used in today`s technological world are: Knoop and Shore hardness test [29, 51].

In the Rockwell method of hardness testing, the depth of penetration of an indenter under certain arbitrary test conditions is determined. The indenter may either be a steel ball of some specified diameter or a spherical diamond-tipped cone of 120° angle and 0.2 mm tip radius, called Brale. The type of indenter and the test load determine the hardness scale (A, B, C, etc).

The Rockwell hardness tester measure the hardness of metal just like the Brinell tester, but in the Rockwell case, the depth of the impression is measured rather than the diametric area. With the Rockwell tester, the hardness is indicated directly on the scale attached to the machine while for Brinell method the average of the diameter reading is used for calculating the hardness [30, 54].

Hardness conversion between different methods and scales cannot be made mathematically exact for a wide range of materials due to the following reasons.

Different loads, different shape of indenters, homogeneity of specimen, cold working properties and elastic properties all complicate the problem. All tables and charts should be considered as giving approximate equivalents, particularly when converting to a method or scale which is not physically possible for the particular test material and thus cannot be verified [31].

### **2.11.1 Microstructural studies**

The microstructure of steel has a significant effect on the strength of steel. For steel with a certain composition the microstructure can be altered through varying the processing route used. For example, different yield strength can be achieved for a fixed composition at different temperatures. Changing the amount of second phase in a predominantly ferrite microstructure has a pronounced effect on the strength of the steel. In the ferrite-pearlite equilibrium microstructure, the soft phase is the ferrite (mainly iron) while the hard phase is the pearlite because of carbon content [32].

### **2.11.2 Cutting and Mounting Metallic Samples**

The material can be cut using the hacksaw blade which is made of secondary-hardened tool steel. A hacksaw has asymmetrical teeth so that the cutting force needs only to be applied during the forward stroke. The reverse force is only needed to restore the hacksaw into its initial position. Small samples can be difficult to hold safely during grinding and polishing operations, they are therefore mounted inside a polymer block [33].

### **2.11.3 Grinding**

Grinding is done using rotating discs covered with silicon carbide paper and water. There are a number of grades of paper: 180, 240, 400, 600, grains of silicon carbide per square inch. 180 grades therefore represent the coarsest particles and this is the grade to begin the grinding operation. Light pressure is applied at the centre of the sample. Grinding should continue until all the blemishes have been removed; the sample surface is flat, and all the scratches are in a single orientation. The sample is washed in water and the next grade is used; the scratches from the previous grade are turned normal to the rotation direction. This makes it easy to see when the coarser scratches have all been removed. After the final grinding operation on 600 silicon carbide paper, the sample is washed in water followed by alcohol and dried before polishing starts [33].

### **2.11.4 Polishing**

The polishers consist of rotating discs covered with soft cloth impregnated with diamond particles (6 and 1 micron size) and an oily lubricant. The polishing is started with the 6 micron grade and continues until the grinding scratches have been removed. It is of vital importance that the sample is thoroughly cleaned using soapy water, followed by alcohol, and dried before moving onto the final 1 micron stage. Any contamination of the 1 micron polishing disc will make it impossible to achieve a satisfactory polish [33, 34].

### **2.11.5 Etching**

Metallographic etching is the process of revealing microstructural details that would otherwise not be evident on the as-polished sample. It is the operation of revealing microstructural features (grain boundaries, phases, precipitates and other micro-structure constituents) of the polished specimen through selective chemical attack of its surface. Etching is not always required as some features are visible in the as-polished condition such as porosity, cracks and inclusions.

The purpose of etching is two-fold. First grinding and polishing operations produce a highly deformed, thin layer on the surface which is removed chemically during etching. Secondly, the etchant attacks the surface with preference for those sites with the highest energy, leading to surface relief which allows different crystal orientations, grain boundaries, precipitates, phases and defects to be distinguished in reflected light microscopy. There are many tried and tested etchants available but there are mandatory safety issues associated with the preparation and use of all of these. Etching should always be done in stages, beginning with light attack, an examination under the microscope and further etching only if required. If you over etch a sample on the first attempt, then the polishing procedure will have to be repeated.

There are different types of etching such as Electrolytic Etching, Heat tinting or thermal etching and Chemical Etching. The sample is then put under the microscope and the microstructure is observed and interpreted [33, 35].

## **2.12 Determination of elemental composition of the iron rods**

The Energy dispersive X-ray fluorescence technology (ED-XRF) provides one of the simplest, most accurate and most economic analytical methods for the determination of the chemical composition of many types of materials. It is non-destructive and reliable, requires no, or very little sample preparation and is suitable for solid, liquid and powdered samples. It can be used for a wide range of elements. The atoms in the sample material, e.g. metals are excited by X-Rays emitted from an X-Ray tube or radioisotope. For increasing sensitivity the primary excitation radiation can be polarized by using specific targets between the X-Ray tube and the metal sample. For all elements specific X-Ray fluorescence signals emitted by the atoms after the photoelectric ionization are measured simultaneously in a fixed mounted semi-conductor detector or sealed gas-proportional counter. The radiation intensity of each element signal, which is proportional to the concentration of the element in the sample, is calculated internally from a stored set of calibration curves and can be shown directly in concentration units by converting softwares on a computerized screen [46].

The mass spectrometer technique is another method for determining elemental composition of a material, which was employed in this work. Mass spectrometer can determine the elements that are present and their relative quantity in the rod. It is basically an analytical technique for the determination of the elemental composition of a sample which can originate as solids, liquids, solutions or vapor.

The technique of mass spectrometry had its beginnings in J.J. Thomson's vacuum tube. Mass spectrometry was used to discover the existence of isotopes; their relative

abundances, and their "exact masses", i.e., atomic masses with a precision of 1 part in  $10^6$  or better. These important fundamental measurements laid the foundation for later developments in diverse fields ranging from geochronology to biochemical research. Mass spectrometry is now widely used to analyze both organic and inorganic substances. It operates at four different stages [36].

### **Stage 1: Gas phase Ions**

The sample is ionized by knocking one or more electrons off to give a positive ion. This can be done by variety of methods (e.g., by impacting them with an electron beam), which results in the formation of positively charged particles (ions) [37]

### **Stage 2: Acceleration**

The ionized ions are accelerated by the heated filament into the electromagnetic region so that they will all have the same kinetic energy.

### **Stage 3: Deflection**

The ions are then deflected by a magnetic field according to their masses to charge ratio  $m/z$  and the groups of ions are collected by a detector. The lighter they are, the more they are deflected. The amount of deflection also depends on the number of positive charges on the ion - in other words, on how many electrons were knocked off in the first stage. The more the ion is charged, the more it gets deflected.

## Stage 4 Analyzing

A data system records the magnitude of these electrical signals as a function of  $m/z$  and converts this into a mass spectrum—a graph of ion intensity as a function of mass to charge ratio. Mass spectra are often depicted graphically.

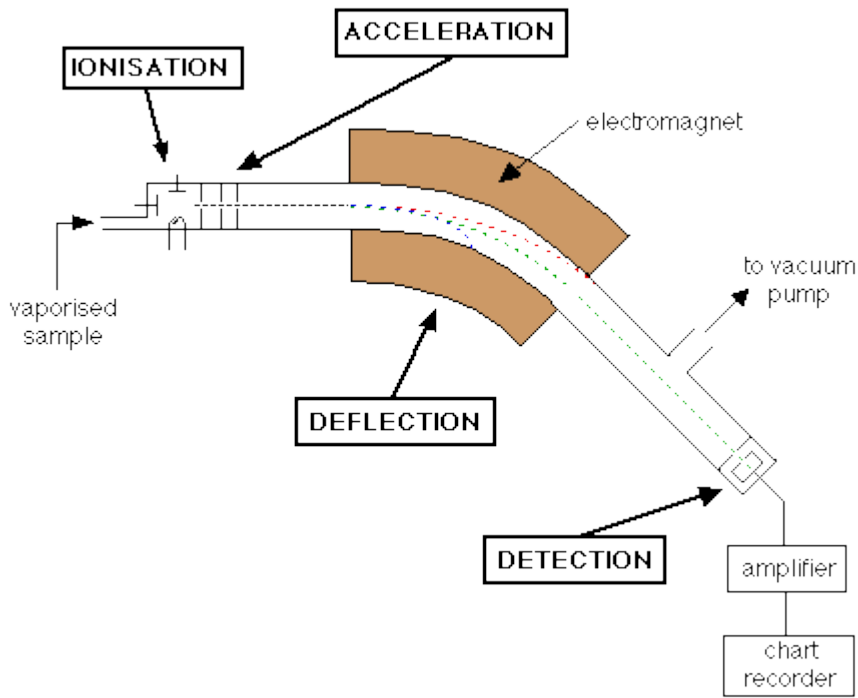


Fig. 2.16 A schematic diagram of internal structure of a mass spectrometer [38, 52].

## **CHAPTER THREE**

### **EXPERIMENTAL DETAILS**

#### **3.1 Introduction**

In this chapter, the procedures used in the characterization of the materials in terms of tensile test, microstructural studies, elemental composition and hardness test are discussed. The rods were cut into pieces with a hacksaw in an alternate order as follow; (0.0254 m) , second (0.4064 m) , followed by another 0.0254 m then another 0.4064 m in that order along the full length of the rod. The 0.0254 m samples were then divided into (0.0127 m), the first 0.0127 m sample were opened up into two along the longitudinal direction and one side was picked for the longitudinal direction microstructure studies while the other half was kept for elemental composition analysis. The other half inch was also used for transverse microstructural studies while the 0.4064 m samples were used for tensile test analysis.

**Table 3.1 Sample codes and their descriptions**

Sample	code
Imported sample from Ukraine*	FU1 , FU2 , FU3 , FU4, FU5 , FU6 , FU7 , FU8 , FU9 and FU10  (Where FU1 stands for the first sample, FU2 the second sample in that order)
Imported sample from Spain*	FS1, FS2, FS3, FS4, FS5, FS6, FS7, FS8, FS9 and FS10  (Where FS1 stands for the first sample, FS2 the second sample in that order)
Locally produced sample from Tema steel Works*	LT1 , LT2 , LT3, LT4, LT5 , LT6, LT7, LT8, LT9, and LT10  (Where LT1 stands for the first sample, LT2 the second sample in that order)
Locally produced sample from Ferro Fabrik*	LF1 , LF2 , LF3, LF4, LF5, LF6, LF7, LF8, F9 and LF10  (Where LF1 stands for the first sample, LF2 the second sample in that order)

\*The rod samples were labeled sequentially from one end to the other

### 3.2.1 Preparation of the specimens for tensile test

The rods of diameter 19 mm and length 40 cm were cut into samples with a hacksaw very slowly to avoid heating up the samples due to friction. The samples were then thoroughly cleaned with a piece of emery cloth to remove clogged up dirt and grease.

The center drill was used to make holes at one end of the samples which were then repositioned in the jaw of the Centre Lathe machine and the mid-portions were then machined to a diameter of 14 mm and an arc was created at the edge of the machined samples to prevent fracturing at the edge. Finally the machined mid-portions of the samples were smoothed with a smooth file and a piece of sand paper to prevent premature necking.

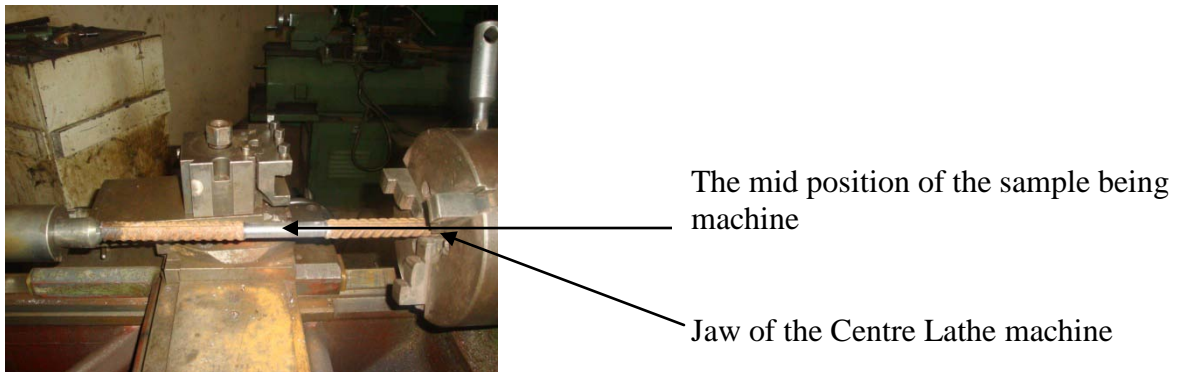


Fig. 3.1 A Picture of the sample in the jaw of the Center Lathe machine



Fig. 3.2 A Picture of the machined samples

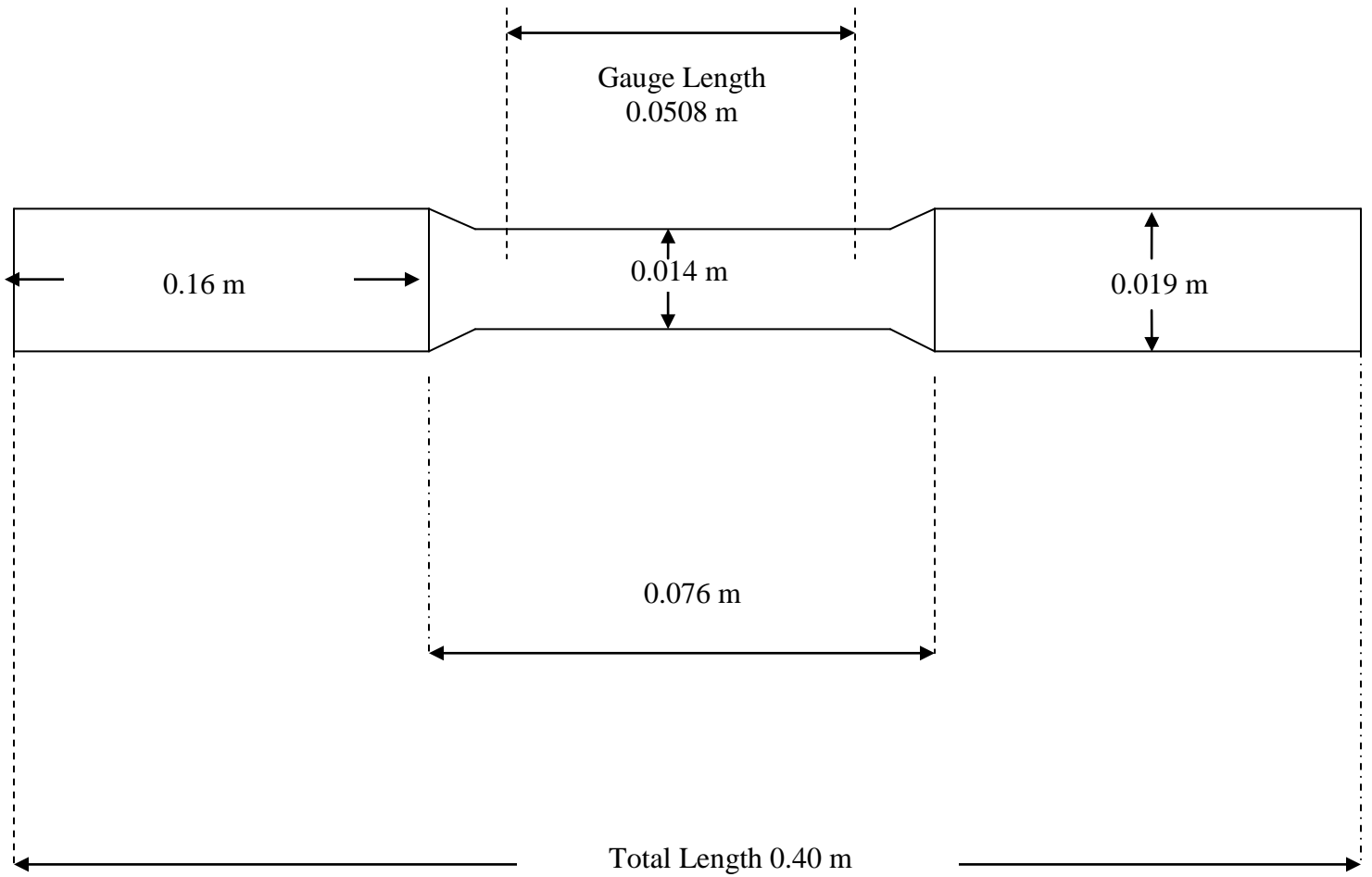


Fig. 3.3 Schematic diagram of a prepared tensile test sample, (not drawn to scale) British Standard [41]

### 3.2.2 Tensile test

1. The sample was position in the jaw of the Avery hydraulic tensile testing machine , as the machined started to stretched the rod readings of loads against extensions were recorded. At the yield point the extensometer was removed to prevent damage. Further readings of load against extension using dividers and calipers at intervals of 0.00127 m increments were recorded. The experiment continued until the specimen fractured and the necking diameter was recorded.

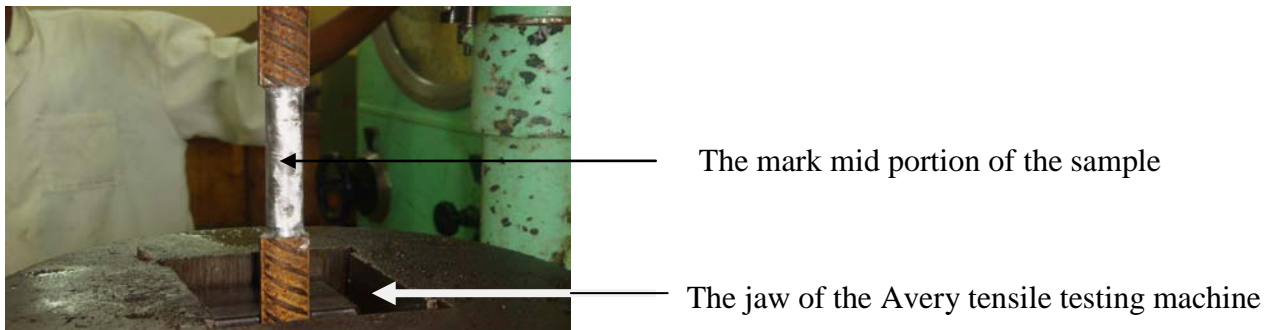


Fig. 3.4 A Picture of the sample in the jaw of the Avery tensile testing machine.

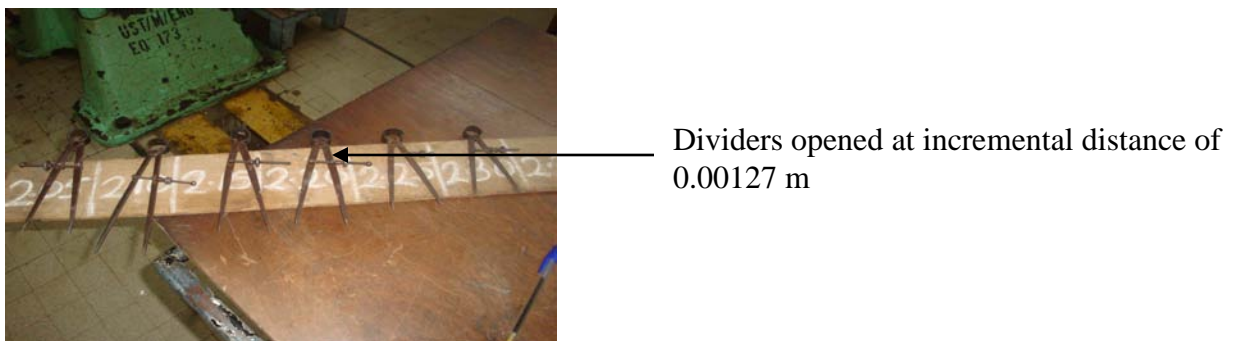


Fig.3.5 A Picture of dividers used at incremental interval of 0.00127 m

### 3.3.1 Preparation of samples for microstructural studies

The samples of height 2.5 cm were ground on different grits of silicon carbide paper from 180, 240, 400, 600 grits (both the transverse and longitudinal cut samples).

Water was poured on the samples regularly every one to two minutes to carry away heat and to enable fast grinding while the sample was turned through an angle of  $90^{\circ}$ , after which they were placed on a rotating wheel covered with emery cloth of grits 1200 while a suspension of alumina powder and water was poured on it at regular interval to carry heat away and to enable fast polishing. The samples were polished to mirror-finished image.

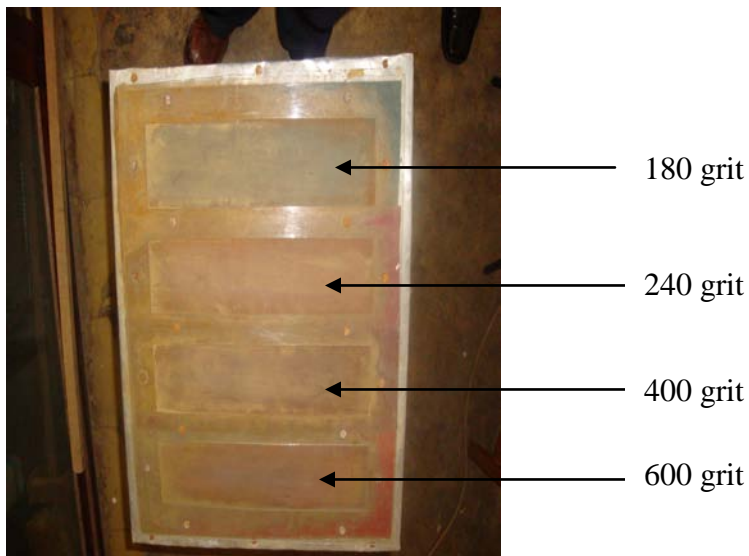


Fig. 3.6 A picture showing the grinding table



Fig. 3.7 A Picture showing a sample being polished on a rotating wheel.

### **3.4 Etching of samples**

- i) 2% (2 vols) Nitric acid was measured and mixed with 98% (98 vols) ethanol with a graduated cylinder in a volumetric flask.
- ii) Three Petri dishes were made available, one with the etchant, the second one with water and the third with ethanol.
- iii) The samples were agitated in the etchant for 40 seconds and quickly wash in water to stop the etchant from attacking more of the phases. Finally they were rinsed in ethanol.
- iv) The hot air blower was used to dry the surface.



Fig. 3.8 A fume chamber for etchant preparation.

### **3.5 Observing the microstructure under the microscope**

- i) The etched sample was placed on a glass slide with plasticine in between.
- ii) The sample is levelled and placed under the microscope.
- iii) The desirable magnification was chosen by selecting one of the objective pieces ( X 500 in this work).
- iv) The focusing was adjusted until a good focus was found by looking into the eye piece.
- v) The image of the microstructure was captured with the help of a computerized system for interpretation.

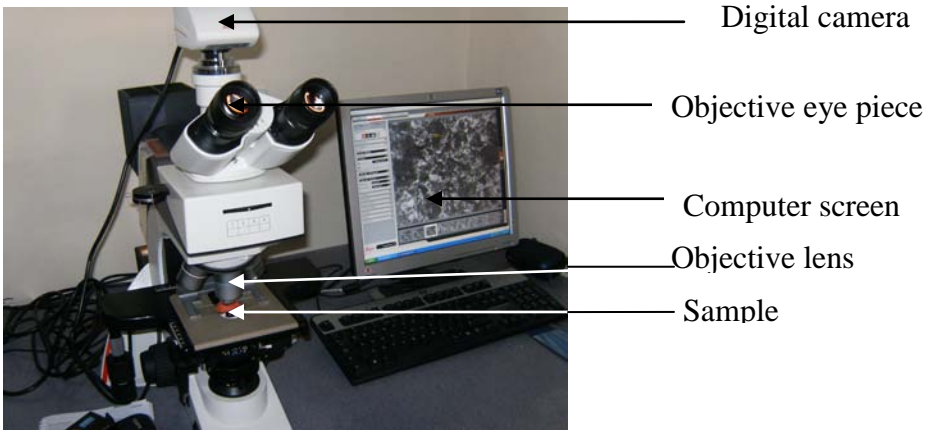


Fig.3.9 A Picture showing a sample mounted on a computerized microscope and its microstructure displayed on the screen

### 3.6 Hardness test

The Brinell hardness test method was used.

First, a standard block from the manufacture of the machine was used to check the accuracy of the machine. The specimen surface was machined flat to provide large surface area for the 10 mm hardened steel ball indenter. The sample was positioned in the machine and the 10 mm diameter hardened steel ball indenter was placed on it and load of 3000 kg was applied for 15 seconds. The diameter of the indentation made on the test material was measured with a low power microscope and the Brinell hardness number was calculated by substituting the diameter measured into equation 3.1.

$$BHN = \frac{F}{\frac{\pi}{2} D * (D - \sqrt{D^2 - D_1^2})} \dots\dots\dots 3.1$$

[55]

Where:  $F$  = Load,  $D$  = The diameter of the steel ball indenter (10 mm) and  $D_1$  = The value of the indentation made by the indenter, (see appendix D, Table1 for the conventional chart)

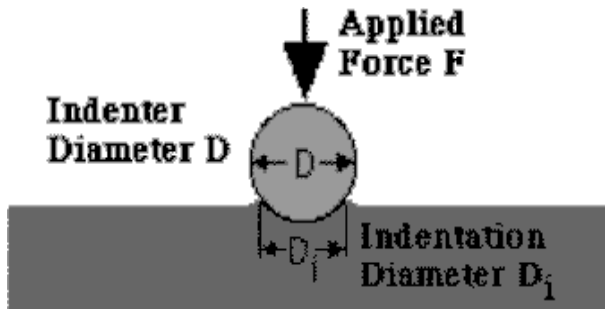


Fig. 3.10 A schematic diagram of a 10 mm steel ball indenter on a test specimen.

A well structured Brinell hardness number reveals the test conditions, and looks like this, "241 BHN 10/3000/30" which means that a Brinell Hardness of 241 was obtained using a 10 mm diameter hardened steel ball with a 3000 kilogram load applied for a period of 30 seconds.

**CHAPTER FOUR**  
**RESULTS AND DISCUSSIONS**

**4.0 Tensile test**

**4.1 Locally produced iron rods**

The stress-strain curve for a particular material provides information on the tensile strength, the Young's modulus, the ultimate tensile strength, percentage elongation, fracture stress as well as the toughness. The various phases present in the microstructure give reason for such mechanical behavior.

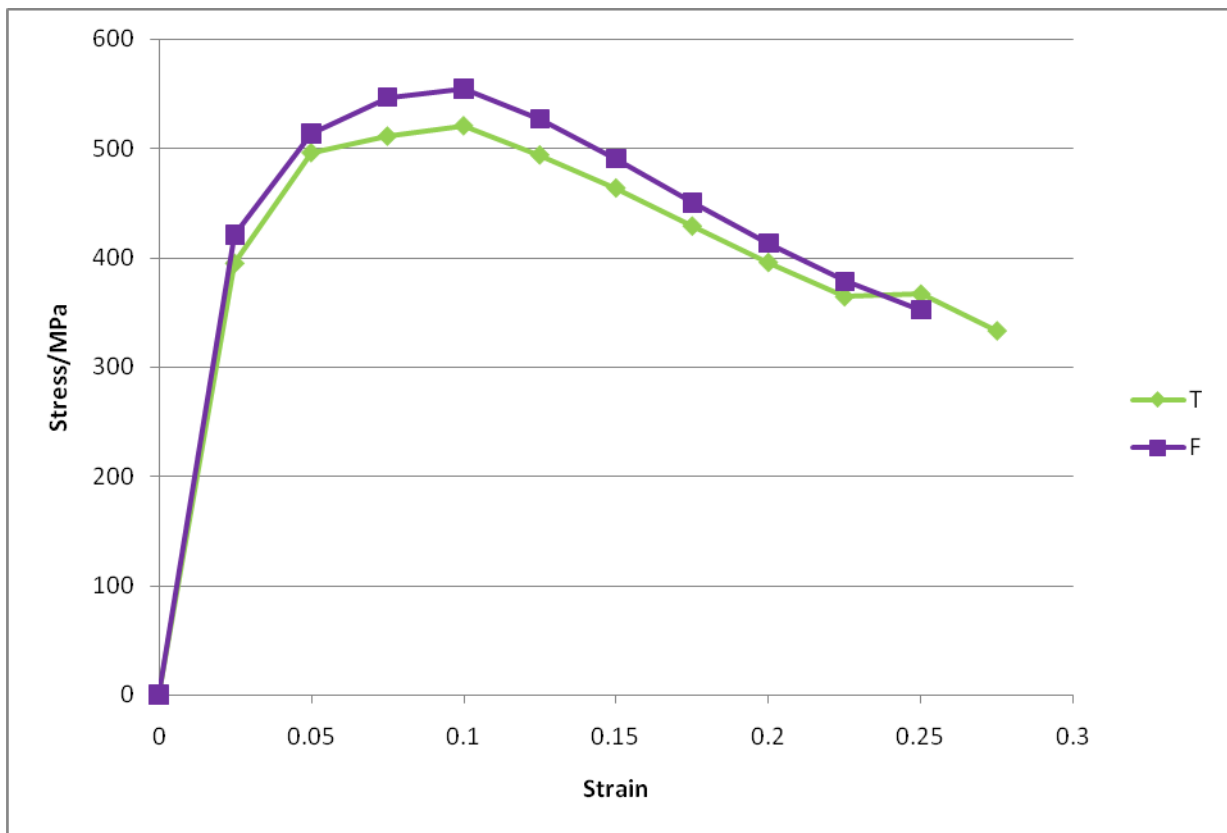


Fig. 4.1 Average Stress-Strain curve of locally produced iron rods (Tema Steel Works [T] and Ferro Fabrik [F])

From Fig.4.1 it can be seen that the initial linear portion of the curves is the proportional limit or elastic limit. This shows that Hooke's law is obeyed, as the strain material being proportional to applied stress, within the elastic limit. This is due to the inter-atomic interaction of carbon atoms and dislocations in the stressed steel. From this portion of the curve, the Young's moduli of elasticity for the Tema Steel Works and Ferro Fabrik rods were  $15.8 \pm 0.4$  GPa and  $16.8 \pm 0.3$  GPa respectively (see appendix C, Table 12 and 16 for details). As the load is increased beyond the elastic limit, the linear behavior ceased giving way to a non-linear trend. In the end the yield point was reached after which the sample underwent a period of strain hardening, in which the stress increased again with the strain up to the ultimate tensile strength as shown in Fig. 4.1. The ultimate tensile strength values were  $520.5 \pm 14.2$  MPa for Tema Steel Works rods and  $550.3 \pm 13.6$  for Ferro Fabrik samples.

Fig.4.1 explained why the Ferro Fabrik rods had higher Young Modulus and Ultimate tensile strength. It can be seen from the graph that Ferro Fabrik samples bore more load than the Tema Steel Works, the fracture stress value for Ferro Fabrik samples were  $374.4 \pm 5.1$  MPa and  $338.5 \pm 7.1$  MPa Tema Steel Works samples. The similarity in the microstructures is the reason for the closeness of the values as can be seen in

Fig.4.2 – 4.5 .The microstructures do not have any distinct grain boundaries because of the processing route used during the production of the rods.

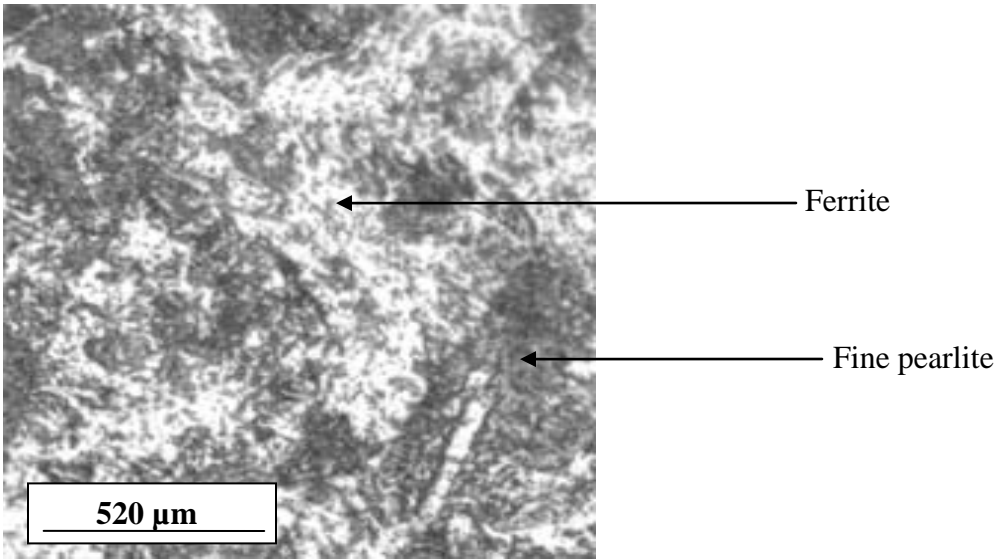


Fig.4.2 Transverse section of Tema steel sample 1

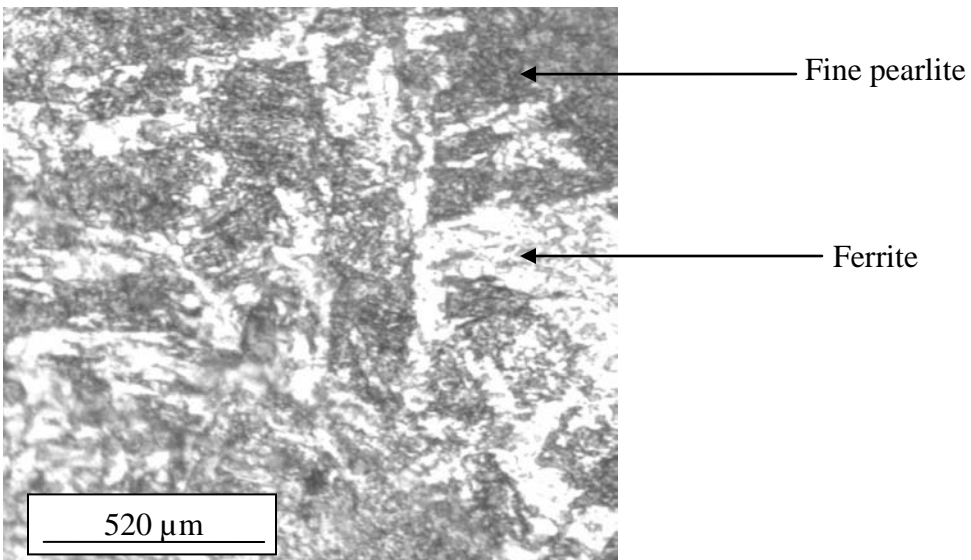


Fig.4.3 Longitudinal section of Tema steel sample 1

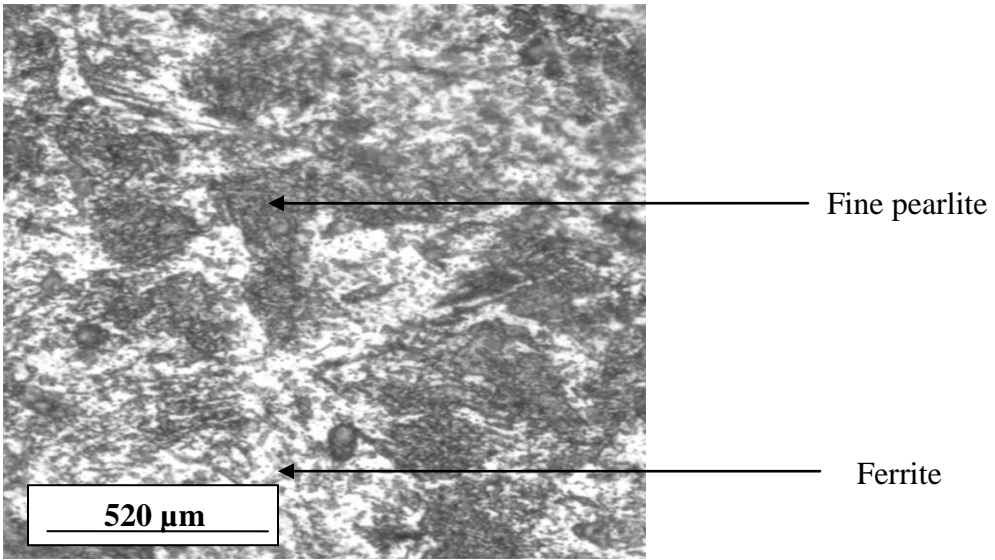


Fig.4.4 Transverse section of Ferro Fabric sample 1

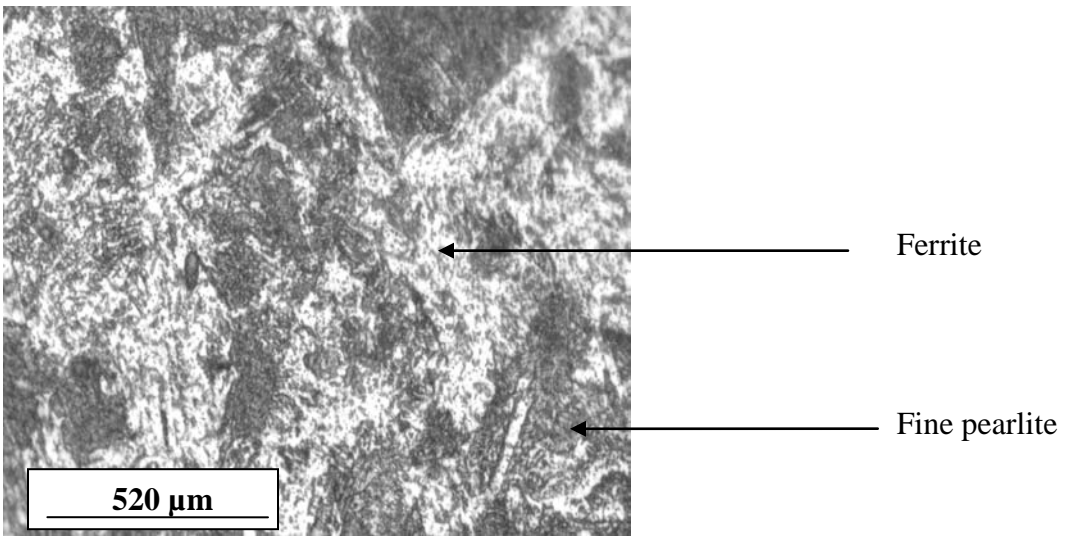


Fig.4.5 Longitudinal section Ferro Fabric sample 1

The local industries used a production process called thermo metallurgical treatment (TMT). It involved rapid cooling of the molten metal from the austenite state to 600-650 °C, before casting the solidified metal into billet, which resulted in the formation of the harder, stronger fine pearlites. The billets were then preheated and pass through a series of circular rollers to produce the desired dimension of the iron rod. The rate at which the steel was cooled through the eutectoid reaction affected the rate at which carbon diffused out of austenite. The fast cooling rate of the local samples from the eutectoid region was a major factor to the formation of the fine pearlite [5]. The microstructure also varied slightly across the whole length of the rod, (see appendix E, Fig.37-72 for details), which showed that the rods were cooled at faster rate which did not allow evenly distribution of the Ferro-alloying elements in the iron.

The elemental analysis in Table 4.1 also explained further why the Ferro Fabrik samples experienced more load than the Tema Steel Works rods. From the table even though the carbon content in the Ferro Fabrik is the lowest, the phosphorus and sulfur content was very high. These elements are undesirable in steel because they cause the material to be hard and brittle hence the ability to bear a higher load before fracture but had poor ductility. The percentage elongation for Ferro Fabrik samples were  $22.8 \pm 0.6$  % and  $25.0 \pm 1.7$ % for Tema Steel Works rods, and their toughness were  $86.5 \pm 3.2$  MJ/m<sup>3</sup> for Ferro Fabrik and  $89.0 \pm 5.2$  MJ/m<sup>3</sup> for Tema Steel Works samples which showed that, the latter is more ductile than the former which is also very evident in Fig.4.1.

**Table 4.1 Elemental composition of iron rods (U – Ukraine, S – Spain, T- Tema steel works, F- Ferro fabric samples respectively)**

SI	Sample Identification	C%	Mn%	Si%	Cr%	P%	S%	Fe%
1	U-1	0.20	0.78	0.03	0.01	0.021	0.019	98.94
2	U-5	0.20	0.78	0.03	0.01	0.022	0.019	98.94
3	U-10	0.20	0.78	0.03	0.01	0.021	0.019	98.94
Average	U	0.20	0.78	0.03	0.01	0.021	0.019	98.94
1	S-1	0.19	0.76	0.03	0.009	0.025	0.033	98.95
2	S-5	0.19	0.77	0.03	0.009	0.026	0.033	98.95
3	S-10	0.19	0.76	0.03	0.009	0.025	0.033	98.95
Average	S	0.19	0.76	0.03	0.009	0.025	0.033	98.95
1	T-1	0.21	0.50	0.15	0.20	0.065	0.039	98.88
2	T-5	0.21	0.50	0.15	0.20	0.065	0.040	98.88
3	T-10	0.22	0.50	0.15	0.21	0.055	0.041	98.86
Average	T	0.21	0.50	0.15	0.20	0.062	0.040	98.88
1	F-1	0.15	0.33	0.28	0.24	0.076	0.045	98.88
2	F-5	0.15	0.33	0.28	0.24	0.077	0.045	98.88
3	F-10	0.15	0.33	0.28	0.24	0.076	0.046	98.88
Average	F	0.15	0.33	0.28	0.24	0.076	0.045	98.88

From the hardness test in Table 4.2, the hardness value for Ferro Fabrik sample were  $258\pm 1$  BHN and  $220\pm 7$  BHN which also explained why the Ferro Fabrik samples bear more load than the Tema Steel Works samples.

All the calculations were done using the convention chart (see appendix D, Table.1 for details), equation 3.1 is used only when the diameter obtain is not found in the convention chart.

Table.4.2. The results of hardness test using Brinell hardness testing method

(U – Ukraine, S – Spain, T- Tema steel works, F- Ferro fabric)

Sample Identification	Diameter of hole (mm)	Brinell Hardness Test (BHN)
U-1	4.65	166
U-5	4.60	170
U-10	4.60	170
<b>U</b>	<b>4.62±0.02</b>	<b>169±1</b>
S-1	4.50	179
S-5	4.40	187
S-10	4.45	183
<b>S</b>	<b>4.45±0.03</b>	<b>183±2</b>
T-1	4.00	239
T-5	4.80	225

T-10	4.50	207
<b>T</b>	<b>4.43±0.23</b>	<b>224±7</b>
F-1	3.65	277
F-5	3.95	235
F-10	3.75	262
<b>F</b>	<b>3.78±0.09</b>	<b>258±1</b>

#### 4.2 Imported iron rods

The stress-strain graphs of the imported iron rods are totally different from those of the local ones as shown in Fig.4.6. This is due to the different mode of production which can be seen clearly in the microstructures in Fig.4.7 – 4.10 and appendix E, Fig.1-36. The microstructures indicated that the rods were cooled at a slow rate which enabled ferrite-pearlite formation. The grains were directed in the rolling direction. The average grain sizes for the Ukraine samples were 213  $\mu\text{m}$  and 237  $\mu\text{m}$  for Spain samples. Due to the similarity in the two microstructures their mechanical property are virtually the same. The Young's Modulus for Ukraine rods were  $11.0\pm 0.6$  and  $10.8\pm 0.1$  for the Spain samples (see Appendix C, Table 4 and 8 for details). The ultimate tensile strength for Ukraine rods were  $456.7\pm 12.4$  MPa and  $453.6\pm 32.7$  MPa for Spain samples. Ukraine samples had fracture stress value of  $247.1\pm 27.7$  MPa while Spain rods had  $225.9\pm 10.3$  MPa. The percentage elongations for the rods were  $30.1\pm 0.1\%$  and  $30.0\pm 0.4\%$  for Ukraine and Spain respectively.

The elemental analysis in Table 4.1 explained further why the two imported samples had almost the same mechanical properties, since their elemental composition are almost the same. The property of steel depends mainly on the Ferro-alloying constituents and the temperatures involved in the production process. Observing the microstructures in Fig.4.7 – 4.10 and appendix E, Fig.1-36, it can be said that the same technology is used to produce the imported samples. The stress-strain curve in Fig.4.6 indicated that the mechanical property of Ukraine and Spain rod were similar.

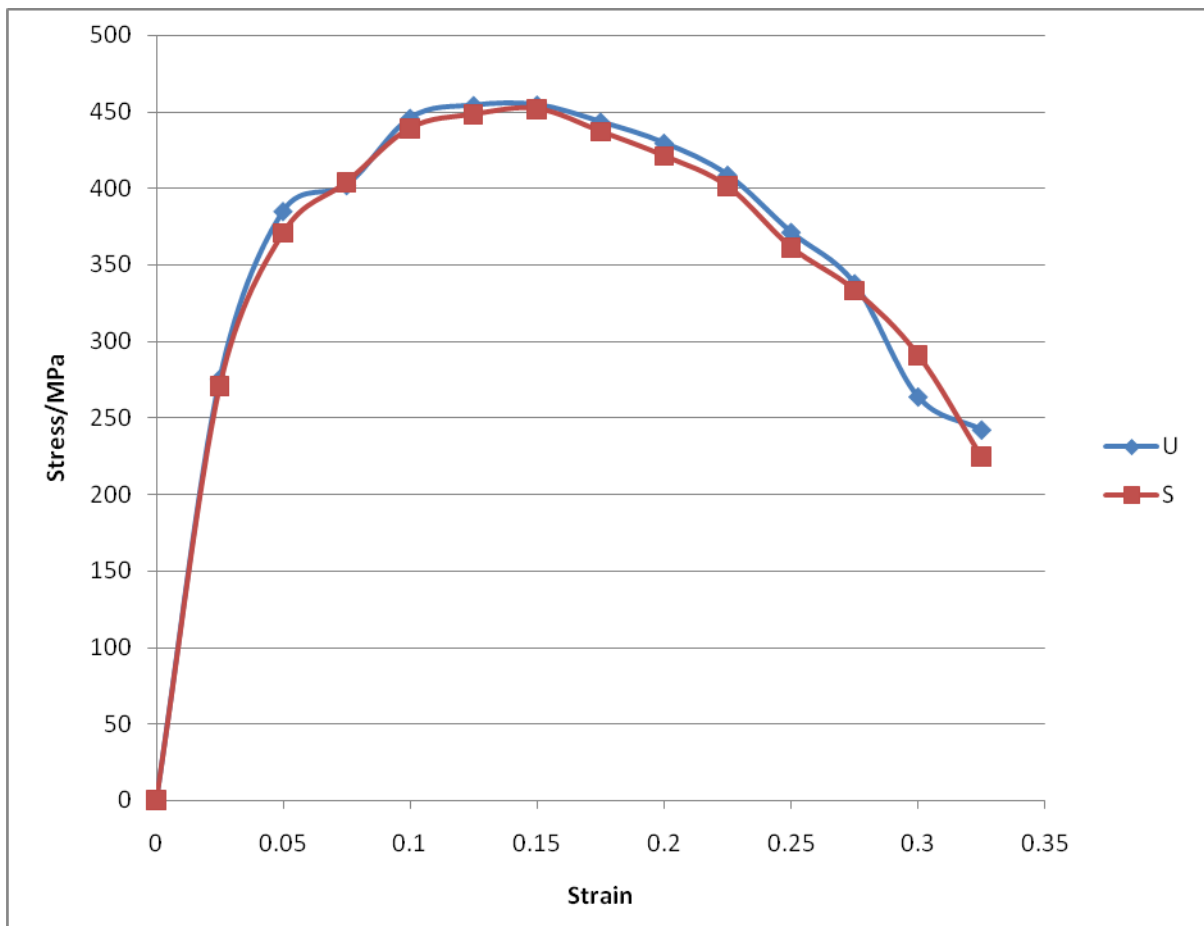


Fig. 4.6 Stress-Strain curve for imported iron rods (Ukraine [U] and Spain [S])

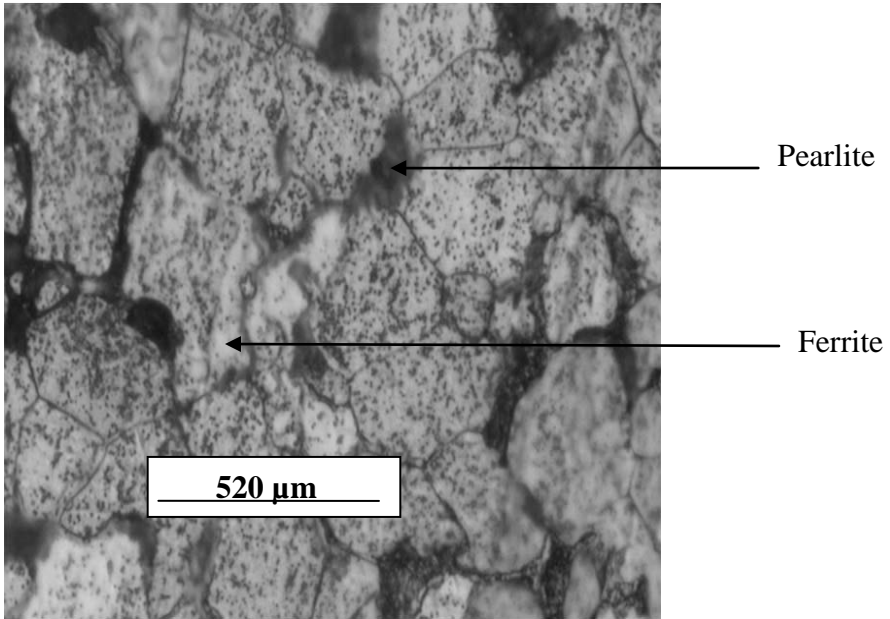


Fig.4.7 Transverse section of Ukraine sample 1

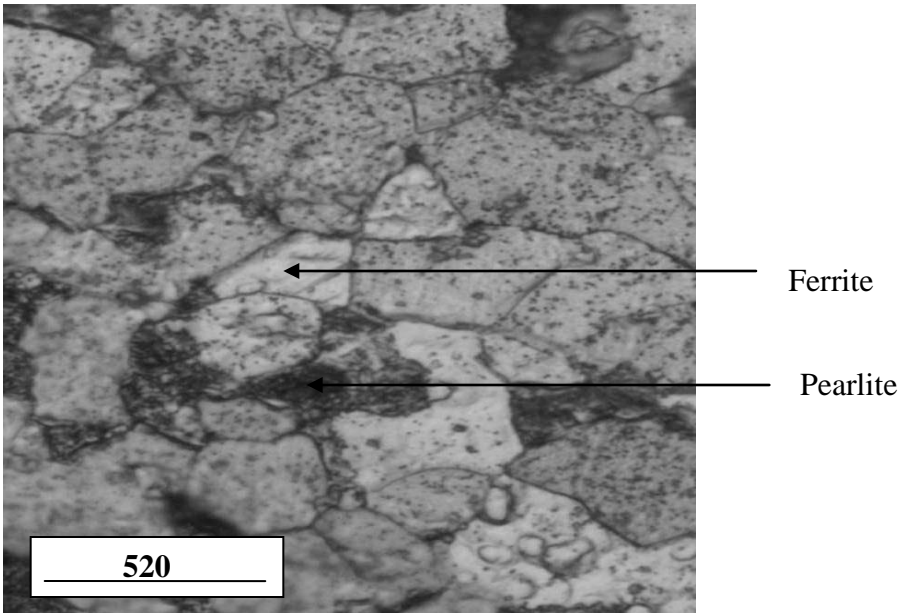


Fig.4.8 Longitudinal section of Ukraine sample 1

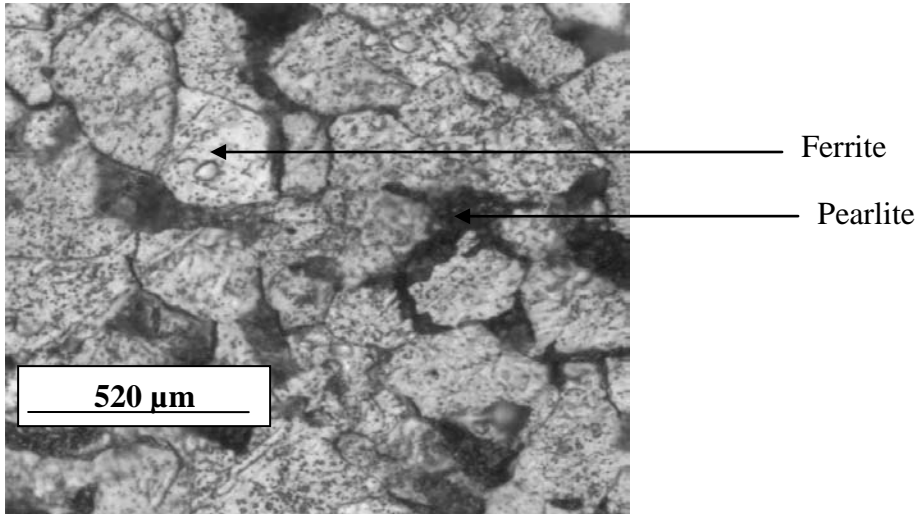


Fig.4.9 Transverse section of Spain sample 1

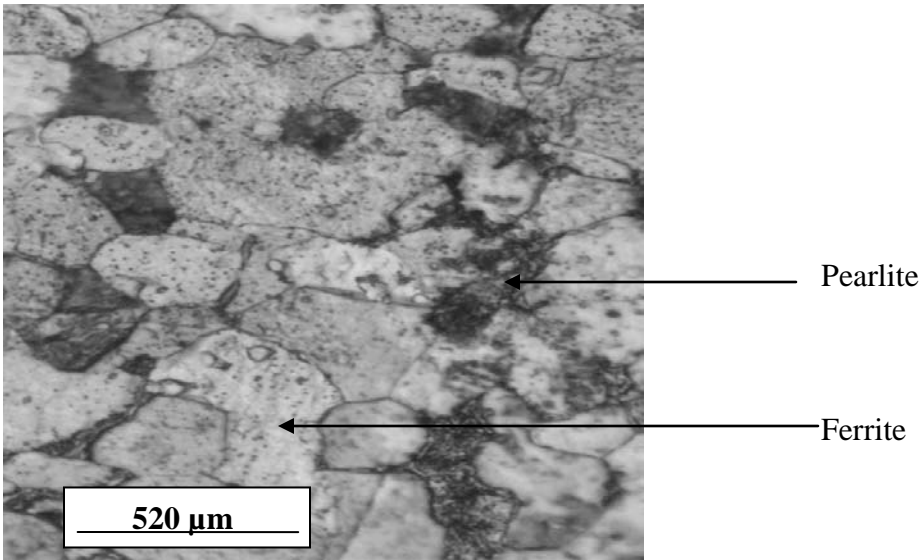


Fig.4.10 Longitudinal section of Spain sample 1

### 4.3 Comparison between locally produced iron rods and imported rods

#### 4.3.1 Mechanical properties

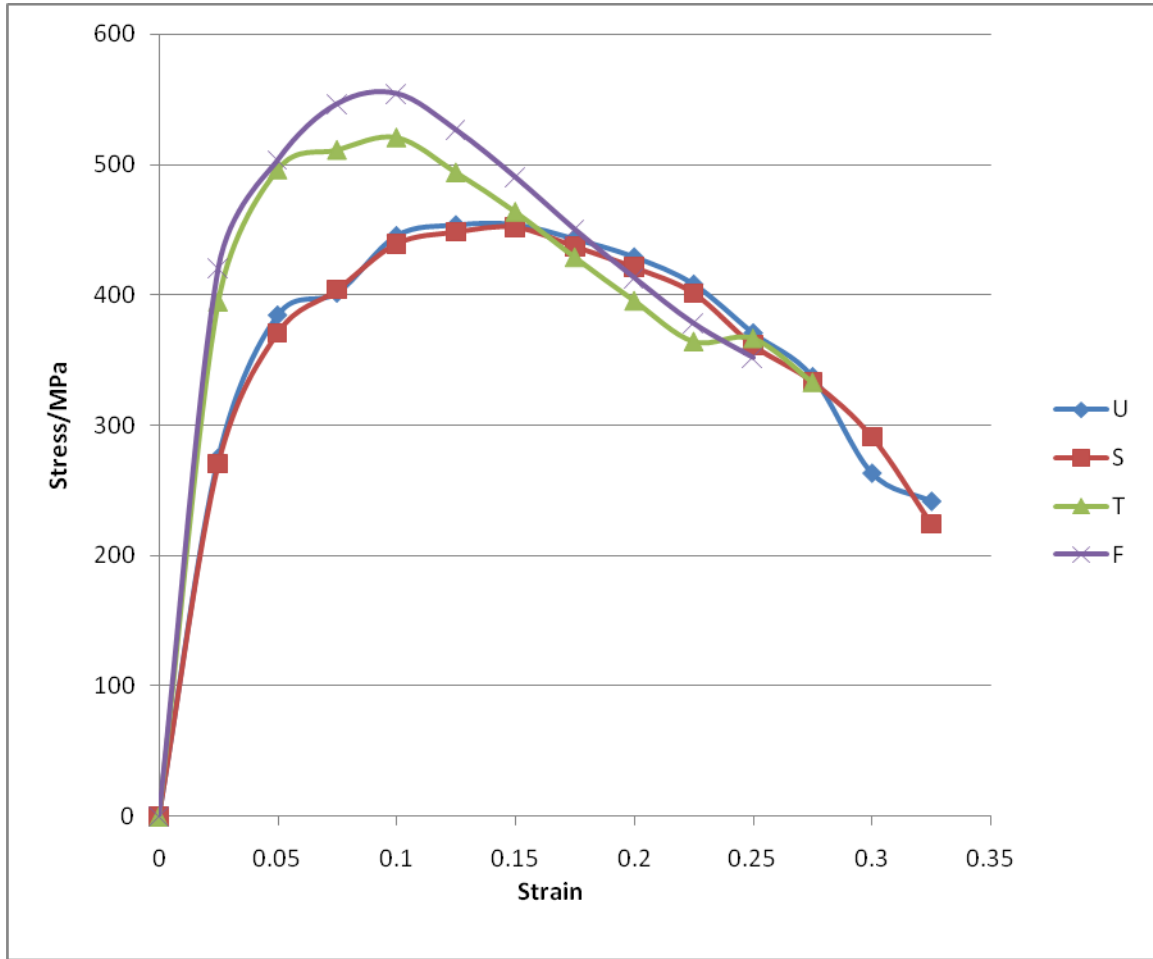


Fig. 4.11 Average Stress-Strain curve for imported and locally produced iron rods (Ukraine [U], Spain [S], Tema Steel Works [T], Ferro Fabrik [F])

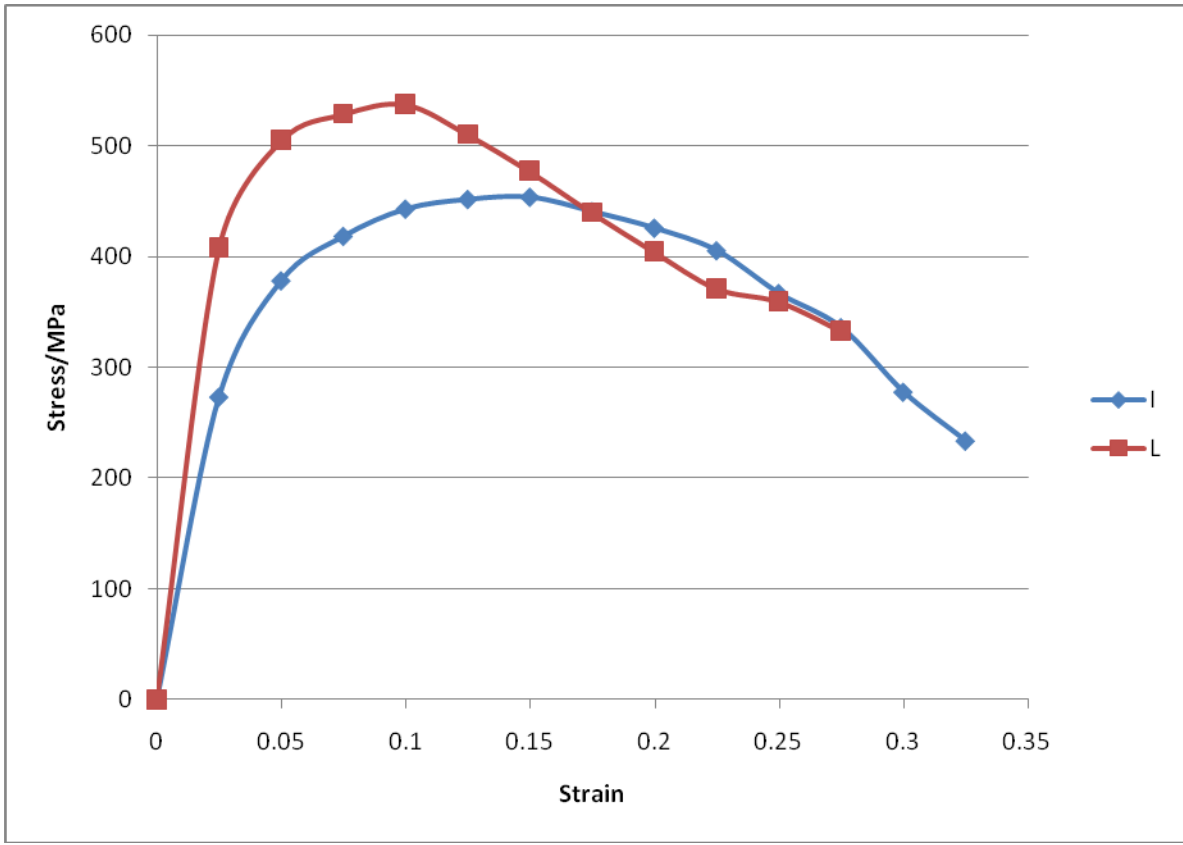


Fig.4.12 Average Stress-Strain curves for the imported (I) and locally produced (L) iron rods.

From the stress-strain curve in Fig. 4.12 the average Young Moduli for the locally produced iron rods and the imported rods were  $16.30 \pm 0.35$  GPa and  $10.92 \pm 0.51$  GPa respectively (see appendix C table 4, 8, 12 and 16, for the details of the calculated values). The bar chart in Fig.4.15 also shows that the local iron rods have a higher Young's Moduli values than the imported samples. These values indicate that the locally produced iron rods develop a greater ability to recover under a given load or stress compared to the imported iron rods.

Considering the processing route of the local samples which resulted in the formation of harder, stronger fine pearlite microstructure which are more stress resistant to deformation than the ferrite-pearlite microstructure of the imported samples, it explained why the local rods are harder and more brittle than the imported samples hence the higher Young's Modulus value. The high sulfur and phosphorus content (see Table 4.1 for details) also increase the hardinability as a result; the local samples bear a higher load than the imported samples.

The yield point of a material gave a most useful indication of its toughness or strength. The above graphs indicated relatively good strength and toughness for the imported iron rods. Using the trapezium rule to calculate the area under the stress-strain curves the imported samples had an average toughness value of  $101.1 \pm 2.7 \text{ MJ/m}^3$  and the local iron rods had an average value of  $87.7 \pm 4.2 \text{ MJ/m}^3$  which shows that the imported samples were tougher than the local samples as indicated by the bar chat in Fig4.13 (see appendix A for the calculation). The locally produced rods can best be described as being exceptionally strong, evident from the higher elastic limit, as shown in Fig.4.12 .The fracture stress value for the local samples was  $356.4 \pm 6.1 \text{ MPa}$  and  $222.0 \pm 19.0 \text{ MPa}$  for the imported samples (see details of the calculation in Appendix C Table 4, 8, 12, 16), which indicate that the local samples could bear more load before fracture than the imported samples. The imported samples were tougher because of the mode of production and the higher content of manganese (see Table 4.1 for details) which main function in steel is to make the material ductile (toughness) [5].

With an increase in load beyond the yield point as shown in Fig.4.11 and 4.12 (and Appendix B, Fig. 1 – 4), the test specimens slowly stretched to a point at which the cross-section would support no additional load. The maximum stress, provided information on the highest stress the metal could withstand, i.e. the maximum load a particular sample could carry before undergoing fracture. The locally produced steel had an average ultimate tensile strength value of  $535.4 \pm 13.9$  MPa and  $455.1 \pm 22.5$  MPa for imported samples, (see Appendix C, Table.4, 8, 12 and 16 for the details). The locally produced iron rod yielded quickly to reach its maximum stress as indicated by Fig.4.12 but showed a shorter total extension before fracture, which shows that the local samples were hard and brittle as the results of the thermo metallurgical treatment (TMT) . The imported samples extended further than local rods even under a less applied load. This is obvious from the stress-strain curves in Fig.4.11 and 4.12, as the stress decreased gradually to the point where the sample fractured.

Since percentage elongation is a measure of the material's ductility and thus, its toughness, it can be seen from Fig.4.11 and 4.12 (see Appendix B, Fig. 1 – 4 for more details) that the imported samples were tougher. In fact, the locally produced sample had an average value of  $23.9 \pm 1.1$  % elongation while that of the imported sample iron rods were  $30.0 \pm 0.2$  % elongation as shown by the bar charts in Fig.4.14 and 4.15 (see details in Appendix C, table. 4, 8, 12 and 16). The imported samples were ductile and had a higher percentage elongation because of the route of production and manganese content. The local samples were hard and brittle because of the processing route used and the high quantity of the phosphorus and sulfur content.

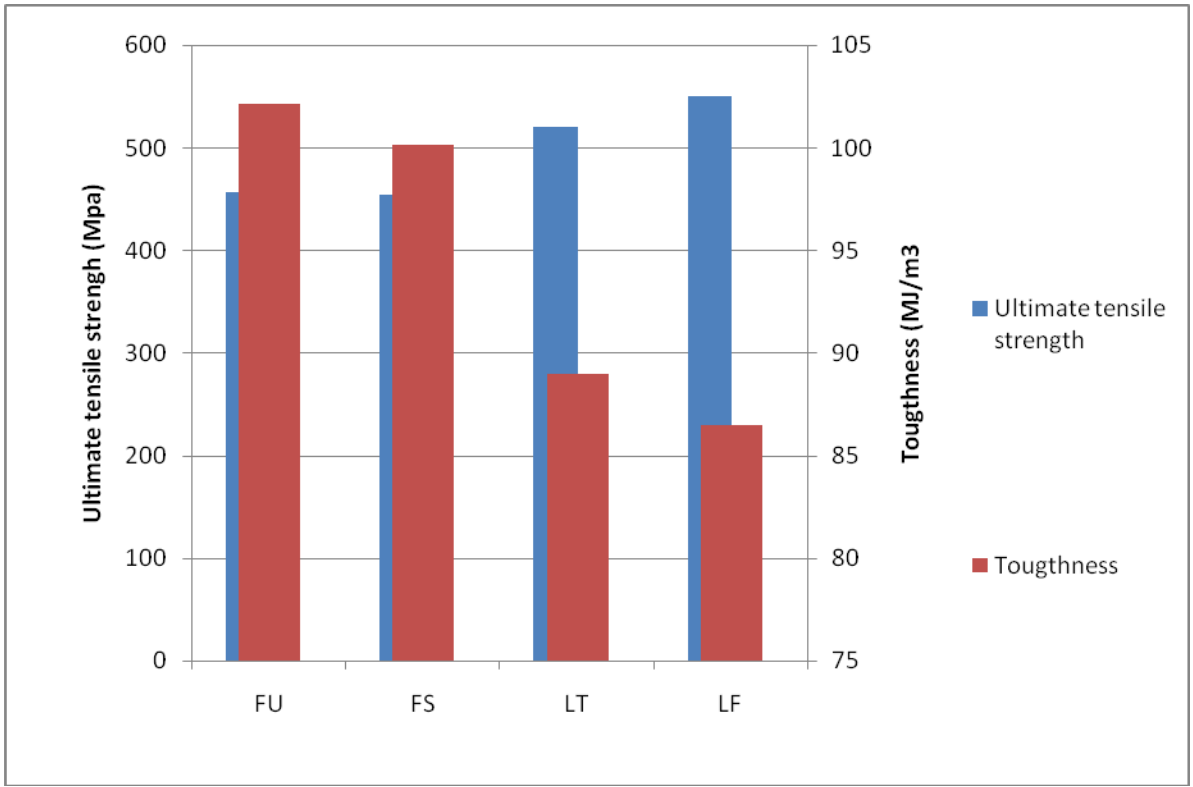


Fig. 4.13 Comparing the Ultimate tensile strength and Toughness of locally produced and imported iron rods.

Observing Fig.4.13 shows that if a metal is tough it does not necessary have a high ultimate tensile strength. A material may not be tough but can bear a lot of load before fracture. Since toughness means the ability of a material to absorb energy and not the amount of load it can bear. The imported samples were tougher and more ductile than the local samples while the local samples had a higher ultimate tensile strength.

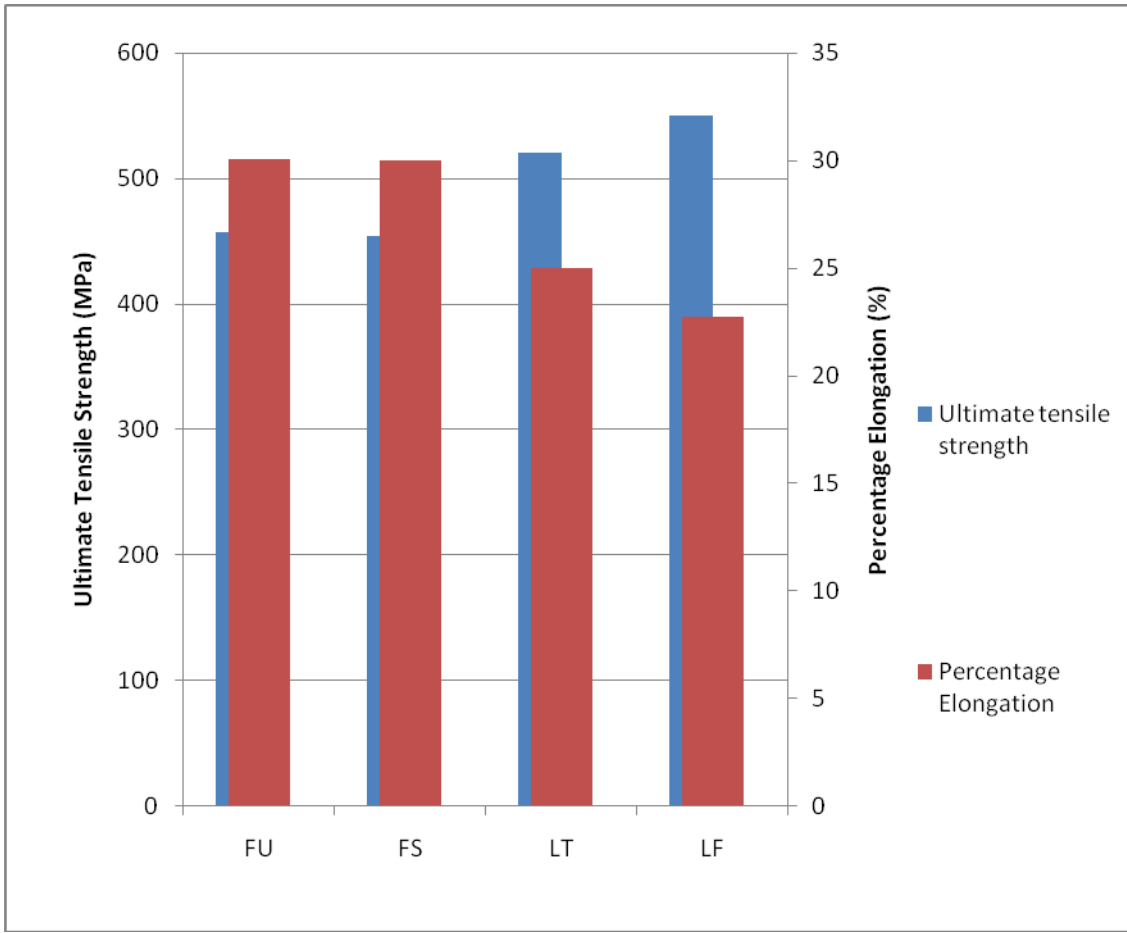


Fig. 4.14 Comparing the Ultimate tensile strength and Percentage elongation of locally produced and imported iron rods

Fig. 4.14 shows that a metal with a high ultimate tensile strength does not necessarily have a good ductility or a good plastic deformation. The local samples can bear more loads but cannot extend more than the imported samples before fracturing because of the harder, stronger fine pearlite microstructure which does not undergo dislocation easily as compared to the ferrite-pearlite microstructure of the imported samples. It is evident that

the imported samples are more ductile than the local ones due to the ferrite-pearlite microstructure.

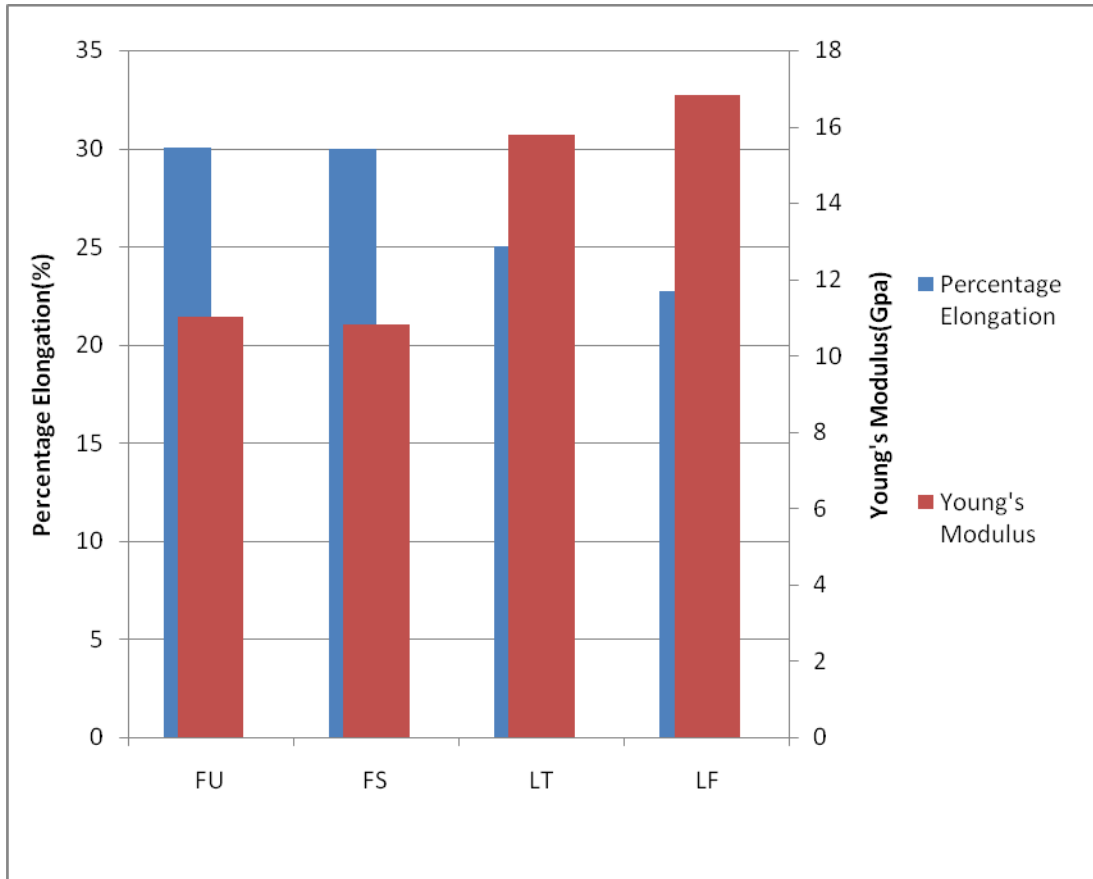


Fig. 4.15 Comparing the Young's modulus and Percentage elongation of locally produced and imported iron rods

Fig. 4.15 shows that, the local samples can bear more loads before fracture as compare with the imported samples. Young's modulus which is stress divided by strain just shows the resistance of the atoms in the structure to plastic deformation.

From the hardness test results in Table.4.2, the imported samples had an average hardness value of  $176\pm 2$  BHN and the local sample  $239\pm 9$  BHN which shows that the local samples were harder while the imported samples were more ductile. It also shows that, the method of production used by the local companies does not allow evenly distribution of the Ferro-alloying elements, because the hardness values obtain along the length of the rods varied more for the local samples than for the imported samples, which did not under go thermo metallurgical treatment. From the elemental composition in Table.4.1 the high level of the impurities (sulfur and phosphorus) also increased the hardness of the local samples. For the imported samples the difference between the hardness values measured along the length of the rod did not vary much like the local samples, which showed that the mode of production allowed sufficient time for the ferro-alloying elements to distribute evenly in to the interstitial position in the iron lattice.

#### **4.3.2 Elemental composition**

From the chemical analysis in Table 4.1, it is obvious that the foreign samples had more preferable tensile properties than the local samples because of their higher manganese content. Manganese major function in steel is to improve the tensile properties such as ductility and toughness, which is within the acceptable range given by Ghana Standard Board (see Table 4.3) [5]. Even tough the Mn content in the local product fell outside the range provided by Ghana Standard Board ,it is not enough to give the rods a good tensile property like ductility and toughness as compared to the imported iron rods. Phosphorous and sulfur are unwanted elements in steel because they eventually form phosphides and sulfides which are harmful to the toughness of the steel. Phosphorus normally induces

fast cooling rate which make the steel non-homogenous. Hence it is desirable to keep these elements less than 0.05% as stated by Ghana Standard Board. But the phosphorus level of the locally produced samples were above the acceptable level by 52% in the Ferro-Fabric steel and for Tema steel works is above it by 24%.

The phosphorus has actually increased the brittleness of the locally produced samples. This shows that local manufactures do not remove all the slag with the impurities. For good steel production the molten metal should be slag three times [5]. Increasing the quantity of manganese in the local samples would have solved the problem, but this would increase the cost of production considerably, (e.g. At the time of carrying out the project work, each of the imported iron rod cost GH¢ 51 while the local ones cost GH¢ 30). To avoid a high cost of production and make the rods affordable to the target market a different technology called Thermo Metallurgical Treatment (TMT) was used. It is rapid cooling of the molten metal before casting begins which would compensate for the right amount of manganese content and give a metallurgical property close to the normal procedure of adding the right amount of manganese [5]. From the elemental analysis and the manufacturing route used it was clear why the local samples were brittle and harder while the imported samples were ductile having more desirable tensile properties than the local samples.

The Ukraine samples were more ductile than the Spain samples because of its higher manganese content and lower phosphorus and sulfur levels. For the local samples even though the quantity of carbon in Ferro Fabrik sample was very minimum, its phosphorus content was too high as compared to the acceptable range given by Ghana Standard Board which is one of the reasons why it was very brittle and hard. The chemistry of the local samples was not fine tuned. The chemical compositions of the foreign samples agreed more with what was provided by Ghana Standard Board than the local samples.

Table 4.3 Approved elemental composition of mild steel from Ghana Standard Board (GS 788-2:2008, Building and construction materials – steel for reinforcement of concrete – part 2: Ribbed bars)

Elements	%
C	$\leq 0.25$
Mn	$\leq 1.65$
Si	$\leq 0.60$
P	$\leq 0.05$
S	$\leq 0.05$
N	$\leq 0.012$

#### 4.4 Grains size Calculation

The grain size of an alloy influence a number of its physical and mechanical properties. The mean linear intercept method is used to calculate the grain size of the imported iron rods, which is the average length of a line segment that crosses a number of grains. The mean linear intercept length is determined by laying a number of randomly placed test lines on the microstructure and counting the number of times the test line segment overlays one grain. One is counted each time the test line overlays a grain and half when the end of the test line falls in a grain (See appendix A for details).

Mathematically it is represented as

$$\bar{L} = \frac{L_T}{P} \dots\dots\dots 4.1$$

[56]

Where  $\bar{L}$  is the mean linear intercept value,  $L_T$  is the total length of the test line and  $P$  is the number of grains the test line overlays. The total length of the test line was 1560  $\mu\text{m}$ . Twenty test lines were overlaid on the microstructure and the average was used in the calculation. The grain size for Ukraine samples were  $223.1 \pm 0.2 \mu\text{m}$  along the transverse section and  $203.1 \pm 0.1 \mu\text{m}$  along the longitudinal section. The size of the grains for Spain samples were  $240.2 \pm 0.3 \mu\text{m}$  and  $233.4 \pm 0.2 \mu\text{m}$  along the transverse and longitudinal sections respectively.

## CHAPTER FIVE

### CONCLUSIONS AND RECOMMENDATIONS

#### 6.1 Conclusions

The research on metallurgical studies of locally produced and imported iron rods on Ghanaian market has the following conclusions.

1. The locally produced iron rods are very hard and brittle. This hardness property of the rod made it possible to withstand more load but fractured quickly just after the yield strength because of its brittleness. The local samples had average hardness value of  $239 \pm 9$  BHN while the imported samples had a value of  $176 \pm 2$  BHN.
2. The locally produced samples are very stiff, that is, they had a high resistance to deformation. This was clearly demonstrated by the high value of Young's modulus. The local samples had a Young's modulus value of  $16.3 \pm 0.4$  GPa while the imported samples had an average value of  $10.9 \pm 0.5$  GPa.
3. The locally produced iron rods had a higher tensile strength than the imported iron rods. The average tensile strength for the local samples was  $535.4 \pm 13.9$  MPa and the imported iron rods had a value of  $455.1 \pm 22.5$  MPa. The average fracture stress value for the local samples was  $356.4 \pm 6.1$  MPa and  $222.0 \pm 19.0$  MPa for the imported samples. The local samples would bear a lot of load before fractured at a lower strain than the imported samples.

4. The imported samples were tougher and more ductile than the locally produced samples. From the area under the stress-strain curve calculations, using the trapezium rule the imported samples had an average toughness of  $101.1 \pm 2.7 \text{ MJ/m}^3$  and  $87.7 \pm 4.2 \text{ MJ/m}^3$  for the local samples. From the percentage elongation, which is a sign of ductility and toughness, the imported samples had an average value of  $30.0 \pm 0.2 \%$  while the locally produced iron rods had an average value of  $23.9 \pm 1.1 \%$ .

5. The strength and toughness of a material are two opposite variables. Thus an increase in the strength of a material leads to a decrease in the toughness. The locally produced iron rods were relatively stronger but were less tough than the imported iron rods.

6. It would be almost impossible to produce very good iron rods with good tensile properties like ductility and toughness without manganese as demonstrated in the imported samples.

7. The hardness of iron rods does not only depend on the carbon content alone but other Ferro-alloy elements like phosphorus and sulfur which are not needed in steel as shown by the locally produced iron rods especially the Ferro Fabric samples.

8. Varying the processing route in steel production would greatly change the microstructure and the mechanical property as shown for the locally produced samples and the imported samples.

### **6.3 Recommendations**

1. A large data should be collected from the same producer over a period of time e.g one year to observe the consistency in the production process.
2. Ghana Standard Board should make sure, acceptable value range given by them is strictly observed by all the local producers.
3. Ghana Standard Board should give more specific values of the mechanical properties such as tensile strength, modulus of elasticity, percentage elongation etc which are good for each type of constructional work in the county.

## REFERENCES

[1] R.A. Higgins, Engineering Metallurgy, sixth edition (1993), Wiley and Sons, Inc., page 140-149.

[2] SubsTech. Substances & Technologies. Steel making (introduction)  
[http://www.substech.com/dokuwiki/doku.php?id=steel\\_making\\_introduction](http://www.substech.com/dokuwiki/doku.php?id=steel_making_introduction)  
[accessed 2008 ,Novemer 16]

[3] D.-H. Choi; C. Miki; R. Plank; C. Roeder. (2010) *International Journal of Steel Structures*, Journal no. 13296

[4] History of metal. A short history of metals by Alan W. Cramb. Department of materials science and engineering. Cambridge Mellon University  
<http://neon.mems.cmu.edu/cramb/Processing/history.html>  
[accessed 2008 ,October 15]

[5] Tema Steel Works company limited (Factory workers).  
[accessed 2009 November]

[6] Wikipedia. Blast furnace. [http://en.wikipedai.org/wiki/Blast furnace](http://en.wikipedai.org/wiki/Blast_furnace)  
[accessed 2008, October 12]

[7] AWS(American Welding Society) Specifications and Standards  
American Welding Society (2008). Amer Welding Society

[8] Ancient metallurgy. A beginner's guide.  
<http://weber.ucsd.edu/~dkjordan/arch/metallurgy.html>  
[accessed 2008 ,October 15]

[9] Classic encyclopedia. Concrete (Material)  
[http://www.1911encyclopedia.org/Concrete\\_\(Material\)](http://www.1911encyclopedia.org/Concrete_(Material))  
[accessed 2008 ,October 12]

[10] History of metal. A short history of metals by Alan W. Cramb. Department of Materials Science and Engineering. Cambridge Mellon University  
<http://neon.memsc.cmu.edu/cramb/Processing/history.html>  
[accessed 2008 ,October 15]

[11] Iron chemistry. Some chemistry of iron.  
<http://wwwchem.uwimona.edu.jm/courses/iron.html>  
[accessed 2008, October 12]

[12] Classic encyclopedia. Concrete (Material)  
[http://www.1911encyclopedia.org/Concrete\\_\(Material\)](http://www.1911encyclopedia.org/Concrete_(Material))  
[accessed 2008, October 12]

[13] American welding society. The ABCs of steel metallurgy.  
<http://www.aws.org/w/a/wj/2003/02/031/index.html>  
[accessed 2008 ,October 12]

[14] W. Alexander and S. Arthur , Metals in the Service of Man , Ninth Edition , Penguin Books Ltd, 27 Wrights Lane London, 1989, p.2-4 , p.111 – 112, p.131-135.

[15] (Literature.pdf). Literature review.  
<http://dspace.unimap.edu.my/bitstream/1123456789/13273151/Literature%20review.pdf>  
[accessed 2008 ,October 18]

[16] Wikipedia. High-strength low-alloy steel.  
[http://en.wikipedia.org/wiki/High-strength\\_low-alloy\\_steel](http://en.wikipedia.org/wiki/High-strength_low-alloy_steel)  
[accessed 2008 ,October 18]

[17] Substech, Substances & Technologies: Iron-carbon phase diagram.  
[http://www.substech.com/dokuwiki/doku.php?id=iron-carbon\\_phase\\_diagram](http://www.substech.com/dokuwiki/doku.php?id=iron-carbon_phase_diagram)  
[accessed 2008 ,November 18]

[18] Plain Iron Carbon steels. Phase diagram.  
[http://www.roymech.co.uk/Useful\\_Tables/Matter/Phase\\_diagram.html](http://www.roymech.co.uk/Useful_Tables/Matter/Phase_diagram.html)  
[accessed 2008, November 16]

[19] C.A. Wart and R.T. Robb ,Materials Science and Engineering Series, Second Edition, McGraw-Hill Book company , 1970, p.85-87.

[20] W.Hayden , W.G. Moffatt and J.Wulff, Mechanical Behavior , Second Editon , John Wiley and Sons , Inc., 1965, p.143-146.

[21] Wipedia. Structural material. [http://en.wikipedia.org/wiki/Structural\\_material](http://en.wikipedia.org/wiki/Structural_material)  
[accessed 2008 ,November 18]

[22] E.C.Rollason, Metallurgy for Engineers, Forth Edition, McGraw-Hill Book Company, (1973), pages 152-155.

[23] Wipedia. Tensile strength. [http://en.wikipedia.org/wiki/Tensile\\_strength](http://en.wikipedia.org/wiki/Tensile_strength)  
[accessed 2008 ,November 18]

[24] Tensile testing of steel. MY3200 Tensile Testing Fall 2002.  
<http://www.mse.mtu.edu/casting/my3200/lab2/tt.html>

[25] W.H. Bowes,L.T. Russel and G.T. Suter, Mechanics of Enginnering Matrials , Third Edition , John Wiley and Sons , Inc. , 1984, p.47-49 , p.50-55.

[26] P.E. Ferdinand and E. R. Johnston , Jr. , Mechanics of Materials , second Edition , McGraw-Hill , Inc., 1992, p.42-47.

[27] The Metallurgy of Carbon Steel. <http://www.gowelding.com/met/carbon.htm>  
[accessed 2008, November 25]

[28] Surface Engineering forum. The brinell hardness test.  
<http://www.gordonengland.co.uk/hardness/brinell.htm>  
[accessed 2009 ,November 20]

[29] Hardness. Material Hardness.  
[http://www.calce.umd.edu/general/Facilities/Hardness\\_ad\\_.htm](http://www.calce.umd.edu/general/Facilities/Hardness_ad_.htm)  
[accessed 2009, November 20]

- [30] Wikipedia. Vickers hardness test.  
[http://en.wikipedia.org/wiki/Vickers\\_hardness\\_test](http://en.wikipedia.org/wiki/Vickers_hardness_test)  
[accessed 2009 ,November 20]
- [31] Wikipedia. Brinell Scale. [http://en.wikipedia.org/wiki/Brinell\\_scale](http://en.wikipedia.org/wiki/Brinell_scale)  
[accessd 2009 November 20]
- [32] Matter. SteelMatter. <http://www.matter.org.uk/steelmatter/>  
[accessed 2008, November 25]
- [33] Metallograghy by H.K.D.H Bhadeshia. An introduction to sample preparation for metallography. University of Cambridge  
<http://www.msm.cam.ac.uk/phasetrans/abstracts/CP1b.html>  
[accessed 2008, December 2]
- [34] Metallurgy. Microstructure  
[http://www.msm.cam.ac.uk/phase-trans/2008/Steel\\_Microstructure/SM.html](http://www.msm.cam.ac.uk/phase-trans/2008/Steel_Microstructure/SM.html)  
[accessed 2009 December 2]
- [35] SubTech. Substances & Technologies.Etching metallographic specimens  
[http://www.substech.com/dokuwiki/doku.php?id=etching\\_metallographic\\_specimens](http://www.substech.com/dokuwiki/doku.php?id=etching_metallographic_specimens)  
[accessed 2008, November 25]
- [36] AMDs Analytical Technology. About mass spectrometer.  
<http://www.mdssciex.com/products/about%20mass%20spectrometry/default.asp?s=1>  
[accessed 2009 November 20]
- [37] Wikipedia. Mass spectrometer. [http://en.wikipedia.org/wiki/Mass\\_spectrometry](http://en.wikipedia.org/wiki/Mass_spectrometry)  
[accessed 2009, November 20]
- [38] The mass spectrometer. How mass spectrometer works.  
<http://www.chemguide.co.uk/analysis/masspec/howitworks.html>  
[accessed 2009, November 20]

[40]. R.G Meadows, Technician Physical Science 1, First Edition, Press Limited Southampton. Great Britain, 1977, p. 2 – 6.

[41]. Schematic diagram of a prepared tensile test sample, (not drawn to scale) British Standard, College of Engineering, Mechanical Engineering, Materials Testing Laboratory, KNUST, Kumasi.

[42] Wikipedia. Metallurgy.  
[http://en.wikipedia.org/wiki/Iron\\_Metallurgy\\_in\\_Africa](http://en.wikipedia.org/wiki/Iron_Metallurgy_in_Africa)  
[accessed 2010 ,January 26]

[43] Africa Sourece  
<http://www.africaresource.com/rasta/sesostris-the-great-the-egyptian-hercules/african-metallurgy-by-nordine-aka-storm/>  
[accessed 2010, January 26]

[44] Eutectoid Steel.pdf. <http://web.utk.edu/~prack/MSE%20300/FeC.pdf>  
[accessed 2010 , January 26]

[45] Martensite. <http://en.wikipedia.org/wiki/Martensite>  
[accessed 2010 , January 26]

[46] Working principle of an EDXRF spectrometer.  
<http://en.wikipedia.org/wiki/EDXRFspectrometer/>  
[accessed 2010, January 26]

[47] Scott, D., (1991). Metallography and Microstructure of Ancient and Historic Metals. Archetype Books.

[48] Rolf, E. (2006). Understanding Materials Science: History, Properties, and Applications. *American Journal of Physics*, 74(6): 559-569

[49] Ishii, K. (2000). Advanced Pulverized Coal Injection Technology and Blast Furnace Operation. Pergamon Title

[50] World Stem Cell Summit 2010. Nature Materials contents: August 2009 Volume 8 Number 8 pp611-689

[51] Samuel R., (2007). Rockwell Hardness of Metallic Materials (SP 960-5). Materials Science and Engineering Laboratory. ASTM-International

[52] Raymond E., Todd, J., (2010). Practical Aspects of Trapped Ion Mass Spectrometry, Theory and Instrumentation

[53] Howard E. Boyer (2007). Practical Heat Treating (06518G) American Society for metals

[54] Low, S., Fink, J. (2006). Effects of Steel and Tungsten Carbide Ball Indenters on Rockwell Hardness Measurements. *Journal of Testing and Evaluation*, 34(3): 187

[55] Wrilreus, S. R. (1942). Hardness and hardness measurements, Cleveland: American Society of Metals, p. 167-762.

[56] Caruta. B.M (2010). Ceramics And Composite Materials: New Research Nova Science Publishers.

## APPENDICES

### APPENDIX A

#### Calculations

##### For a particular local sample (LF1)

$$\text{Young's Modulus} = \frac{\text{change in stress}}{\text{Change in strain}} = \frac{443.8 - 0}{0.025 - 0} = 17.75 \text{ GPa}$$

$$\% \text{ Elongation} = \frac{\text{Final length} - \text{Initial length}}{\text{Original length}} = \frac{(0.06223 - 0.0508)}{0.0508} = 22.50 \%$$

$$\text{Ultimate tensile stress} = \frac{\text{Maximum Load}}{\text{Initial Area}} = \frac{12116.5 \times 9.81}{1.98057 \times 10^{-4}} = 600.10 \text{ MPa}$$

$$\text{Fracture stress} = \frac{\text{Load at fracture}}{\text{Initial Area}} = \frac{7738.1 \times 9.81}{1.98057 \times 10^{-4}} = 383.30 \text{ MPa}$$

##### Calculating toughness by trapezium rule for (LF1, data collected from Table. 15)

$$\int_{x_0}^{x_n} f(x) dx = \frac{1}{2} h [(y_0 + y_n) + 2(y_1 + y_2 + \dots + y_{n-1})]$$

Since the original interval was split up into n smaller intervals, then h is given by:

$$h = (x_n - x_0)/n$$

$$\begin{aligned} \text{Area} &= [(0.225-0.025)/9] \times (443.8/2 + 564.8 + 595.5 + 600.1 + 542.7 + 559.8 + 504.3 + \\ &443.8 + 383.3/2) \\ &= 93.87\text{MJ/m}^3 \end{aligned}$$

This was how the trapezium rule was used to calculate the toughness for all the other samples.

### **Error calculations**

It was calculated using the inbuilt formula in Microsoft Excel. The data for the error calculation were imported into excel and the error values were calculated by excel. The inbuilt formula use the following procedures

The standard deviation of a data sample can be calculated using the root-mean-square (RMS) deviation of its values from the mean:

If one sample e.g. (FL1) takes on  $N$  values  $x_1, \dots, x_N$  which are real numbers then its standard deviation  $\sigma$  can be calculated as follows:

1. Find the mean,  $\bar{x}$ , of the values.
2. For each value  $x_i$  calculate its deviation  $(x_i - \bar{x})$  from the mean.
3. Calculate the squares of these deviations.
4. Find the mean of the squared deviations which is the variance  $\sigma^2$ .
5. Take the square root of the variance.

This calculation is described by the following formula:

$$\sigma = \sqrt{\frac{1}{N} \sum_{i=1}^N (x_i - \bar{x})^2},$$

Where  $\bar{x}$  is the arithmetic mean of the values  $x_i$ , defined as:

## Calculating the error values for LF1

### 1. Young's Modulus error for LF1

Arithmetic Mean ( $\bar{x}$ ):

$$17.75 + 17.12 + 15.73 + 16.05 + 15.73 + 17.70 + 18.12 + 17.56 + 16.65 + 15.80 = 168.2$$

x	$(x_i - \bar{x})$	$(x_i - \bar{x})^2$
17.75	0.93	0.86
17.12	0.30	0.09
15.73	-1.09	1.19
16.05	-0.77	0.60
15.73	-1.09	1.19
17.70	0.88	0.77
18.12	1.30	1.69
17.56	0.74	0.55
16.65	-0.17	0.03
15.80	-1.02	1.04
		$\sum(x_i - \bar{x})^2 = 8.00$

$$\text{Standard deviation } \sqrt{\frac{1}{10}(8.00)} = 0.89$$

$$\text{Error} = 0.89 / \sqrt{10} = 0.28$$

## 2. Percentage Elongation error for LF1

Arithmetic Mean ( $\bar{x}$ ):

$$22.5 + 25.0 + 25.0 + 20.0 + 25.5 + 25.5 + 25.5 + 25.5 + 20.0 + 25.0 = 22.75$$

<b>x</b>	$(x_i - \bar{x})$	$(x_i - \bar{x})^2$
22.5	-0.25	0.06
25.0	2.25	5.06
25.0	2.25	5.06
20.0	-2.75	7.56
22.5	-0.25	0.06
22.5	-0.25	0.06
22.5	-0.25	0.06
22.5	-0.25	0.06
20.0	-2.75	7.56
25.0	2.25	5.06
		$\sum(x_i - \bar{x})^2 = 30.63$

$$\text{Standard deviation} = \sqrt{\frac{1}{10}(30.63)} = 1.75$$

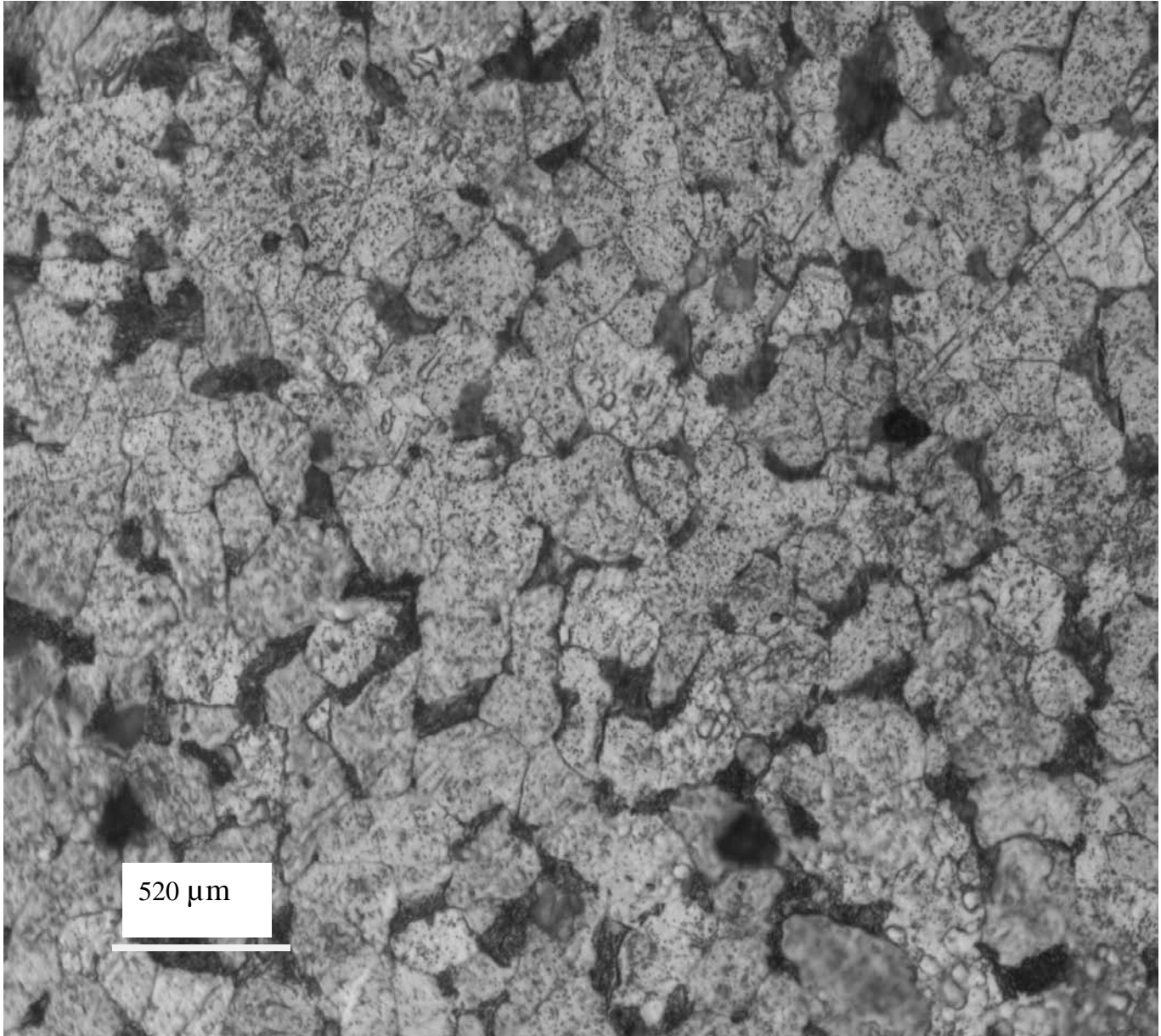
$$\text{Error} = 1.75/\sqrt{10} = 0.55$$

This is how the error values for all the other parameters (Ultimate tensile

Strength/MPa , Fracture Stress/MPa , Toughness/(MJ/m<sup>3</sup>) and the other samples were calculate from excel.

### Calculating of grain size by the mean linear intercept length method

Twenty of the test lines were placed randomly on the microstructure and the grain sizes were determined.



- 1) Calculation of grain size for Ukraine samples along the transverse section

$$\bar{L} = \frac{L_T}{P} = \frac{1560}{7} = 223 \mu\text{m}$$

- 2) Calculation of grain size for Ukraine samples along the longitudinal section

$$\bar{L} = \frac{L_T}{P} = \frac{1560}{7.5} = 208 \mu\text{m}$$

- 3) Calculation of grain size for Spain samples along the transverse section

$$\bar{L} = \frac{L_T}{P} = \frac{1560}{6.5} = 240 \mu\text{m}$$

- 4) Calculation of grain size for Spain samples along the longitudinal section

$$\bar{L} = \frac{L_T}{P} = \frac{1560}{6.7} = 233 \mu\text{m}$$

## APPENDIX B

### Stress Strain curves for imported and locally produced iron rods

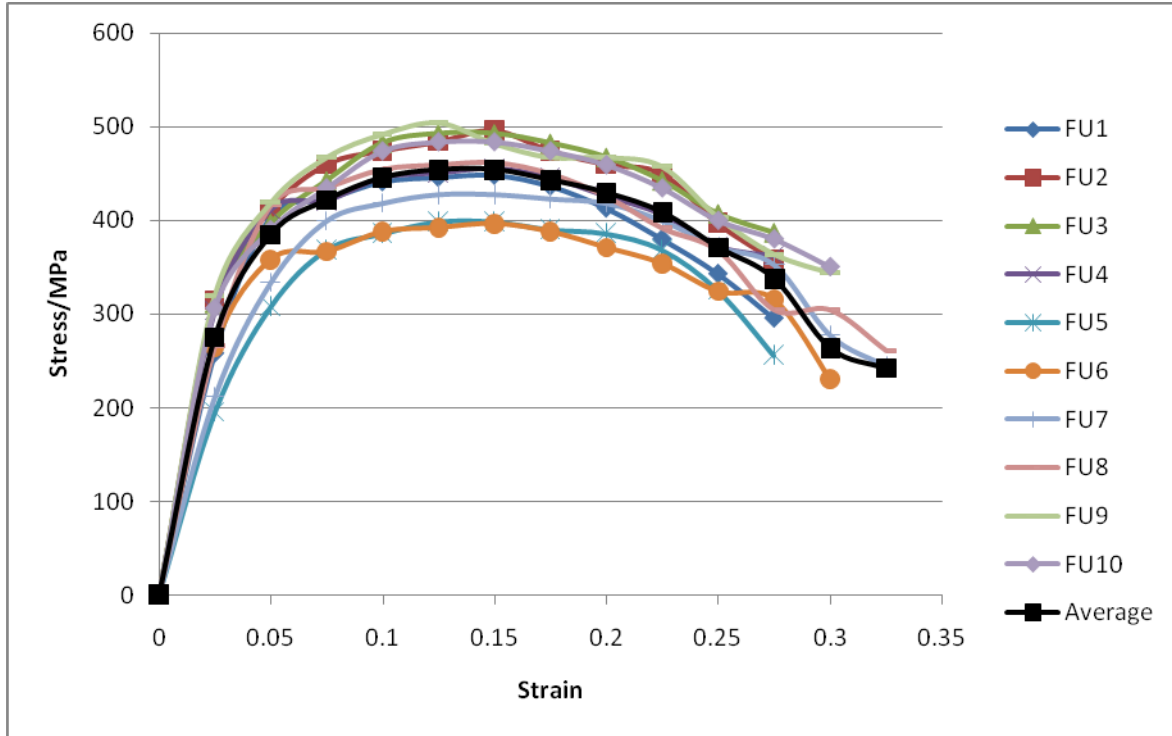


Fig.1 Graph of Stress-Strain curve for all the imported samples from Ukraine

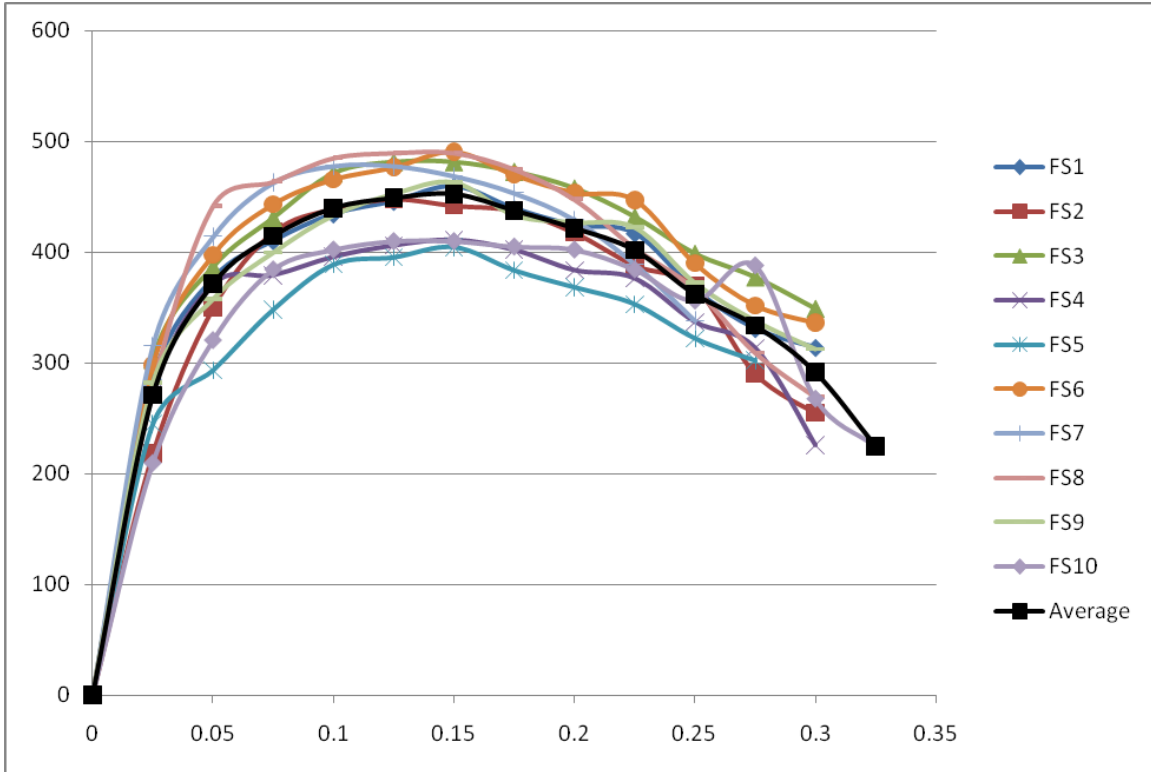


Fig. 2 Graph of Stress-Strain curve for all the imported samples (FS-Series) from Spain

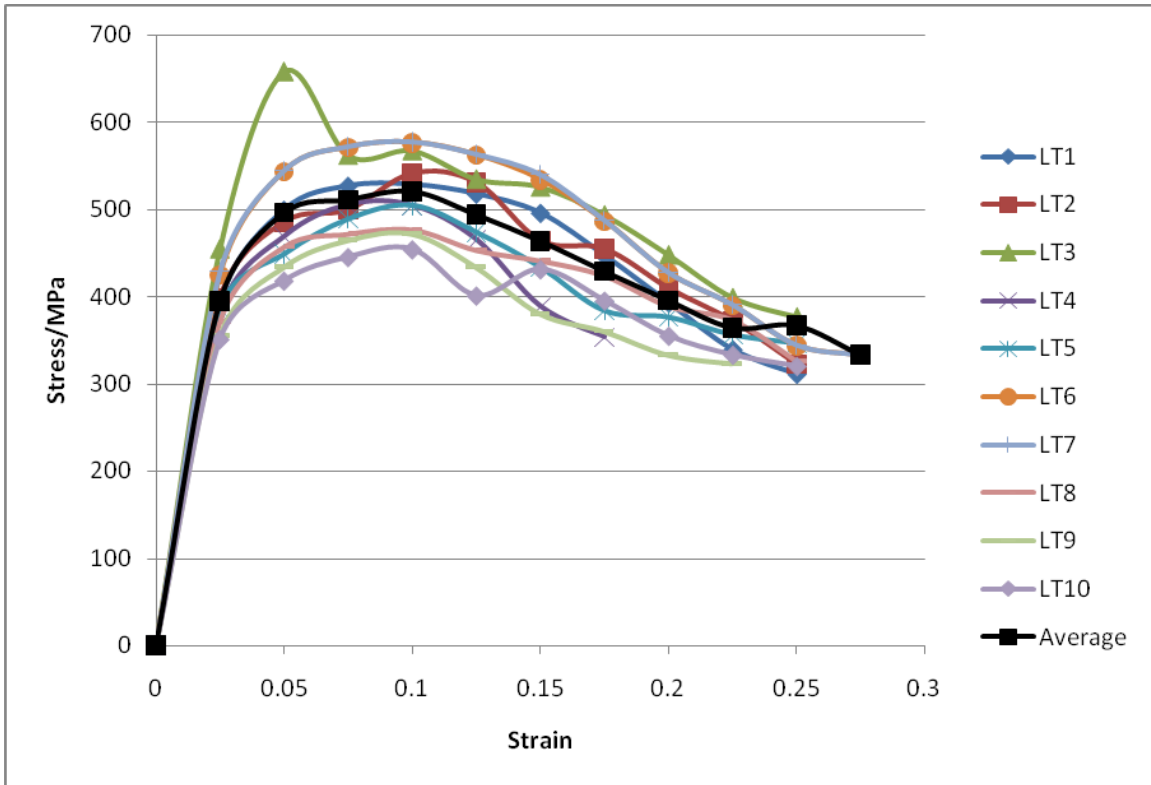


Fig. 3 Graph of Stress-Strain curve for locally produced samples (LT-Series) from Tema steel works.

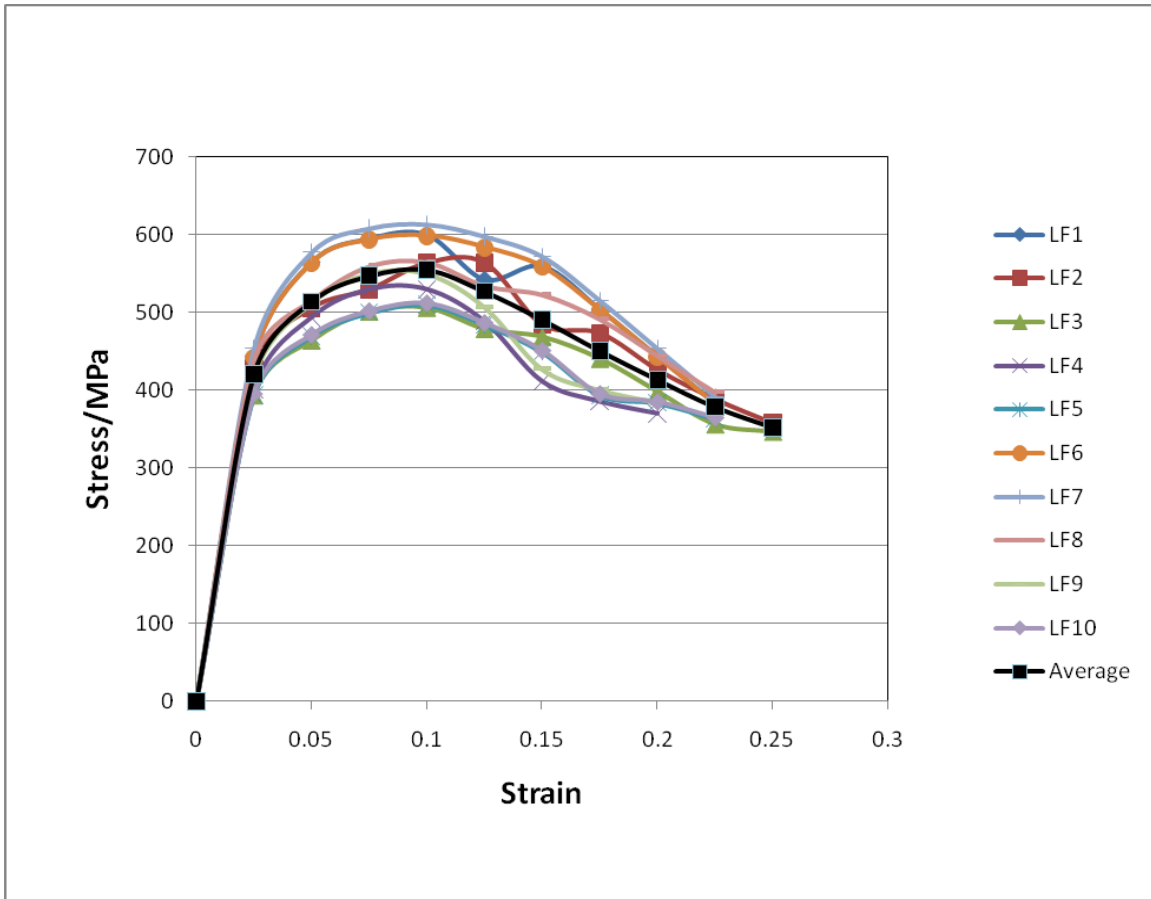


Fig..4 Graph of Stress-Strain curves of locally produced iron samples (LF – Series) from Ferro Fabrik.

## APPENDIX C

### Load - extension tables and calculated values for imported and locally produced iron rods

**Table.1 Load and extension values for imported iron rods from Ukraine**

Sample	FU1	FU2	FU3	FU4	FU5
Extension/m	Load/kg	Load/kg	Load/kg	Load/kg	Load/kg
0.00127	5600.2	6618.5	6313.0	6313.1	4582.1
0.00254	8756.7	8654.9	8044.1	8553.2	7229.3
0.00381	9164.0	9673.1	8960.5	8756.4	8654.9
0.00508	9571.3	9978.6	9774.9	9265.8	9062.3
0.00635	9673.1	10182.3	9978.7	9367.6	9265.8
0.00762	9723.9	10436.8	9978.7	9469.5	9265.8
0.00889	9469.5	9978.6	9774.9	9265.9	9164.0
0.01016	8960.5	9673.1	9469.5	8858.5	9062.2
0.01143	8247.6	9469.5	8960.4	8451.4	8654.9
0.0127	7738.5	8349.4	8247.6	7738.5	8044.1
0.01397	6414.9	7534.9	7840.3	7534.9	7636.7
0.01524	5498.5	7127.6	7229.5	5498.5	6007.6
	FU6	FU7	FU8	FU9	FU10
Extension/m	Load/kg	Load/kg	Load/kg	Load/kg	Load/kg
0.00127	6312.9	4582.1	5600.3	6618.5	6313.3
0.00254	8553.0	7229.5	8756.8	8655.1	8043.9
0.00381	8756.6	8654.9	9163.9	9673.1	8960.4
0.00508	9265.3	9062.4	9571.5	9978.6	9774.9
0.00635	9367.6	9265.8	9673.1	10182.3	9978.6
0.00762	9469.5	9265.8	9724.2	10436.8	9978.6
0.00889	9265.8	9164.0	9469.9	9978.5	9774.9
0.01016	8858.5	9062.2	8960.5	9673.2	9469.5
0.01143	8451.5	8654.9	8247.7	9469.6	8960.5
0.0127	7738.5	8044.1	7738.5	8349.5	8247.7
0.01397	7534.9	7636.7	6414.9	7534.9	7840.5
0.01524	5498.5	6007.9	5498.5	7127.8	7229.5
0.01651		5296.1			

**Table.2 Diameter and area data for imported samples from Ukraine**

Sample	Original diameter/m	Necking diameter/m	Original area/m <sup>2</sup>	Necking area/m <sup>2</sup>
FU1	0.01646	0.008865	2.1279 x10 <sup>-4</sup>	6.1723 x10 <sup>-5</sup>
FU2	0.01621	0.009042	2.0637 x10 <sup>-4</sup>	6.4212 x10 <sup>-5</sup>
FU3	0.01590	0.009499	1.9856 x10 <sup>-4</sup>	7.0867 x10 <sup>-5</sup>
FU4	0.01612	0.008687	2.0409 x10 <sup>-4</sup>	5.9269 x10 <sup>-5</sup>
FU5	0.01712	0.008738	2.3019 x10 <sup>-4</sup>	5.9967 x10 <sup>-5</sup>
FU6	0.01727	0.008331	2.3425 x10 <sup>-4</sup>	5.4511 x10 <sup>-5</sup>
FU7	0.01644	0.008636	2.1227 x10 <sup>-4</sup>	5.8575 x10 <sup>-5</sup>
FU8	0.01621	0.008484	2.0637 x10 <sup>-4</sup>	5.6531 x10 <sup>-5</sup>
FU9	0.01608	0.008814	2.0308 x10 <sup>-4</sup>	6.1014 x10 <sup>-5</sup>
FU10	0.01605	0.009042	2.0232x10 <sup>-4</sup>	6.4212 x10 <sup>-5</sup>

**Table.3 Data on stresses and strains for imported samples from Ukraine**

Strain	FU1 Stress/ MPa	FU2 Stress/ MPa	FU3 Stress/ MPa	FU4 Stress/ MPa	FU5 Stress/ MPa	FU6 Stress/ MPa	FU7 Stress/ MPa	FU8 Stress/ MPa	FU9 Stress/ MPa	FU10 Stress /MPa	Average Sress/ MPa
0	0	0	0	0	0	0	0	0	0	0	0
0.025	258.2	314.6	311.9	303.5	195.3	264.4	211.8	<sup>266.2</sup>	319.7	306.1	275.2
0.05	403.7	411.4	397.4	411.1	308.1	358.2	334.1	416.3	418.9	390.0	384.9
0.075	422.5	459.8	442.7	420.9	368.8	366.7	400.0	435.6	467.3	434.5	421.9
0.1	441.3	474.3	482.9	445.4	386.2	388.0	418.8	455.0	491.9	474.0	445.8
0.125	446.0	484.0	493.0	450.3	398.9	392.3	428.2	459.8	504.2	483.8	454.1
0.15	448.3	496.1	493.0	455.2	398.9	396.6	428.2	462.2	482.0	483.8	454.4
0.175	436.6	474.3	482.9	445.4	390.5	388.0	423.5	450.2	467.3	474.0	443.3
0.2	413.1	459.8	467.8	425.8	386.2	371.0	418.8	425.9	467.3	459.2	429.5
0.225	380.2	450.1	442.7	406.2	368.8	353.9	400.0	392.1	457.4	434.5	408.6
0.25	343.1	396.9	407.5	372.0	325.5	324.1	371.8	367.9	403.3	400.0	371.2
0.275	295.7	358.2	387.4	362.2	256.2	315.5	352.9	304.9	364.0	380.2	337.7
0.3						230.3	277.7	304.9	344.3	350.5	263.7
0.325							244.8	261.4			242.1

**Table.4 Young's Modulus, Percentage elongation. Ultimate tensile strength and Fracture stress values for Ukraine iron rods**

Sample	Young's Modulus/GPa	Percentage Elongation	Ultimate tensile Strength/MPa	Fracture Stress/MPa	Toughness/ (MJ/m <sup>3</sup> )
FU1	10.328	30.0	448.3	523.5	91.18
FU2	12.584	30.0	496.1	338.8	100.98
FU3	12.476	30.0	493.0	357.2	101.35
FU4	12.140	30.0	455.2	264.3	94.66
FU5	7.812	30.0	398.9	256.0	89.41
FU6	10.576	30.0	396.6	230.3	103.44
FU7	8.472	30.5	428.2	244.8	109.35
FU8	10.648	30.0	462.2	261.4	111.27
FU9	12.788	30.0	504.2	344.3	111.19
FU10	12.244	30.0	483.8	350.8	108.68
<b>Average</b>	<b>11.01±0.57</b>	<b>30.05±0.05</b>	<b>456.65±12.35</b>	<b>317.14±27.68</b>	<b>102.15±2.59</b>

**Table.5 Load and extension values for imported iron rods from Spain**

Sample	FS1	FS2	FS3	FS4	FS5
Extension/m	Load/kg	Load/kg	Load/kg	Load/kg	Load/kg
0.00127	6450.4	4483.9	6260.3	6260.5	6021.5
0.00254	8496.8	7191.8	7992.6	8504.9	7215.3
0.00381	9489.6	8600.7	8908.6	8698.2	8567.6
0.00508	9811.5	9038.5	9742.6	9079.8	9565.3
0.00635	10069.5	9216.6	9952.3	9314.9	9725.9
0.00762	10376.2	9094.3	9952.3	9429.3	9954.3
0.00889	9922.8	9000.5	9770.7	9199.8	9435.5
0.01016	9580.6	8592.8	9460.4	8800.8	9084.6
0.01143	9418.9	7983.8	8928.5	8424.6	8625.6
0.0127	8267.6	7586.5	8241.0	7730	7923.5
0.01397	7472.7	5973.2	7800.5	7189.8	7432.5
0.01524	7088.9	5242.6	7212.9	5178.6	6012.3
0.01651					
	FS6	FS7	FS8	FS9	FS10
Extension/m	Load/kg	Load/kg	Load/kg	Load/kg	Load/kg
0.00127	6243.0	6513.2	5421.3	6248.6	4684.3
0.00254	8324.6	8553.8	8645.6	7925.4	7158.8
0.00381	9284.3	9565.4	9068.4	8854.1	8584.9
0.00508	9752.3	9875.5	9489.6	9600.4	8984.3
0.00635	9980.5	9875.5	9578.8	10025.3	9154.7
0.00762	10277.9	9685.7	9578.8	10258.6	9154.7
0.00889	9835.8	9369.2	9289.7	9600.4	9045.6
0.01016	9501.9	8868.2	8756.3	9457.3	8984.3
0.01143	9366.8	8040.8	7900.6	9354.9	8584.9
0.0127	8165.2	7532.5	7425.9	8245.9	7957.5
0.01397	7370.5	7058.6	6047.0	7489.1	7548.1
0.01524	6980.4		5265.1	6921.7	5978.3
0.01651					5014.4

**Table.6 Diameter and area values for imported rods samples from Spain**

Sample	Original diameter/m	Necking diameter/m	Original area/m <sup>2</sup>	Necking area/m <sup>2</sup>
FS1	0.0168	0.00917	2.2167x10 <sup>-4</sup>	6.604x10 <sup>-5</sup>
FS2	0.01603	0.00925	2.0182 x10 <sup>-4</sup>	6.72 x10 <sup>-5</sup>
FS3	0.01607	0.009425	2.0283 x10 <sup>-4</sup>	6.977 x10 <sup>-5</sup>
FS4	0.01692	0.0096	2.2485 x10 <sup>-4</sup>	7.238 x10 <sup>-5</sup>
FS5	0.01753	0.0112	2.4135 x10 <sup>-4</sup>	9.852 x10 <sup>-5</sup>
FS6	0.01617	0.01005	2.0536 x10 <sup>-4</sup>	7.933 x10 <sup>-5</sup>
FS7	0.01607	0.009425	2.0283 x10 <sup>-4</sup>	6.977 x10 <sup>-5</sup>
FS8	0.01563	0.00927	1.9187 x10 <sup>-4</sup>	6.749 x10 <sup>-5</sup>
FS9	0.01663	0.009195	2.1721 x10 <sup>-4</sup>	6.640 x10 <sup>-5</sup>
FS10	0.0167	0.009265	2.1904 x10 <sup>-4</sup>	6.742 x10 <sup>-5</sup>

**Table.7 Stress and Strain data for imported iron rods from Spain**

Strain	FS1 Stress/ MPa	FS2 Stress/ MPa	FS3 Stress/ MPa	FS4 Stress/ MPa	FS5 Stress/ MPa	FS6 Stress/ MPa	FS7 Stress/ MPa	FS8 Stress/ MPa	FS9 Stress/ MPa	FS10 Stres s/MP a	Average Sress/ MPa
0	0	0	0	0	0	0	0	0	0	0	0
0.025	285.5	218.0	302.8	273.1	244.8	298.2	315.0	277.2	282.2	209.8	270.7
0.05	376.0	349.6	386.6	371.1	293.3	397.7	413.7	442.0	357.9	320.6	370.9
0.075	410.0	418.1	430.9	379.5	348.2	443.5	462.5	463.7	399.9	384.5	414.1
0.1	434.2	439.3	471.2	396.1	388.8	465.9	477.6	485.2	433.6	402.4	439.4
0.125	445.6	448.0	481.3	406.4	395.3	476.8	477.6	489.7	452.8	410.0	448.4
0.15	459.2	442.1	481.3	411.4	404.6	491.0	468.5	489.7	463.3	410.0	452.1
0.175	439.1	437.5	472.6	402.4	383.5	470.0	453.1	475.0	433.6	405.1	437.2
0.2	424.0	417.7	457.6	384.0	368.3	453.9	428.9	447.7	427.1	402.4	421.2
0.225	416.8	388.1	431.8	376.6	353.0	447.4	388.9	403.9	422.5	384.5	401.4
0.25	365.9	368.8	398.6	337.3	322.1	390.0	337.9	366.6	372.4	356.4	361.6
0.275	330.7	290.3	377.3	313.7	302.1	352.1		309.2	338.2	388.1	333.5
0.3	313.7	254.8	348.9	226.0		336.4		269.2	312.6	267.7	291.2
0.325										224.6	224.6

**Table.8 Young's Modulus, Percentage elongation. Ultimate tensile strength and Fracture stress values for Spain iron rods**

Sample	Young's Modulus/GPa	Percentage Elongation	Ultimate tensile Strength/MPa	Fracture Stress/MPa	Toughness/ (MJ/m <sup>3</sup> )
FS1	11.420	30.0	459.2	313.7	100.86
FS2	8.720	30.0	448.0	254.8	97.07
FS3	12.112	30.0	481.3	348.9	108.05
FS4	10.924	30.0	411.4	225.9	92.31
FS5	9.792	30.0	404.6	244.4	80.24
FS6	11.928	30.0	491.0	333.5	107.84
FS7	12.600	27.5	477.6	341.4	107.17
FS8	11.088	30.0	489.7	269.2	106.47
FS9	11.288	30.0	463.3	312.6	100.80
FS10	8.392	32.5	410.0	224.6	100.36
<b>Average</b>	<b>10.826±0.45</b>	<b>30.00±0.38</b>	<b>453.61±32.65</b>	<b>286.90±10.32</b>	<b>100.12±2.75</b>

**Table.9 Load and extension values for locally produced iron rods from Tema Steel works**

Sample	LT1	LT2	LT3	LT4	LT5
Extension/m	Load/kg	Load/kg	Load/kg	Load/kg	Load/kg
0.00127	9010.1	9126.8	8852.8	7966.2	8016.5
0.00254	11443.6	10730.3	12809.0	9781.3	9533.2
0.00381	12064.5	11040.8	10941.5	10541.6	10142.6
0.00508	12166.2	11963.2	11047.7	10525.4	10486.8
0.00635	11856.2	11732.8	10407.7	9710.9	9844.0
0.00762	11352.4	10256.5	10234.1	8125.9	9010.3
0.00889	10237.9	10048.1	9609.2	7598.7	7974.7
0.01016	8995.7	9054.1	8716.2	7381.0	7821.3
0.01143	7767.7	8224.2	7762.8		7401.9
0.0127	7124.3	7534.1	7334.1		7204.6
0.01397		7125.2			
	LT6	LT7	LT8	LT9	LT10
Extension/m	Load/kg	Load/kg	Load/kg	Load/kg	Load/kg
0.00127	8964.7	9026.3	8616.2	8037.6	7953.3
0.00254	11466.0	11440.7	11011.4	9830.5	9472.1
0.00381	12052.4	12063.8	10934.5	10525.3	10085.6
0.00508	12167.1	12188.4	11050.2	10690.2	10285.6
0.00635	11864.6	11874.6	10501.3	9825.5	9085.2
0.00762	11372.9	11367.8	10220.6	8614.9	9766.7
0.00889	10271.2	10208.3	9821.3	8158.2	9058.2
0.01016	9010.7	9074.5	9010.8	7542.6	8954.2
0.01143	8231.9	8940.9	8642.9	7321.2	8040.0
0.0127	7256.8	7821.6	7548.2		7545.2
0.01397	7012.3				7254.3

**Table.10 Diameter and area values for local samples from Tema steel works**

Sample	Original diameter/m	Necking diameter/m	Original area/m <sup>2</sup>	Necking area/m <sup>2</sup>
LT1	0.01691	0.01004	2.2458x10 <sup>-4</sup>	7.9169x10 <sup>-5</sup>
LT2	0.01661	0.0095	2.1669 x10 <sup>-4</sup>	7.0882 x10 <sup>-5</sup>
LT3	0.01560	0.0110	1.9113 x10 <sup>-4</sup>	9.5033 x10 <sup>-5</sup>
LT4	0.01614	0.009421	2.0460 x10 <sup>-4</sup>	6.9708 x10 <sup>-5</sup>
LT5	0.01611	0.00916	2.0384 x10 <sup>-4</sup>	6.5899 x10 <sup>-5</sup>
LT6	0.01623	0.009254	2.0688 x10 <sup>-4</sup>	6.6317 x10 <sup>-5</sup>
LT7	0.01622	0.009189	2.0663 x10 <sup>-4</sup>	6.6317 x10 <sup>-5</sup>
LF8	0.01701	0.009261	2.2725 x10 <sup>-4</sup>	6.7346 x10 <sup>-5</sup>
LT9	0.01682	0.00925	2.2220 x10 <sup>-4</sup>	6.736 x10 <sup>-5</sup>
LT10	0.01604	0.00921	2.2220 x10 <sup>-4</sup>	6.662 x10 <sup>-5</sup>

**Table.11 Stress and Strain data for iron rods from Tema steel works**

Strain	LT1 Stress/ MPa	LT2 Stress/ MPa	LT3 Stress/ MPa	LT4 Stress/ MPa	LT5 Stress/ MPa	LT6 Stress/ MPa	LT7 Stress/ MPa	LT8 Stress/ MPa	LT9 Stress/ MPa	LT10 Stress /MPa	Average Sress/ MPa
0	0	0	0	0	0	0	0	0	0	0	0
0.025	393.6	398.7	454.4	382.0	385.8	425.1	428.5	371.9	354.9	351.1	394.6
0.05	499.4	485.8	657.4	469.0	448.8	543.7	544.4	457.3	434.0	418.2	495.8
0.075	527.0	499.8	561.6	505.4	489.0	571.5	572.2	472.0	464.7	445.3	510.9
0.1	528.6	541.6	567.0	504.7	504.7	577.0	577.6	477.0	472.0	454.1	520.4
0.125	517.9	531.2	534.2	465.6	473.8	562.6	563.3	453.3	433.8	401.1	493.7
0.15	495.9	464.3	525.3	389.0	433.6	534.3	540.0	441.2	380.3	431.2	463.5
0.175	447.2	454.9	493.2	353.9	383.8	487.0	487.6	424.0	360.2	395.3	428.7
0.2	392.9	409.9	447.4		376.4	427.3	427.8	389.0	333.0	355.0	395.4
0.225	339.3	372.3	398.4		356.2	390.3	390.8	373.1	323.2	333.1	364.1
0.25	311.2	322.6	376.4		346.7	344.1	344.5	325.8		320.3	366.5
0.275						332.8	332.9				332.9

**Table.12 Young's Modulus, Percentage elongation. Ultimate tensile strength and Fracture stress values for iron rods from Tema Steel works**

Sample	Young's Modulus/GPa	Percentage Elongation	Ultimate tensile Strength/MPa	Fracture Stress/MPa	Toughness/ (MJ/m <sup>3</sup> )
LT1	15.744	25.0	528.6	311.2	92.26
LT2	15.948	27.5	541.6	322.6	92.71
LT3	18.176	25.0	567.0	376.4	103.50
LT4	15.280	20.0	505.4	353.9	57.89
LF5	15.432	25.0	504.7	347.5	86.23
LT6	17.004	27.5	577.0	332.5	109.47
LT7	17.140	25.0	577.6	371.3	109.75
LF8	14.876	25.0	477.0	325.8	86.30
LT9	14.196	22.5	472.0	323.2	71.49
LT10	14.044	27.5	454.1	320.3	80.30
<b>Average</b>	<b>15.784±0.42</b>	<b>25.00±1.69</b>	<b>520.50±14.24</b>	<b>338.47±7.14</b>	<b>88.99±5.22</b>

**Table.13 Load and extension values for locally produced iron rods from Ferro Fabric**

Sample	LF1	LF2	LF3	LF4	LF5
Extension/m	Load/kg	Load/kg	Load/kg	Load/kg	Load/kg
0.00127	8960.1	9062.1	8552.8	7942.2	7942.1
0.00254	11403.9	10691.2	10080.0	97747.7	9469.3
0.00381	12014.8	10990.2	10894.5	10487.3	10080.2
0.00508	12116.5	11924.1	10996.7	10487.5	10283.8
0.00635	11811.0	11924.1	10407.2	9672.8	9774.9
0.00762	11302.1	10243.5	10182.1	8145.5	9062.3
0.00889	10182.3	10011.1	9571.2	7636.5	7942.1
0.01016	8960.2	9012.1	8654.7	7331.0	7738.2
0.01143	7738.1	8214.2	7738.5		7331.0
0.0127		7564.1	7534.5		
0.01397					
	LF6	LF7	LF8	LF9	LF10
Extension/m	Load/kg	Load/kg	Load/kg	Load/kg	Load/kg
0.00127	8961.2	8964.2	8554.9	7945.0	7944.1
0.00254	11404.7	11405.7	10042.4	9776.8	9472.1
0.00381	12013.5	12016.8	10896.7	10490.2	10082.1
0.00508	12116.5	12118.4	10998.9	10490.2	10285
0.00635	11811.4	11813.6	10409.7	9674.9	9
0.00762	11304.2	11305.2	10185.3	8147.9	9776.7
0.00889	10184.1	10184.2	9574.3	7637.9	9064.2
0.01016	8962.3	8963.5	8654.8	7334.0	7944.2
0.01143	7735.9	7740.5	7739.9		7740.0
0.0127					7333.0

**Table.14 Diameter and area data for local samples from Ferro Fabric**

Sample	Original diameter/m	Necking diameter/m	Original area/m <sup>2</sup>	Necking area/m <sup>2</sup>
LF1	0.01588	0.01069	1.98057x10 <sup>4</sup>	8.9752x10 <sup>5</sup>
LF2	0.01626	0.01033	2.07649x10 <sup>4</sup>	8.3809x10 <sup>5</sup>
LF3	0.01648	0.00861	2.13306x10 <sup>4</sup>	5.1529x10 <sup>5</sup>
LF4	0.01572	0.01056	1.94086x10 <sup>4</sup>	8.7582x10 <sup>5</sup>
LF5	0.01588	0.01039	1.98057x10 <sup>4</sup>	8.4785x10 <sup>5</sup>
LF6	0.01590	0.01033	1.98556x10 <sup>4</sup>	8.3808x10 <sup>5</sup>
LF7	0.01572	0.00899	1.94086x10 <sup>4</sup>	6.3475x10 <sup>5</sup>
LF8	0.01560	0.01041	1.91134x10 <sup>4</sup>	8.5112x10 <sup>5</sup>
LF9	0.01544	0.00947	1.87233x10 <sup>4</sup>	7.0435x10 <sup>5</sup>
LF10	0.01585	0.00960	1.97309x10 <sup>4</sup>	7.2382x10 <sup>5</sup>

**Table.15 Data on Stress and Strain for local samples from Ferro Fabric**

Strain	LF1 Stress/ MPa	LF2 Stress/ MPa	LF3 Stress/ MPa	LF4 Stress/ MPa	LF5 Stress/ MPa	LF6 Stress/ MPa	LF7 Stress/ MPa	LF8 Stress/ MPa	LF9 Stress/ MPa	LF10 Stress /MPa	Average Sress/ MPa
0	0	0	0	0	0	0	0	0	0	0	0
0.025	443.8	428.1	393.3	401.4	393.4	442.7	453.1	439.1	416.3	395.0	420.6
0.05	564.8	505.1	463.6	494.1	469.0	563.5	576.5	515.4	512.3	470.9	513.5
0.075	595.1	529.2	501.0	530.1	499.3	593.5	607.4	559.3	549.6	501.3	546.6
0.1	600.1	563.3	505.7	530.1	509.4	598.6	612.5	564.5	549.6	511.4	554.5
0.125	542.7	563.3	478.6	488.9	484.2	583.6	597.1	534.3	506.9	486.1	526.6
0.15	559.8	483.9	468.3	411.7	448.9	558.5	571.4	522.8	426.9	450.7	490.3
0.175	504.3	473.0	440.2	386.0	393.4	503.2	514.8	491.4	400.2	395.0	450.2
0.2	443.8	425.8	398.0	370.5	383.3	442.8	453.1	444.2	384.3	384.8	413.1
0.225	383.3	388.1	355.9		363.1	382.2	391.2	397.3		364.6	378.2
0.25		357.4	346.5								352.0

**Table.16 Young's Modulus, Percentage elongation. Ultimate tensile strength and Fracture stress values for Ferro fabrik iron rods**

Sample	Young's Modulus/GPa	Percentage Elongation	Ultimate tensile Strength/MPa	Fracture Stress/MPa	Toughness/ (MJ/m <sup>3</sup> )
LF1	17.75	22.5	600.1	383.3	93.87
LF2	17.12	25.0	563.3	357.4	97.30
LF3	15.73	25.0	505.7	346.5	89.58
LF4	16.05	20.0	530.1	370.5	70.59
LF5	15.73	22.5	509.4	363.1	79.24
LF6	17.70	22.5	598.6	382.2	94.58
LF7	18.12	22.5	612.5	391.2	96.78
LF8	17.56	22.5	564.5	397.3	90.00
LF9	16.65	20.0	506.9	384.3	73.19
LF10	15.80	25.0	511.4	364.6	79.56
<b>Average</b>	<b>16.82±0.28</b>	<b>22.80±0.55</b>	<b>550.25±13.55</b>	<b>374.40±5.11</b>	<b>86.47±3.15</b>

## APPENDIX D

**Table.1 The convention chart for hardness test [5]**

ROCKWELL			SUPERFICIAL ROCKWELL			BRINELL		VICKERS OR FIRTH DIAMOND HARDNESS NUMBER	SCLERO-SCOPE	TENSILE STRENGTH
						10 m/m Ball				
Diamond Brale			1/16" Bull	"N" Brale Penetrater			3000 kgm Load			
150 kgm C Scale	60 kgm A Scale	100 kgm D Scale	100 kgm B Scale	15 kg Load N	30 kg Load 30N	45 kg Load 45N	Diam. Of Ball Impression in m/m	Hardness Number		Equivalent 1000 lb. Sq. In.
80	92	87		97	92	87			1865	
79	92	86			92	87			1787	
78	91	85		96	91	86			1710	
77	91	84			91	85			1633	
76	90	83		96	90	84			1556	
75	90	83			89	83			1478	
74	89	82		95	89	82			1400	
73	89	81			88	81			1323	
72	88	80		95	87	80			1245	
71	87	80			87	79			1160	99
70	87	79		94	86	78			1076	98
69	86	78		94	85	77			1004	97
68	86	77			85	79			942	96
67	85	76		93	84	75			894	95
66	85	76		93	83	73			854	93
65	84	75		92	82	72	2.25	745	820	91
64	84	74			81	74	2.30	710	789	88
63	83	73		92	80	70	2.30	710	763	87
62	83	73		91	79	69	2.35	682	746	85
61	82	72		91	79	68	2.35	682	720	83
60	81	71		90	78	67	2.40	653	697	82
59	81	70		90	77	66	2.45	627	674	80
										326

58	80	69		89	76	65	2.55	578	653	78	315
57	80	69		89	75	63	2.55	578	633	77	304
56	79	68		88	74	62	2.60	555	613	75	294
55	79	67		88	73	61	2.60	555	595	74	287
54	78	66		87	72	60	2.65	534	577	72	279
53	77	65		87	71	59	2.70	514	560	71	269
52	77	65		86	70	57	2.75	495	544	69	261
51	76	64		86	69	56	2.75	495	528	68	254
50	76	63		86	69	55	2.80	477	513	67	245
49	75	62		85	68	54	2.85	461	498	65	238
48	75	61		85	67	53	2.90	444	484	64	232
47	74	61		84	66	51	2.90	444	471	63	225
46	73	60		84	65	50	2.95	432	458	62	219
45	73	59		83	64	49	3.00	415	446	61	211
44	73	59		83	63	48	3.00	415	434	59	206
43	72	58		82	62	47	3.05	401	423	58	202
42	72	57		82	61	46	3.10	388	412	56	198
41	71	56		81	60	44	3.10	388	402	55	191
40	70	55		80	60	43	3.15	375	392	54	185
39	70	55		80	59	42	3.20	363	382	53	181
38	69	54		79	58	41	3.25	352	372	51	176
37	69	53	109	79	57	40	3.30	341	363	50	171
36	68	52	109	78	56	39	3.35	331	354	49	168
35	68	52	108	78	55	37	3.35	331	345	48	163
34	67	51	108	77	54	36	3.40	321	336	46	159
33	67	50	107	77	53	38	3.45	311	327	45	154
32	66	49	106	76	52	34	3.50	302	318	44	150
31	66	48	106	76	51	33	3.55	293	310	43	146
30	65	48	105	75	50	32	3.60	285	302	42	142
29	65	47	104	75	50	30	3.65	277	294	41	138
28	64	46	103	74	49	29	3.70	269	286	40	134
27	64	45	103	73	48	28	3.75	262	279	39	131
26	63	45	102	73	47	27	3.80	255	272	38	126
25	63	44	101	72	46	26	3.80	255	266	37	124
24	62	43	100	72	45	24	3.85	248	260	37	122

23	62	42	99	71	44	23	3.90	241	254	36	118
22	62	42	99	71	43	22	3.95	235	248	35	116
21	61	41	98	70	42	21	4.00	229	243	35	113
20	61	40	97	69	42	20	4.05	223	238	34	111
18			95				4.10	217	230	33	107
16*			94				4.15	212	222	32	102
14*			92				4.25	203	213	31	98
12*			90				4.35	192	204	29	92
10*			89				4.40	187	195	28	90
8*			87				4.50	179	187	27	87
6*			85				4.60	170	180	26	83
4*			84				4.65	166	173	25	79
2*			82				4.80	156	166	25	77
0*			81				4.80	156	160	25	74
			79				4.90	149	156	23	73
			77				5.00	143	150	22	70
			74				5.10	137	143	21	67
			72				5.20	131	137		65
			70				5.30	126	132	20	62
			68				5.40	121	127	19	60
			65				5.50	116	122	18	58
							5.60	112	117	15	56

Microstructure of Ukraine samples

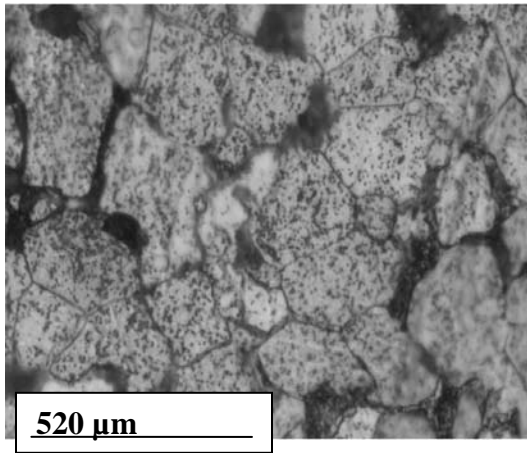


Fig.1 Transverse section of Ukraine sample 2

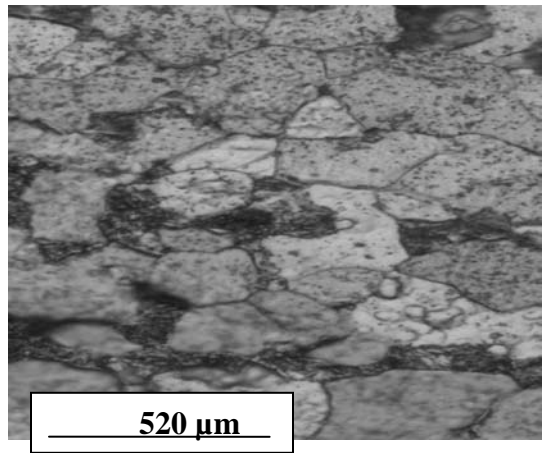


Fig.2 Longitudinal section of Ukraine sample 2

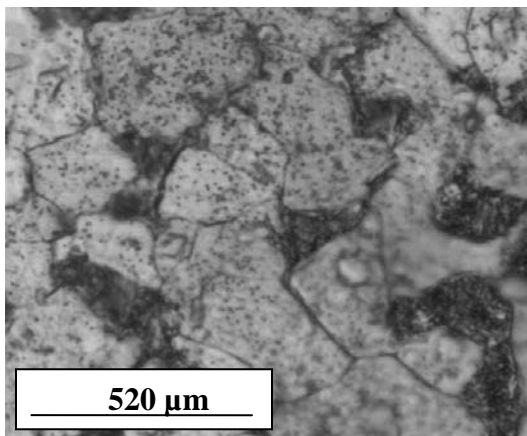


Fig. 3 Transverse section of Ukraine sample 3

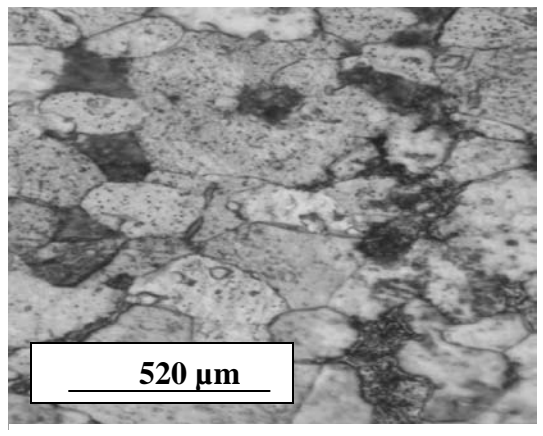


Fig.4 Longitudinal section of Ukraine sample 3

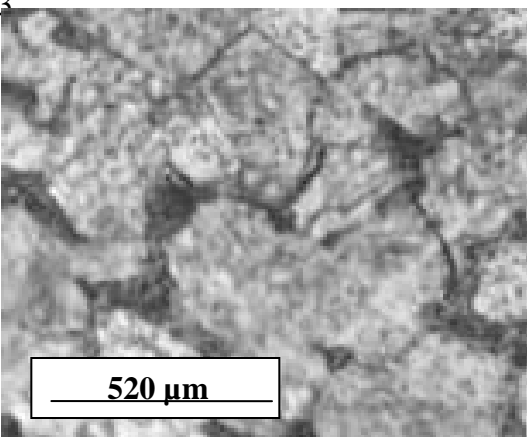


Fig.5 Transverse section of Ukraine sample 4

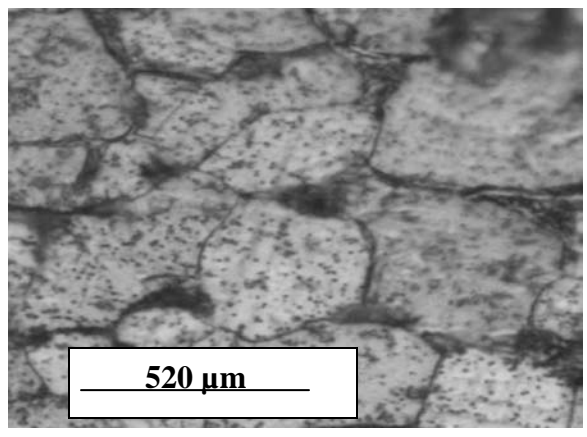


Fig.6 Longitudinal section of Ukraine sample 4

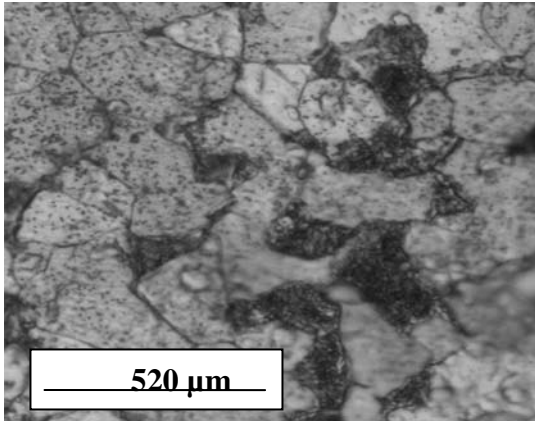


Fig.5 Transverse section of Ukraine sample 5

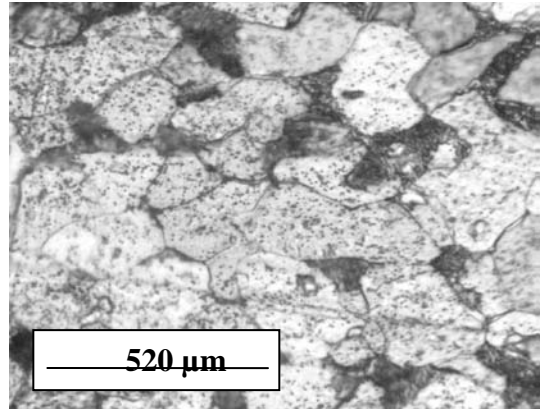


Fig.8 Longitudinal section of Ukraine sample 5

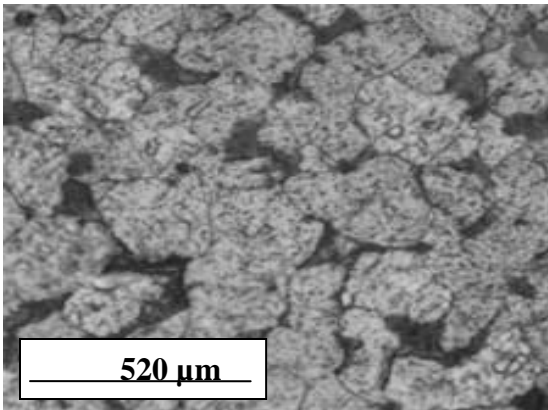


Fig.9 Transverse section of Ukraine sample 6

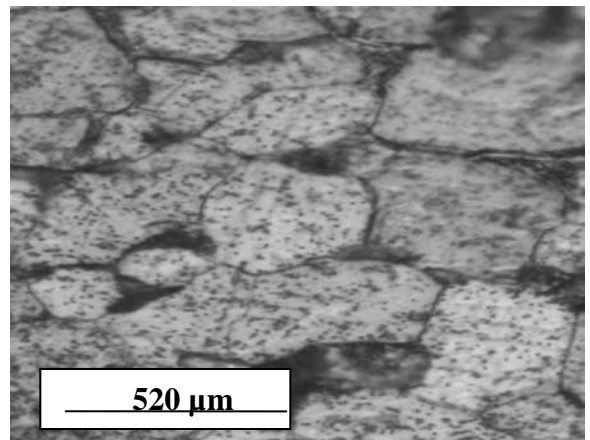


Fig.10 Longitudinal section of Ukraine sample 6

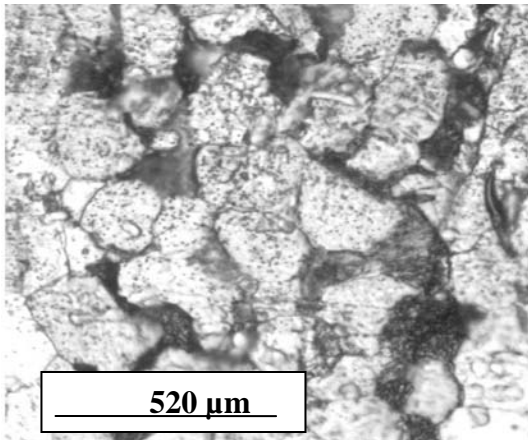


Fig.11 Transverse section of Ukraine sample 7

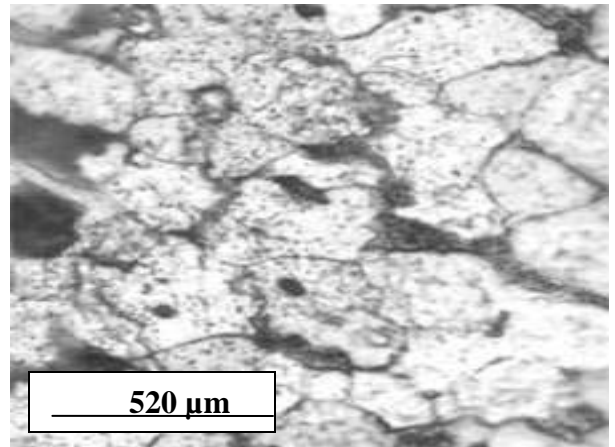


Fig.12 Longitudinal section of Ukraine sample 7

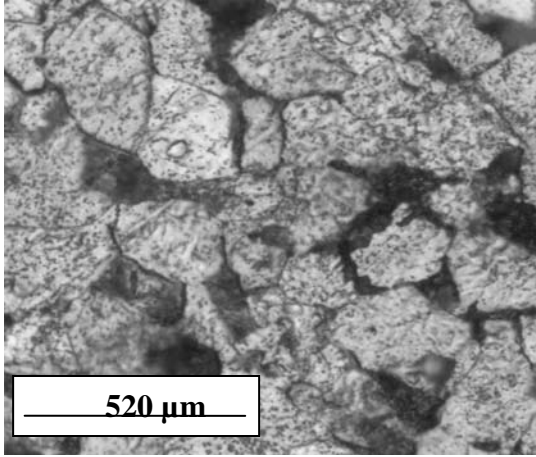


Fig.13 Transverse section of Ukraine sample 8

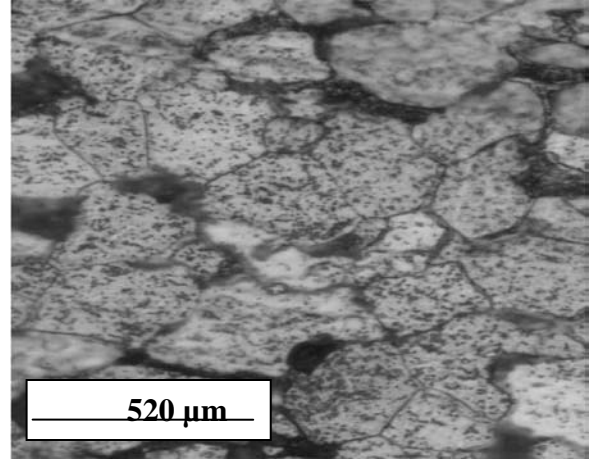


Fig.14 Longitudinal section of Ukraine sample 8

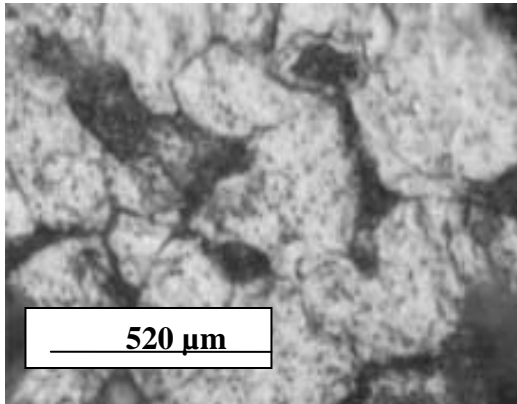


Fig.15 Transverse section of Ukraine sample 9

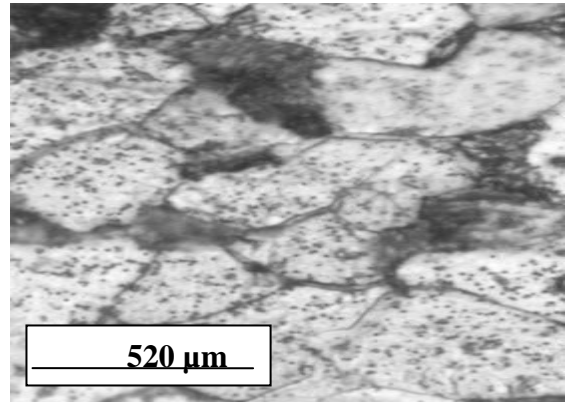


Fig.16 Longitudinal section of Ukraine sample 9

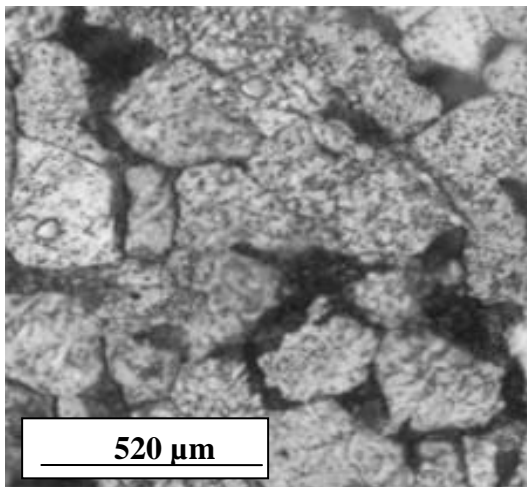


Fig.17 Transverse section of Ukraine sample 10

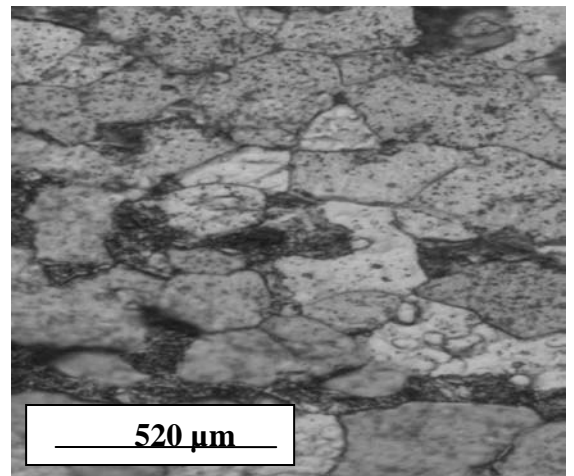


Fig.18 Longitudinal section of Ukraine sample

## Macrostructure of Spain samples

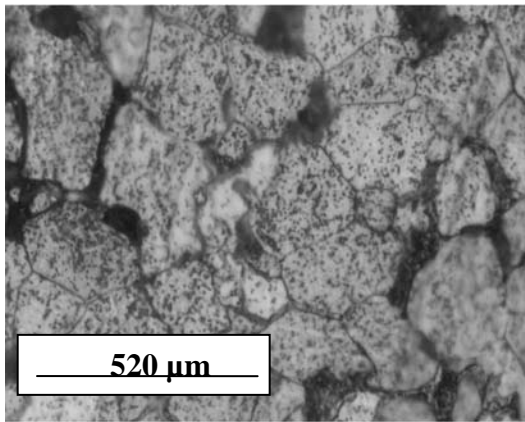


Fig.19 Transverse section of Spain sample 2

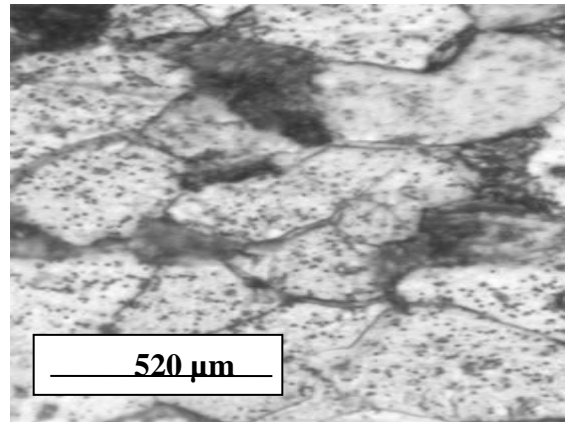


Fig.20 Longitudinal section of Spain sample 2

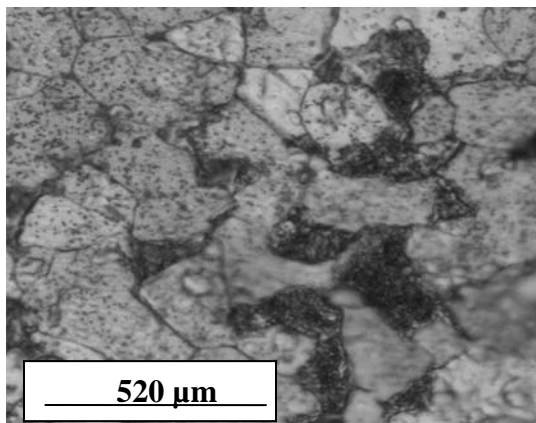


Fig.21 Transverse section of Spain sample 3

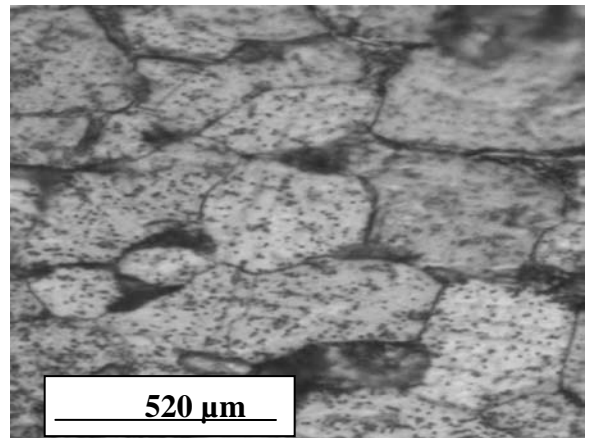


Fig.22 Longitudinal section of Spain sample 3

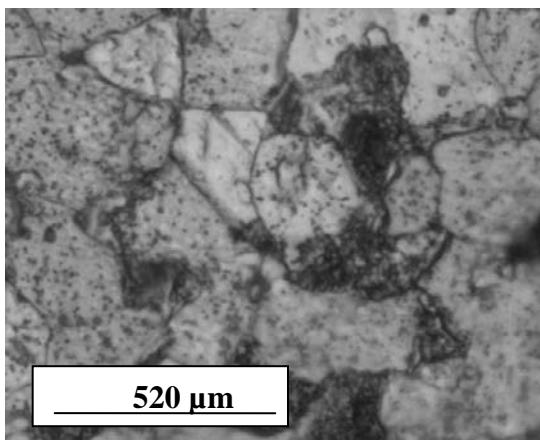


Fig.23 Transverse section of Spain sample 4

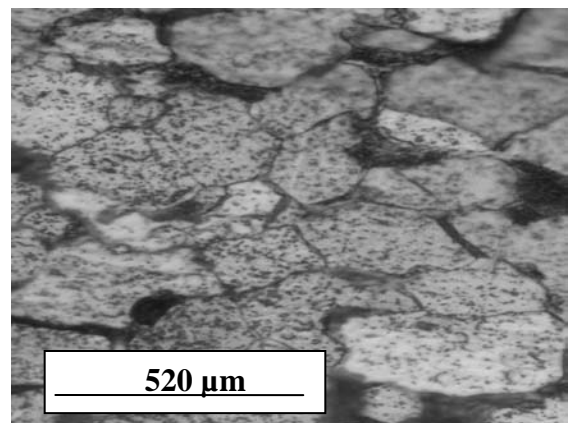


Fig.24 Longitudinal section of Spain sample 4

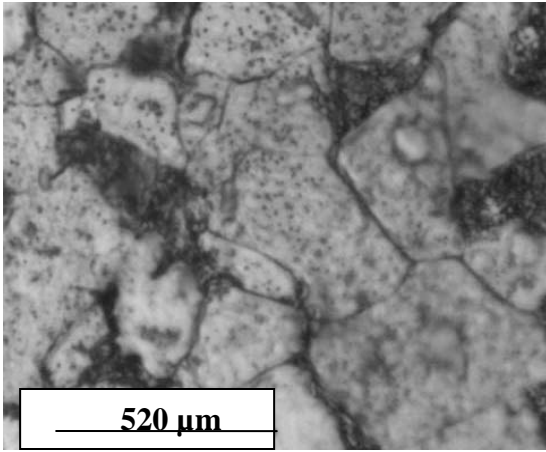


Fig.25 Transverse section of Spain sample 5

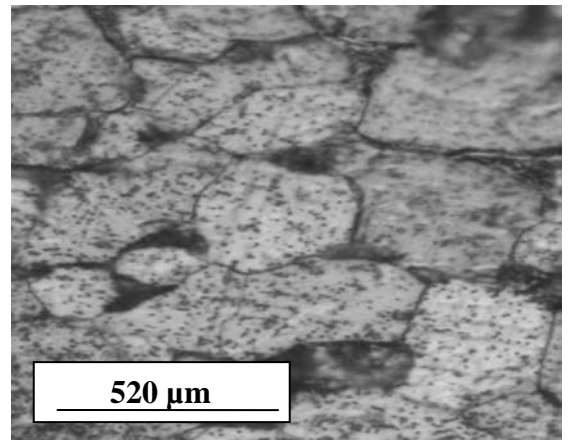


Fig.26 Longitudinal section of Spain sample 5

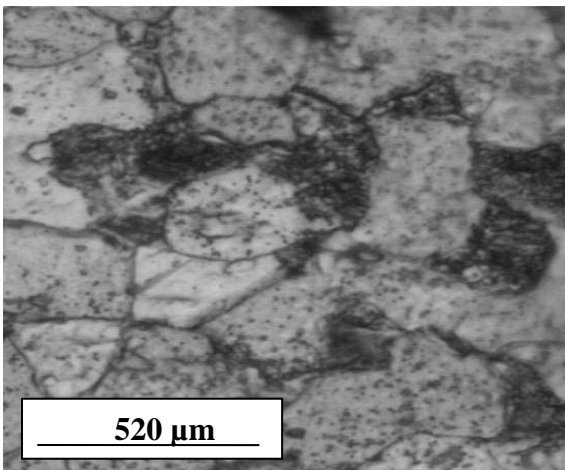


Fig.27 Transverse section of Spain sample 6

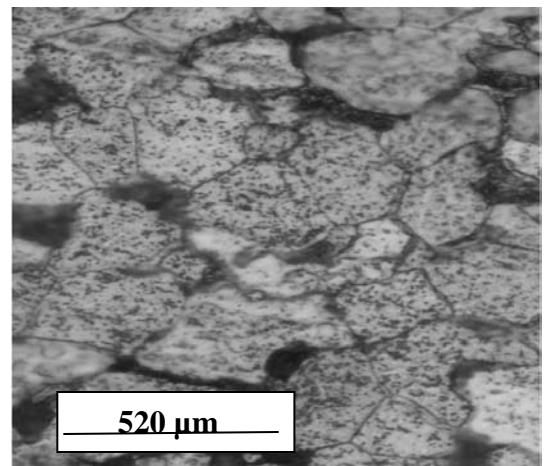


Fig.28 Longitudinal section of Spain sample 6

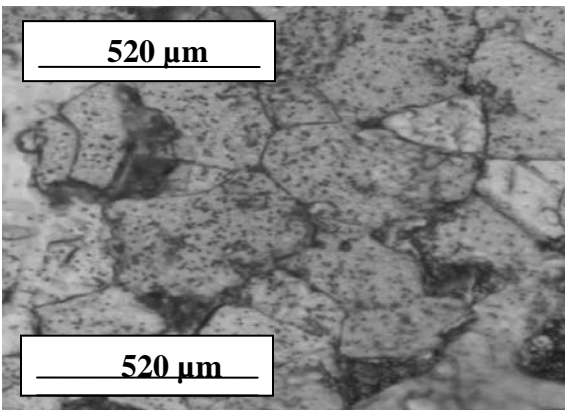


Fig.29 Transverse section of Spain sample 7

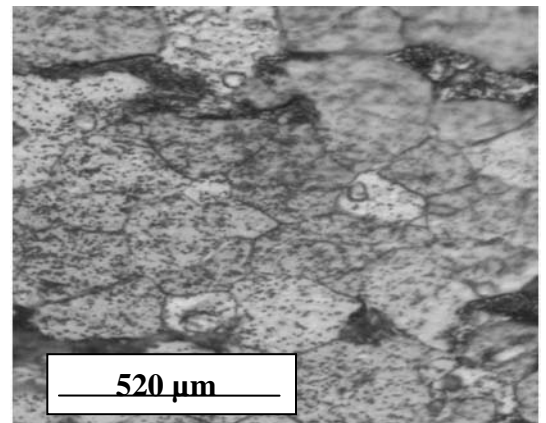


Fig.30 Longitudinal section of Spain sample 7

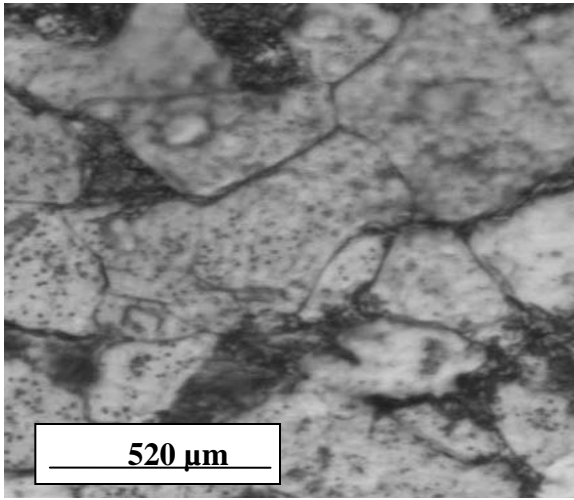


Fig.31 Transverse section of Spain sample 8

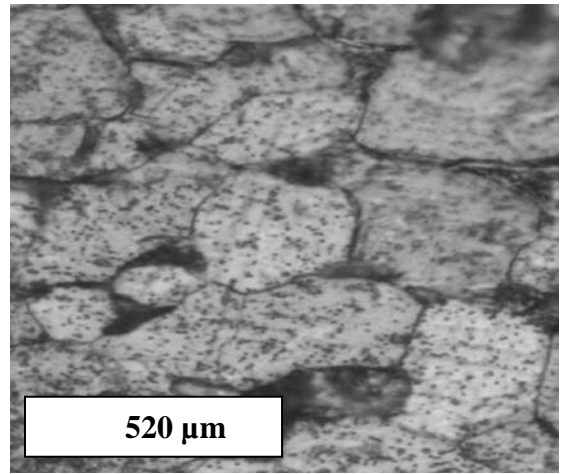


Fig.32 Longitudinal section of Spain sample 8

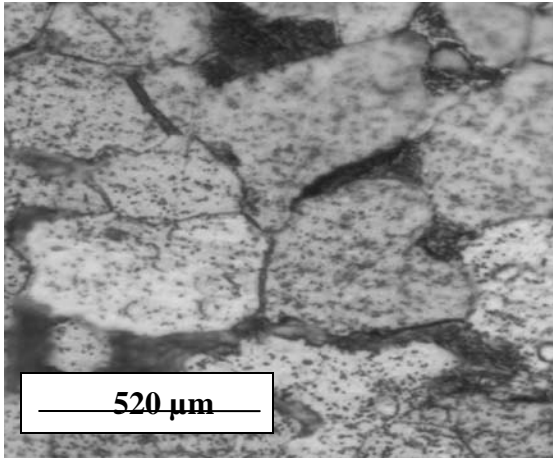


Fig.33 Transverse section of Spain sample 9

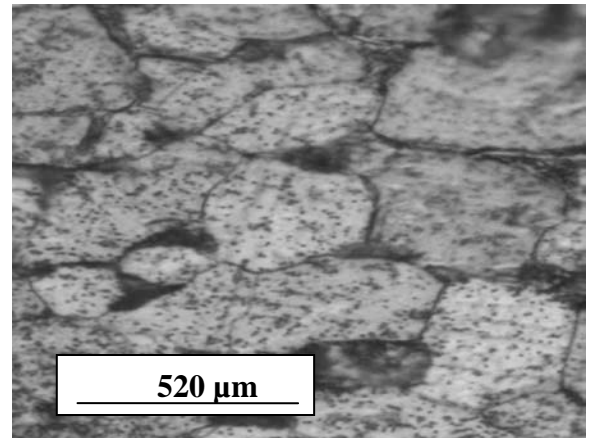


Fig.34 Longitudinal section of Spain sample 9

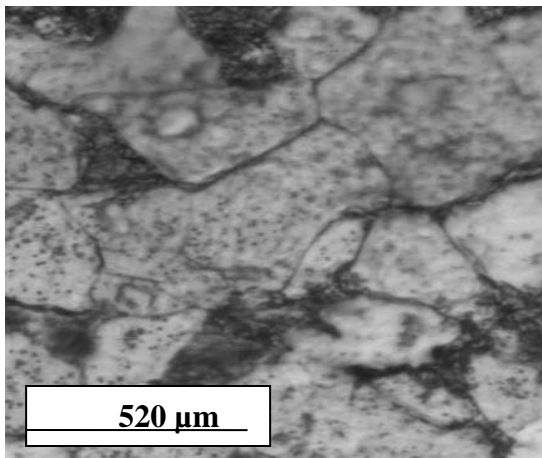


Fig.35 Transverse section of Spain sample 10

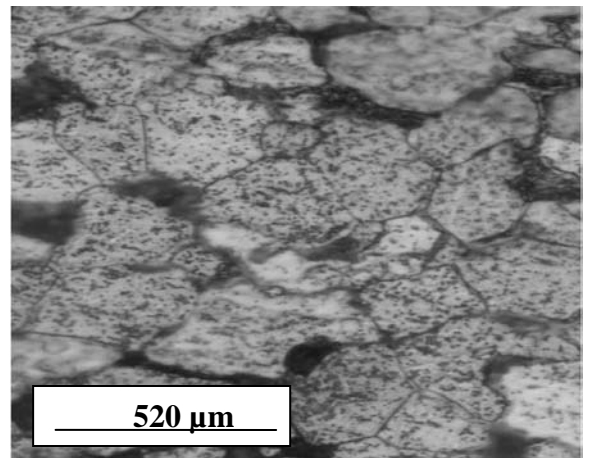


Fig.36 Longitudinal section of Spain sample 10

## Microstructure of Tema Steel Works

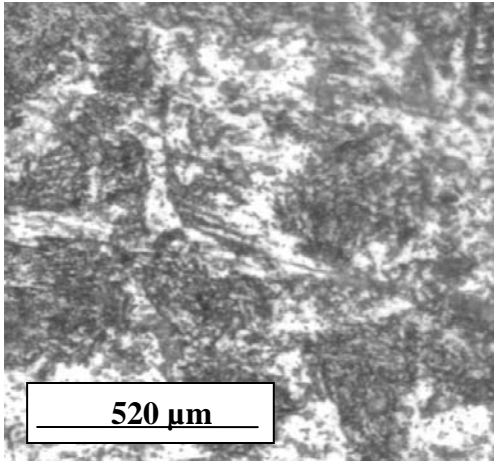


Fig.37 Transverse section of Tema steel sample 2

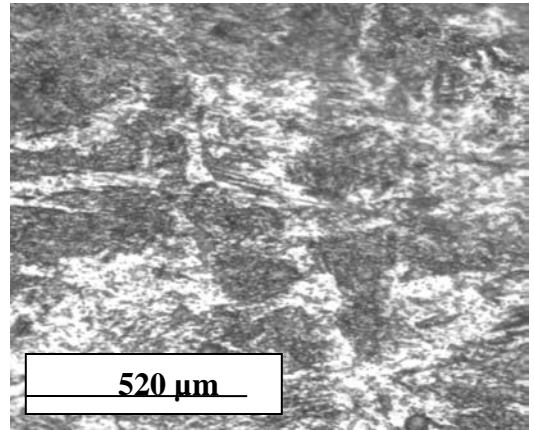


Fig.38 Longitudinal section of Tema steel sample 2

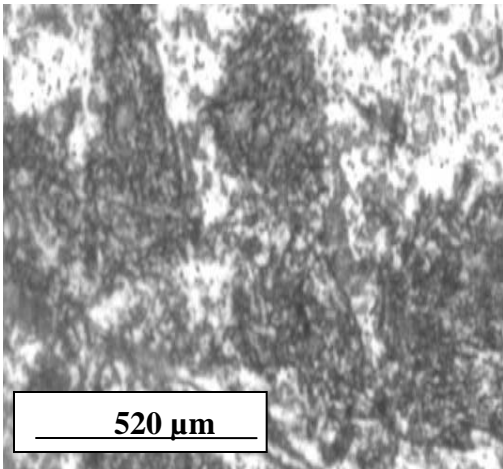


Fig.37 Transverse section of Tema steel sample 3

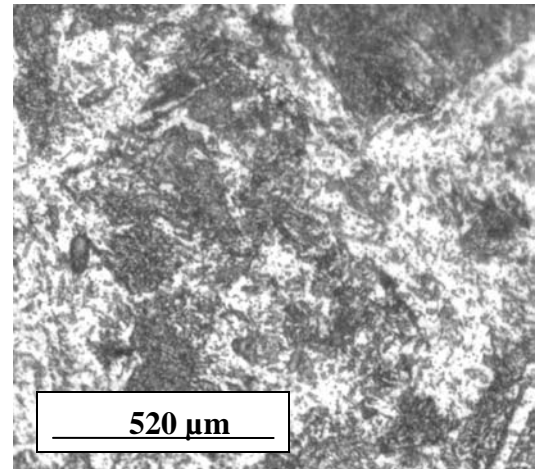


Fig.40 Longitudinal section of Tema steel sample 3

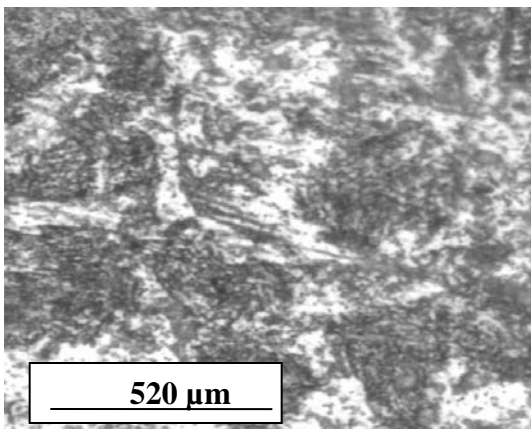


Fig.41 Transverse section of Tema steel sample 4

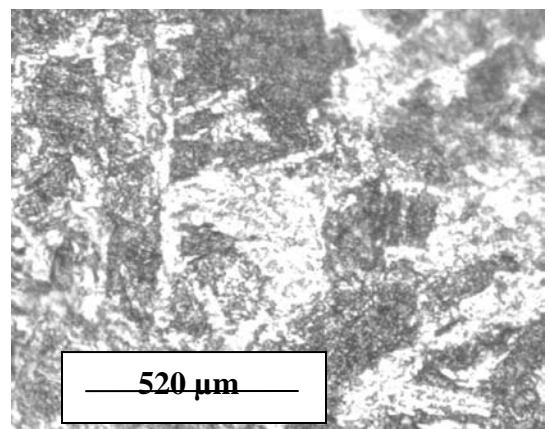


Fig.42 Longitudinal section of Tema steel sample 4

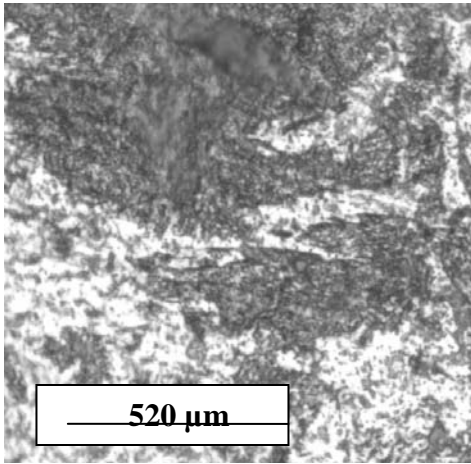


Fig.43 Transverse section of Tema steel sample 5

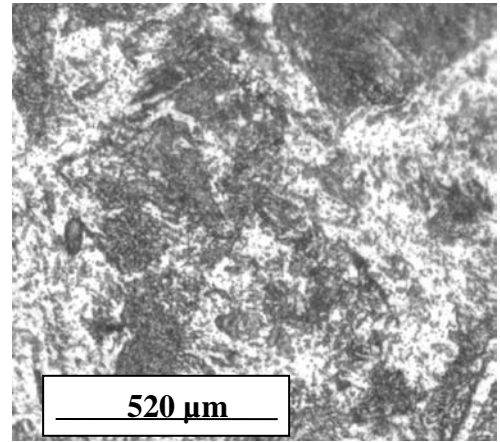


Fig.44 Longitudinal section of Tema steel sample 5

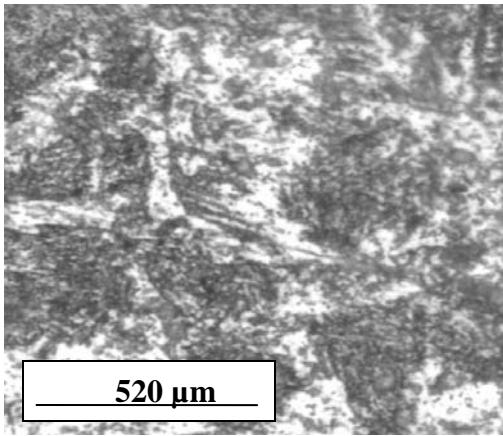


Fig.45 Transverse section of Tema steel sample 6

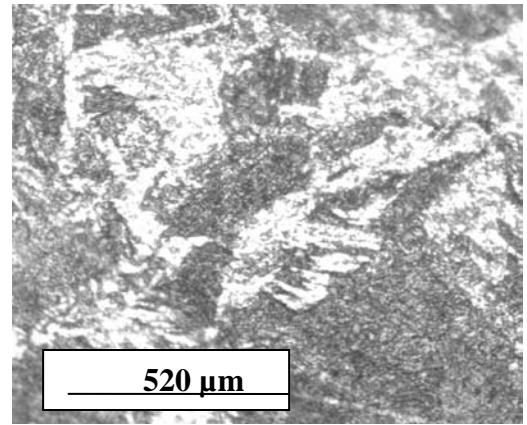


Fig.46 Longitudinal section of Tema steel sample 6

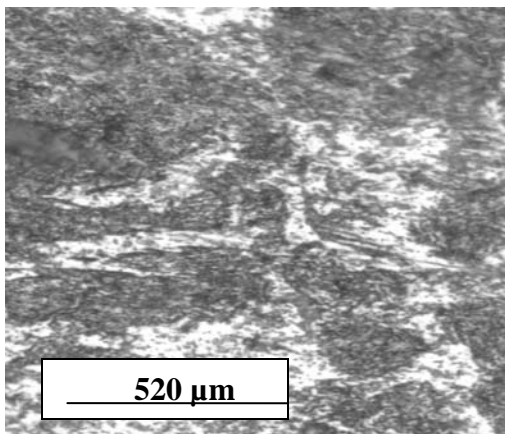


Fig.47 Transverse section of Tema steel sample 7

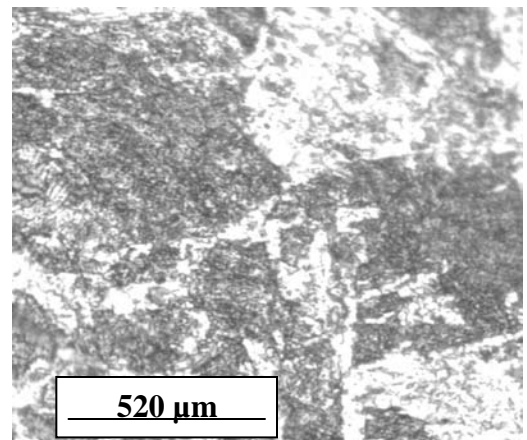


Fig.48 Longitudinal section of Tema steel sample 7

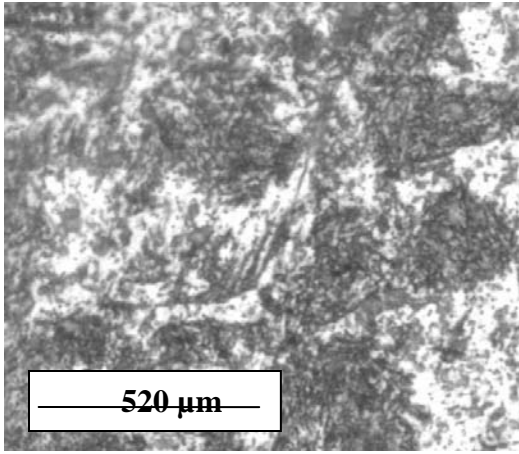


Fig.49 Transverse section of Tema steel sample 8

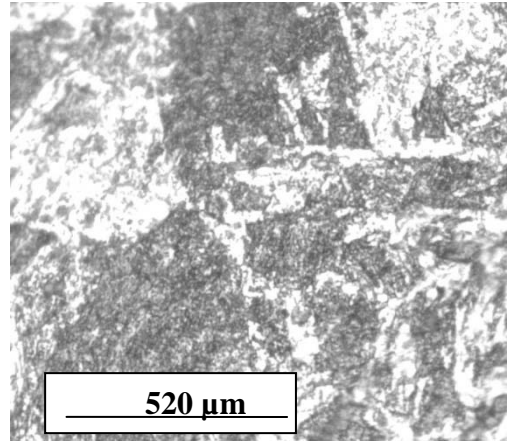


Fig.50 Longitudinal section of Tema steel sample 8

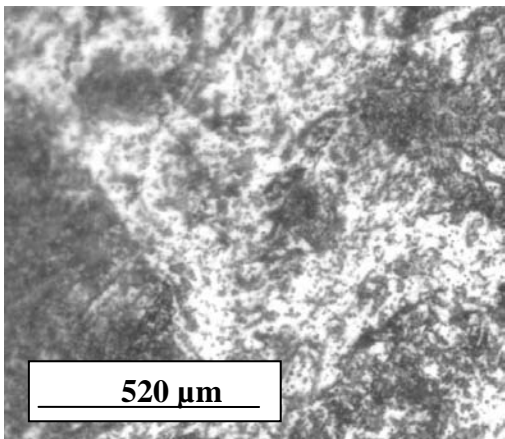


Fig.49 Transverse section of Tema steel sample 9

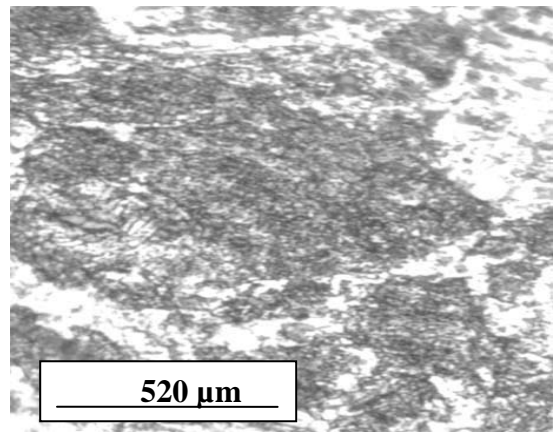


Fig.52 Longitudinal section of Tema steel sample 9

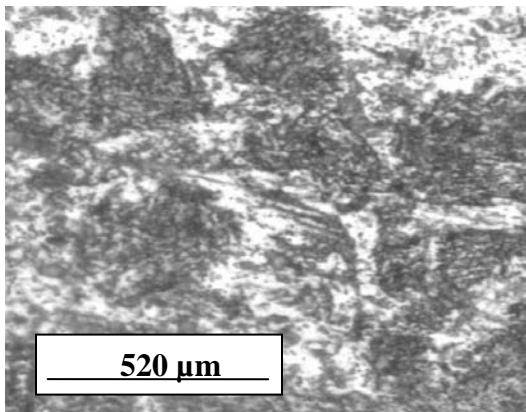


Fig.49 Transverse section of Tema steel sample 10

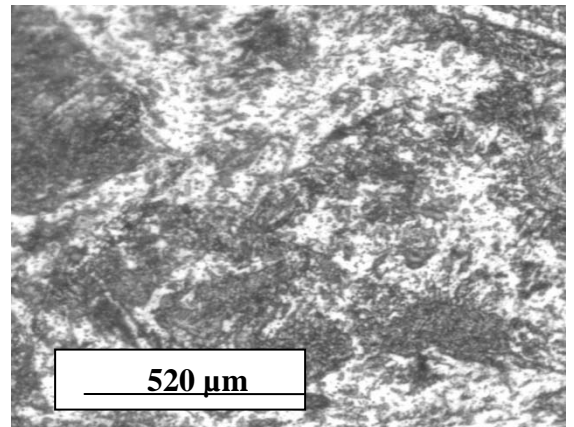


Fig.54 Longitudinal section of Tema steel sample 10

**Microstructure of Ferro Fabrik Samples**

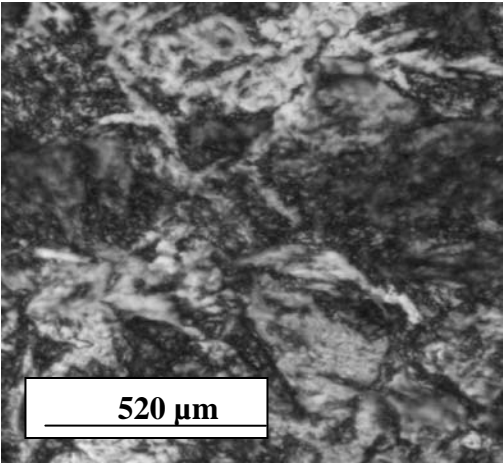
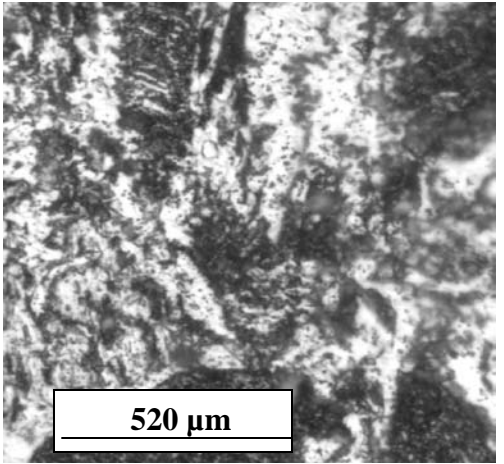


Fig.55 Transverse section of Ferro Fabrik sample 2



56 Longitudinal section of Ferro Fabrik sample 2

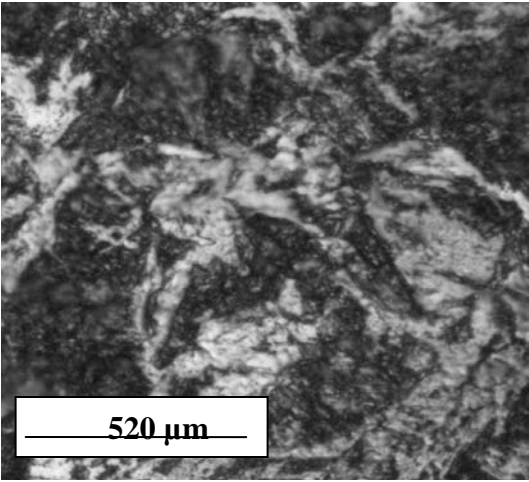


Fig.57 Transverse section of Ferro Fabrik sample 3

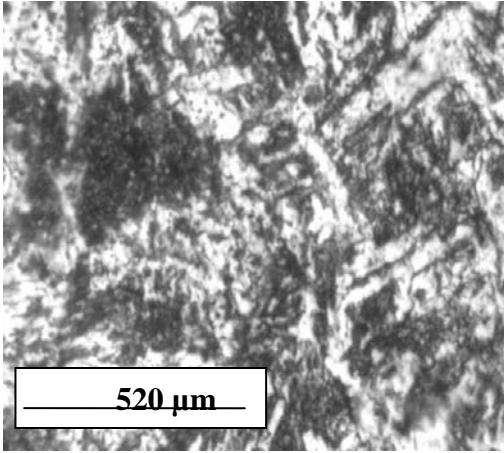


Fig.58 Longitudinal section of Ferro Fabrik sample 3

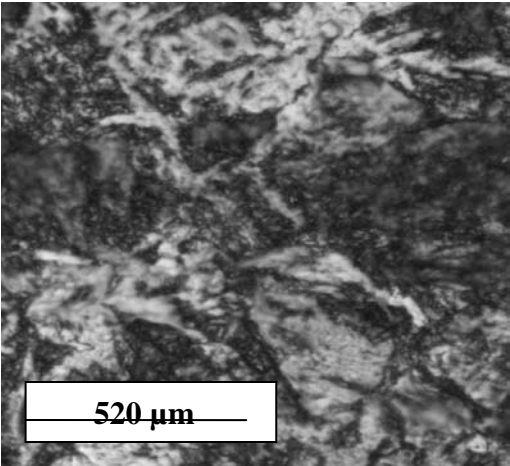


Fig.59 Transverse section of Ferro Fabrik sample 4

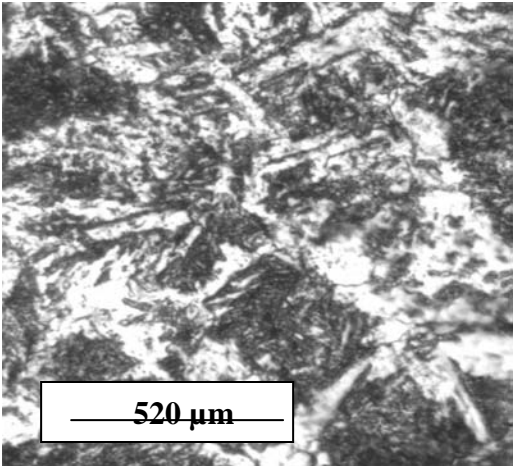


Fig.60 Longitudinal section of Ferro Fabrik sample 4

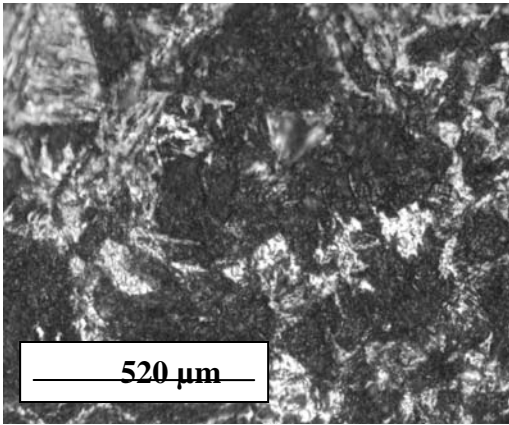


Fig.61 Transverse section of Ferro Fabrik sample 5

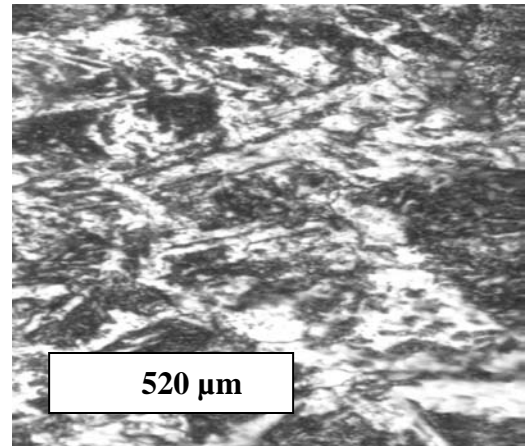


Fig.62 Longitudinal section of Ferro Fabrik sample 5

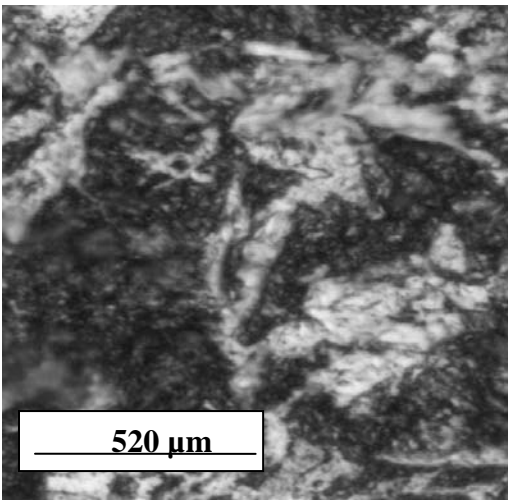


Fig.63 Transverse section of Ferro Fabrik sample 6

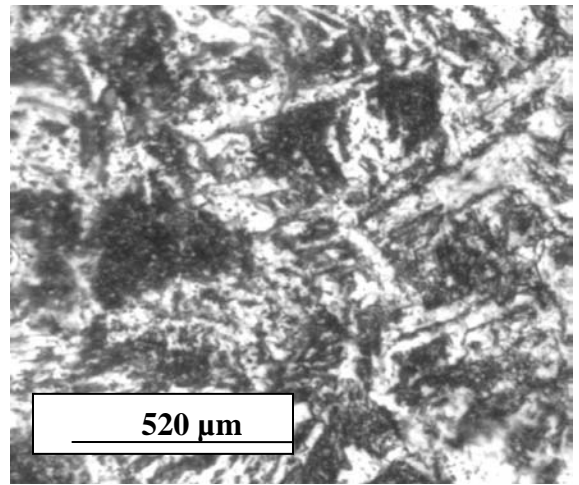


Fig.64 Longitudinal section of Ferro Fabrik sample 6

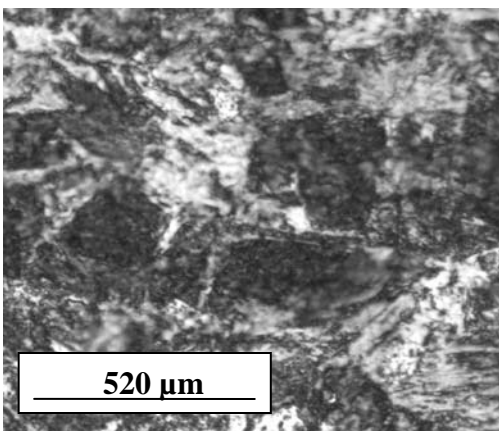


Fig.65 Transverse section of Ferro Fabrik sample 7

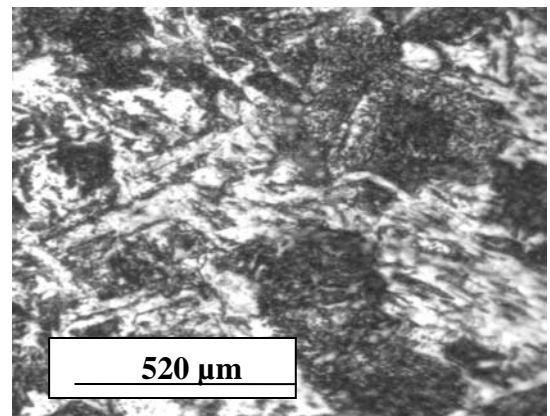


Fig.66 Longitudinal section of Ferro Fabrik sample 7

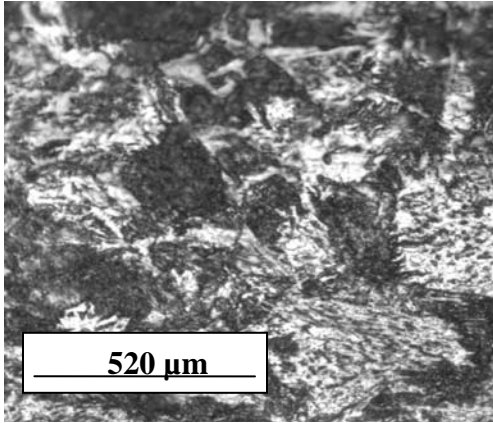


Fig.67 Transverse section of Ferro fabrik sample 8

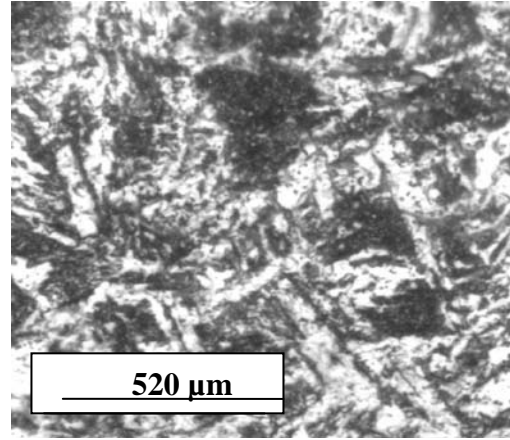


Fig.68 Longitudinal section of Ferro Fabrik sample 8

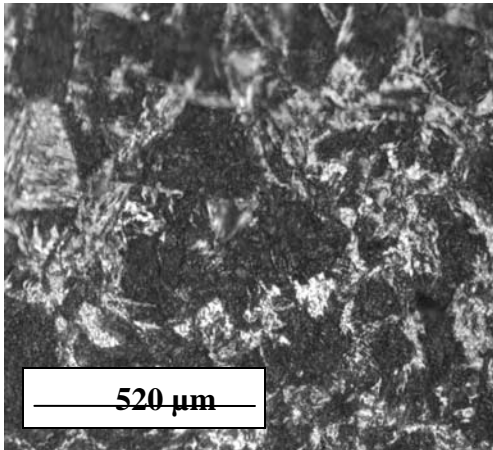


Fig.69 Transverse section of Ferro Fabrik sample 9

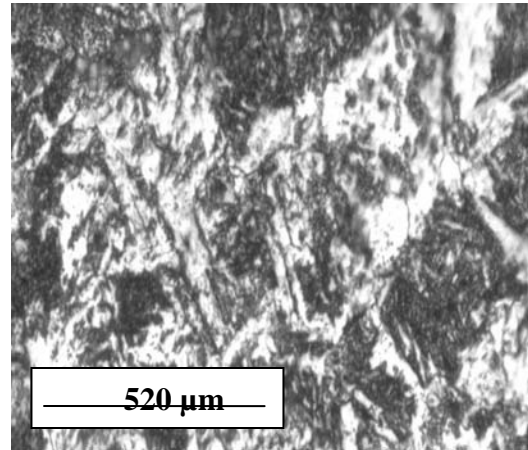


Fig.70 Longitudinal section of Ferro Fabrik sample 9

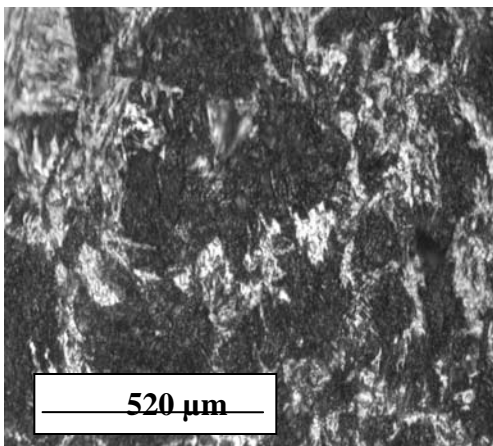


Fig.71 Transverse section of Ferro Fabrik sample 10

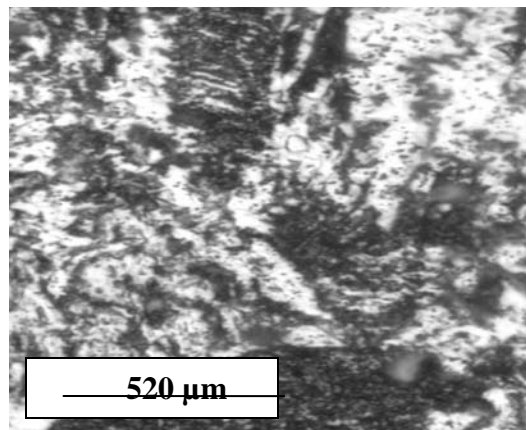


Fig.72 Longitudinal section of Ferro Fabrik sample 10